A STUDY OF THE POWDER PROCESSING, TRIBOLOGICAL PERFORMANCE AND METALLURGY OF ALUMINIUM-BASED, DISCONTINUOUSLY REINFORCED METAL MATRIX COMPOSITES

C A Mitchell

A thesis submitted in partial fulfillment of the requirements of Napier University for the degree of Doctor of Philosophy

July 2002

C A Mitchell
Doctor of Philosophy

A Study of the Powder Processing, Tribological Performance and Metallurgy of Aluminium-based, Discontinuosly Reinforced Metal Matrix Composites

The principal objectives of the research reported in this thesis are: to determine the effect that sinter time has on the metallurgical behaviour of alumina-reinforced aluminium-6061matrix composites; compare and assess the wear resistance of alumina and silicon carbide reinforced aluminium 6061-matrix composites, together with monolithic aluminium 6061 alloy; determine the effect that reinforcement particle size has on the wear resistance of aluminium 6061-matrix composites; identify the relative merits of two techniques for depositing copper coatings on to alumina reinforcements.

Through investigation, a successful method of processing silicon carbide and alumina particulate-reinforced AA6061 composites, fabricated by cold uniaxial pressing with vacuum sintering, has been determined. The processing route is as follows: pressing at 400 MPa; vacuum sinter at 600^0C for 30 minutes; solution heat treat for 30 minutes at 530^0C then water quench; precipitation (ageing) heat treat for 7 hours at I 75^0C, then air cool.

Metallurgical examination of composites revealed that magnesium was found to collect at interface regions around alumina particulates, resulting in the depletion of magnesium from the aluminium 6061 matrix. The severe depletion of magnesium from the AA6061 matrix when alumina is used as a reinforcement was found to occur during long (greater than 30 minutes) sintering times using a sintering temperature of 600^0C. It is postulated that the formation of spinel ($MgAl_2O_4$) formed from the reaction of magnesium with alumina is a probable cause for the Mg migration. The composites containing alumina particulates were found to have lower hardness values than the monolithic alloy and composites containing silicon carbide, when sintering took place for longer than 30 minutes. Adding 5 wt% silicon to the AA6061 matrix in composites reinforced with alumina particulates was found to reduce the magnesium depletion for sinter times up to one hour at 600^0C and give improved composite bulk hardness.

During the research, a need for an improved wear testing machine was identified. Therefore a wear test rig, which allows samples of different materials (under different applied loads if required) to be tested simultaneously without interference between test pieces, was designed and commissioned.

Two electroless methods for copper coating alumina particulates were also investigated. One method used formaldehyde as the reducing agent, while the other employed hydrazine-hydrate as the reducing agent. The latter method has proven to be quicker, and with improved results, compared to the traditional method using formaldehyde as the reducing agent.

DECLARATION

I hereby declare that the work presented in this thesis was solely carried out by myself at Napier University, Edinburgh, except where acknowledgement is made, and that it has not been submitted for any other degree.

Colin A. Mitchell (candidate)

5 AUGUST 2002

(Date)

Abstract

The principal objectives of the research reported in this thesis are: to determine the effect that sinter time has on the metallurgical behaviour of alumina-reinforced aluminium-6061matrix composites; compare and assess the wear resistance of alumina and silicon carbide reinforced aluminium 6061-matrix composites, together with monolithic aluminium 6061 alloy; determine the effect that reinforcement particle size has on the wear resistance of aluminium 6061-matrix composites; identify the relative merits of two techniques for depositing copper coatings on to alumina reinforcements.

Through investigation, a successful method of processing silicon carbide and alumina particulate-reinforced AA6061 composites, fabricated by cold uniaxial pressing with vacuum sintering, has been determined. The processing route is as follows: pressing at 400 MPa; vacuum sinter at 600^0C for 30 minutes; solution heat treat for 30 minutes at 530^0C then water quench; precipitation (ageing) heat treat for 7 hours at I 75^0C, then air cool.

Metallurgical examination of composites revealed that magnesium was found to collect at interface regions around alumina particulates, resulting in the depletion of magnesium from the aluminium 6061 matrix. The severe depletion of magnesium from the AA6061 matrix when alumina is used as a reinforcement was found to occur during long (greater than 30 minutes) sintering times using a sintering temperature of 600^0C. It is postulated that the formation of spinel ($MgAl_2O_4$) formed from the reaction of magnesium with alumina is a probable cause for the Mg migration. The composites containing alumina particulates were found to have lower hardness values than the monolithic alloy and composites containing silicon carbide, when sintering took place for longer than 30 minutes. Adding 5 wt% silicon to the AA6061 matrix in composites reinforced with alumina particulates was found to reduce the magnesium depletion for sinter times up to one hour at 600^0C and give improved composite bulk hardness.

During the research, a need for an improved wear testing machine was identified. Therefore a wear test rig, which allows samples of different materials (under different applied loads if required) to be tested simultaneously without interference between test pieces, was designed and commissioned.

Two electroless methods for copper coating alumina particulates were also investigated. One method used formaldehyde as the reducing agent, while the other employed hydrazine-hydrate as the reducing agent. The latter method has proven to be quicker, and with improved results, compared to the traditional method using formaldehyde as the reducing agent.

Contents

Tables

Figures

Acknowledgements

I wish to acknowledge the role my supervisor, Mr. Alan Davidson, has played in the completion of this thesis. His continual support, encouragement and faith have never wavered, and I thank him for this. I also thank him for being supportive in more personal aspects, which have occurred over the period of study, and being there to talk to.

My thanks to Mr. William Brownlee and Mr. David Kane, technicians at Napier University, for their technical expertise, support and friendship. Without the technical skills of Bill and Davie many aspects of this research would not have been possible.

I also wish to thank and acknowledge the support, good conversation and friendship of other research students in the School of Engineering at Napier University. I won't mention any names for fear that I leave someone out.

My thanks also to the staff at Otto von Guericke Universitat, Magdeburg for their technical assistance, especially to Stephan for being my guide and interpreter.

Finally thanks to Mum and Yvonne. You gave me the support and help to finish this thesis, and I thank you both for it.

Chapter 1

Introduction

"there is no new thing under the sun", Ecclesiastes 1, 9.

1.1 An Historical Overview

Metal Matrix Composites (MMCs) are generally considered to be a relatively recent development in the field of materials technology, with research and development tracing its roots back to the 1950s [Harris 1999]. However, it is recorded that some ancient civilisations were constructing laminated structures consisting of metallic and non-metallic materials [Muhly 1988].

The advantages of MMCs over their monolithic counterparts are well documented and include superior specific strength, stiffness and wear resistance. In the 1970s and 1980s, there was an increase in research and development of MMCs due to their potential improvement at high temperatures [Hunt 2000]. The latter part of the 20^{th} century resulted in research which was not only performance driven, but also involved the economics of MMCs [Hunt 2000]. Partly due to economic benefits, research began to evaluate particulates as reinforcements for MMCs, including silicon carbide (SiC), aluminium oxide or alumina (Al_2O_3), titanium carbide (TiC), titanium diboride (TiB_2) and boron carbide (B_4C). While not quite having the increased levels of specific strength and stiffness shown by their fibre-reinforced counterparts, particulate reinforced MMCs provided significant improvements in such properties when compared with the monolithic materials and their associated processing costs were

significantly less than those associated with continuous reinforcements. However, there were still problems associated with the processing of composite materials and the remit of this current research includes work in this area.

1.2 Scope of Thesis

The scope of the thesis is to identify and investigate the procedures required for a low cost processing route of MMCs containing particulate ceramic reinforcements for wear resistant applications. A major reason for the slow commercial exploitation of MMCs is their relatively high cost of processing. The current research uses a low cost (cold pressing and vacuum furnace), pressureless sintering technique, which has the following advantages over liquid state methods of lower processing temperatures:

- reducing the likelihood of the matrix reacting unfavourably with the reinforcement
- improved ceramic particle distribution
- potentially lower energy consumption
- cost effective material usage
- little or no machining required, and
- low operator costs (i.e. simplified operation methods with a low time scale).

However, solid-state processing also has disadvantages over liquid methods including higher cost of matrix (powder production costs), problematic composite consolidation and longer times to achieve consolidation. The current research addresses the issue in terms of investigating the effect of sintering time and heat treatment time on the hardness and wear resistance of particulate alumina and silicon carbide reinforced

composites. The performance of aluminium alloy-based metal matrix composites reinforced with a hybridised alumina/silicon carbide combination is also examined.

To achieve high wear rates, wear testing is carried out using a dry sliding wear method. Metallographic examination of the composites is performed using optical microscopy, scanning electron microscopy and energy dispersive x-ray analysis. Since particulate alumina is less expensive than particulate silicon carbide, it is clear that if their employment in aluminium alloy-based composites results in comparable wear characteristics, then the economic benefits would be attractive.

The study will also identify and attempt to overcome any deleterious effects found in the MMCs due to processing procedures.

1.3 The Objectives of this Study

The objectives associated with this work are to investigate and explain the following factors associated with aluminium based discontinuously reinforced metal matrix composites:

- The effect that sinter time has on the metallurgical behaviour of alumina-reinforced aluminium-6061matrix composites.
- To compare and assess the wear resistance of alumina and silicon carbide reinforced aluminium 6061-matrix composites, together with monolithic aluminium 6061 alloy.
- The determination of the effect that reinforcement particle size has on the wear resistance of aluminium 6061-matrix composites.

- To identify the relative merits of two techniques for depositing copper coatings on to alumina reinforcements.

1.4 The Aims of this Study

The work carried out during this research has the following overall aims:

- To progress the understanding of powder metallurgy techniques in producing aluminium metal matrix composites.
- The furtherance of the lowering of costs in the processing of metal matrix composites.

Chapter 2

Literature Review

2.1 Overview of Composite Technology

2.1.1 Classification of Metal Matrix Composites (MMCs)

MMCs are multi-phase materials in which a strong, stiff reinforcing phase, typically a ceramic, is incorporated throughout a softer, ductile metal phase. There are however particular classes of MMC, which are unorthodox, for example, gas as the dispersed phase creating a metallic foam [Clyne 2000]. Also the inclusion of graphitic plates, refractory metals, intermetallics or semi-conductors can be used to obtain a specific property or properties. The various classes of orthodox MMCs are discussed below.

2.1.1.1. Dis-continuously Reinforced MMCs.

Particulate MMCs.

This classification can be further divided into two sub-categories [Callister 1994], Dispersion strengthened and large particle (or true-particle) composites. Dispersion strengthened composites can themselves be divided into two sub-categories:

(A) Dispersion hardening - in this case small, 10 nm to 250 nm diameter particles (usually oxides) are dispersed into a metal matrix;

(B) Precipitation hardening - in this case a precipitate is nucleated and grown within the metal matrix.

In dispersion strengthened composites the particles, which usually constitute ~1 wt% of the material, must be closely spaced (< ~ 1μm). This spacing is necessary because

of the strengthening process (dislocation obstruction) involved. Due to the mechanism of strengthening, these materials are not considered true composites [Clyne 2000].

Large particle composites consist of a metallic matrix with large (1μm - 50μm diameter), usually ceramic particles distributed throughout the matrix. The strengthening process here is primarily load transfer between the matrix and the reinforcing particle [Clyne 2000].

Short Fibre MMCs.

These consist of a metal matrix with ceramic fibres distributed throughout. The fibres range in diameter from ~1μm - 150μm [Hull 1996], with aspect ratios ranging, typically, from 3 to 100. The fibres (e.g. "Saffil", short alumina fibres) are fine-grained polycrystalline in structure.

Whisker Reinforced MMCs.

These MMCs are essentially similar to the short fibre type, the exception being that the whiskers are mono crystalline [Levitt 1970] and usually have a diameter < 1μm, with aspect ratios up to several hundred [Clyne 2000]. Their mechanical properties have been found to be superior when compared with polycrystalline short fibres [Parvizi-Majidi 1993].

2.1.1.2. Continuously Reinforced MMCs.

Monofilament MMCs.

Continuous monofilament reinforcements are large diameter (typically 100μm - 150μm) fibres, usually consisting of SiC or boron, which has been deposited (e.g. by chemical vapour deposition) on to a carbon or tungsten wire core [Clyne 2000]. The monofilament fibres are usually aligned in a unidirectional manner within the matrix. These large diameter fibres do not display a high degree of flexibility and are usually used as single fibres. They typically have a large bend radius (see Table 1) and care must be taken to avoid over bend during processing.

Multifilament MMCs.

Multifilament reinforcements are small diameter (5μm - 30μm diameter) fibres, which can be woven, knitted, stitched, braided or wound. These fibres have a small bend radius (see Table 1), which improves their flexibility. Because of the flexibility of these fibres they can be incorporated into a matrix in a unidirectional manner, or combined (e.g. woven into a multi directional reinforcement).

Table 1. Curvature data for various fibres [Hull 1996].

Material	Trade Name	Diameter d (μm)	Young's Modulus E (GPa)	Fracture Strength σ_f (GPa)	Maximum Curvature K_{max} (mm^{-1})	Minimum Bend Radius (mm)
SiC monofilament continuous	Sigma (UK)	150	400	2.4	0.08	12.5
SiC multifilament continuous	Nicalon (Japan)	15	190	2.0	1.4	0.71
$Al_2O_3 + SiO_2$ short fibre discontinuous	Saffil (UK)	3	300	2.5	5.5	0.18
SiC whisker discontinuous	N/A	1	450	5.0	22.2	0.045

Note: in Table 1, maximum curvature values are calculated from -

$$K_{max} = \frac{2\sigma_f}{Ed} \qquad \text{eqn. 1.}$$

Where K_{max} = maximum curvature / mm^{-1} σ_f = fracture strength / GPa

E = Young's Modulus / GPa d = diameter of the fibre / mm

Layered MMCs.

Layered MMCs consist of alternate layers of, usually, two constituent materials. These composites can contain layers from a few nanometres thickness up to thickness of several centimetres. This category of MMC includes coatings and / or film deposition (e.g. ceramic coating of metals to improve wear resistance). Also included in this category is the use of fibre-reinforced tapes or fabrics when used in alternate layers [Askeland 1998].

2.1.1.3. MMCs Containing High Percentage of Ceramic.

This group of composites are commonly known as cermets. In this group the volume percent of ceramic should be greater than 70% [Tinklepough 1960]. Ceramic particles are held together by a small amount of metallic phase. They may be considered as high particulate volume ceramic reinforced metal matrix composites.

2.1.2. Reinforcement Influence on Directional Properties of MMCs.

The geometry of the reinforcement within the matrix affects the mechanical properties of the MMC. Below are schematics of the geometry and orientation of reinforcements and their effect on an MMCs mechanical properties.

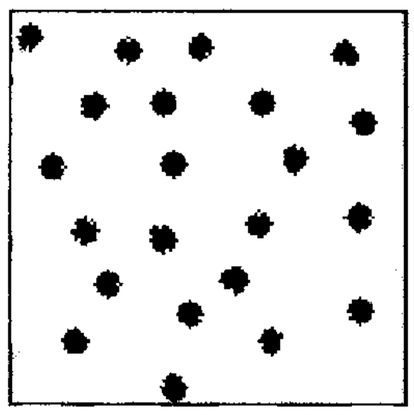

Equiaxed particles;
isotropic behaviour

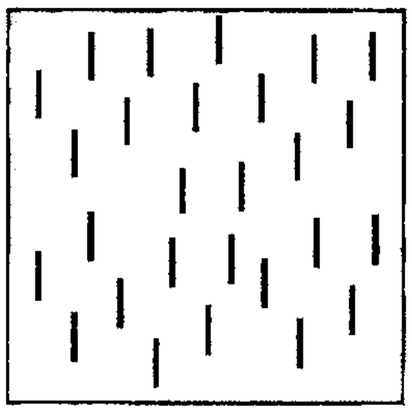

Aligned short fibres/whiskers;
anisotropic behaviour

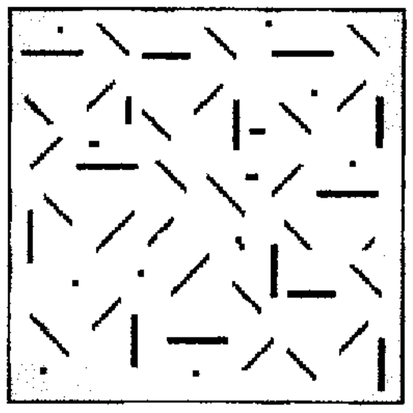

Random short fibres/whiskers;
isotropic behaviour

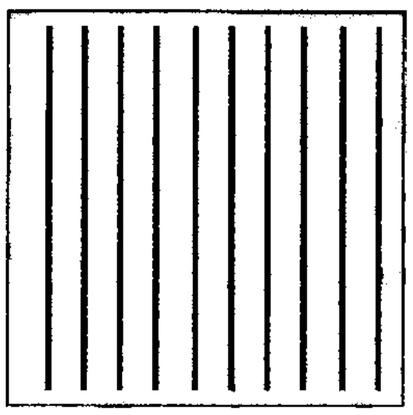

Aligned continuous monofilament fibres;
anisotropic behaviour

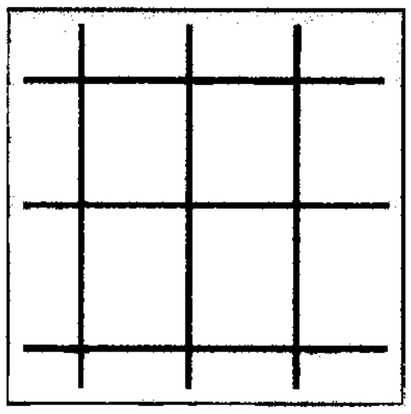

Woven multifilament fibres;
bi-directional properties

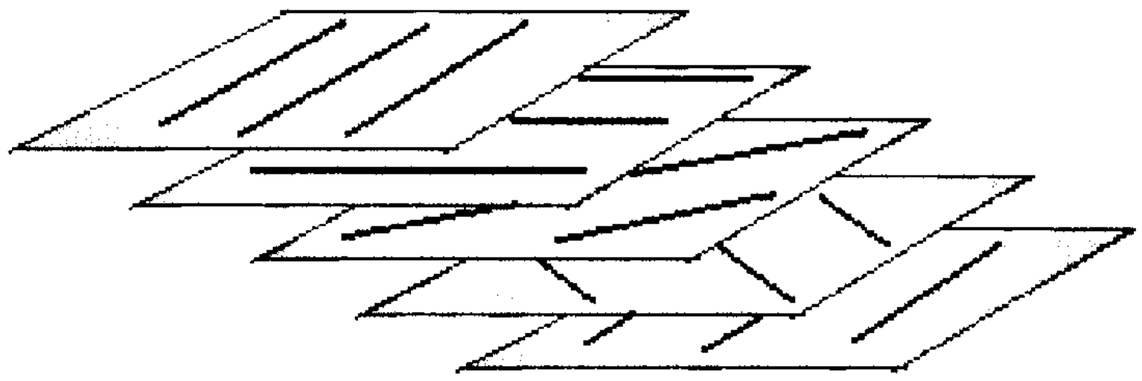

Cross-plied fibre tapes;
quasi-isotropic behaviour

Figure 1. Effects of reinforcement orientation on mechanical properties.

There are other orientations possible (e.g. three dimensional weaves or knits). However it is observed that the simplest method of achieving isotropy is by using particulate or random short fibre/ whisker reinforcements in MMCs.

2.1.3 Examples of Methods of Manufacture for MMCs.

2.1.3.1 Powder Metallurgy

Powder Metallurgy (PM) is widely used for the production of discontinuously reinforced MMCs and at Napier University the processing consists of three stages:

(1) Blending - the metal powder and the reinforcement are mixed together to form a homogenous mixture;

(2) Cold compaction - the powders are pressed to form a "green" billet;

(3) Hot consolidation - the powders are heated to obtain a fully dense compact.

Other commercial variations include hot isostatic pressing (HIPing), high-energy-high-rate processing, and resistance sintering [Liu 1993].

The powder metallurgy route is discussed in more detail in Chapter 3.

2.1.3.2 Alternative MMC Processing Routes.

Reactive metal penetration: this process involves the penetration of a reactive metal into a dense ceramic preform [Gao, Y. 1996]. The method described by Gao involves the penetration of molten aluminium (Al) into a mullite ($Al_6Si_2O_{13}$) preform (rod) at a temperature higher than 900°C. The ceramic preform was dipped into the molten metal. The formation of a Al - Al_2O_3 composite is completed when the molten Al reacts with $Al_6Si_2O_{13}$ according to the reaction equation -

$$3Al_6Si_2O_{13} + (8 + x)Al \rightarrow 13Al_2O_3 + 6Si + xAl \qquad \text{eqn. 2}$$

This process produces a composite containing interconnected Al_2O_3 and Al. A composite formation rate of 3 mm h^{-1} at a temperature of 1100°C was reported. When the Al was replaced with the aluminium alloy 6061 (typically containing 1wt% Mg, 0.6 wt % Si, balance Al) the composite formation rate was reported to be slower, suggesting Mg inhibited the reaction [Gao, Y. 1996].

Pressureless metal infiltration: this method of manufacture was developed by the Lanxide Corporation and is given the trade name of PRIMEX™ [Schiroky 1997]. In the PRIMEX™ method a ceramic preform (typically SiC or Al_2O_3 particulates) is infiltrated by a molten aluminium alloy. The aluminium alloy contains between 2 - 7

wt% magnesium. The process is carried out at 800°C in a nitrogen atmosphere. At 800°C the Mg vapour pressure is high enough to cause the Mg to slowly evaporate. With the molten alloy in contact with the ceramic preform, the Mg diffuses into the preform. Within the preform Mg reacts with nitrogen in the process atmosphere, this reaction product, Mg_3N_2, coats the ceramic particles. As the molten aluminium contacts with the Mg_3N_2 coating, the coating is reduced to AlN and Mg, according to the reaction [Schiroky 1997]:-

$$Mg_3N_2 + 2Al \rightarrow 2AlN + 3Mg \qquad \text{eqn. 3}$$

The Mg_3N_2 coating on the particles promotes wetting of the aluminium on the ceramic [Lee 1998] and therefore drives the spontaneous infiltration process. The kinetics of infiltration depend upon preform permeability, Mg concentration, N concentration and process temperature. Several hours are required for infiltration of only a few millimetres [Schiroky, G.H. 1997].

High pressure infiltration casting: this type of composite production consists of two methods, (a) squeeze casting infiltration, using a piston to drive the molten metal into the reinforcement preform; (b) gas driven pressure infiltration, using a pressurised gas to achieve the metal infiltration of the preform.

(a) this method forces molten metal (e.g. aluminium) into a porous ceramic, particulate or fibre, preform [Dynan 1993]. A pressure is required which will overcome any surface tension effects (poor wettability) between the molten metal and the ceramic reinforcement. The method, described by Dynan, involved heating a ceramic (alumina - silicate fibres) preform to 1000°C for 30 minutes, then pouring molten aluminium A356 alloy on to the upper surface of the preform. A pressure of 100 MPa was applied for approximately 45 seconds, then the composite billet was removed.

(b) This method again uses high pressure (> 1MPa) to achieve infiltration. This process [Mortensen 2000] uses a ceramic preform inserted into a gas tight mould, which is contained within a pressure vessel. Above the preform mould is a container containing the matrix metal and the container has a facility for pouring the molten metal from the base. The pressure vessel is heated to a temperature, which ensures the melting of the metal. Air is evacuated from the pressure vessel producing a vacuum within. The molten metal is then poured over the perform and an inert gas is pumped into the vessel to the required pressure. Since the ceramic preform is not exposed to the pressurised gas (the molten metal sealing the preform from the gas), it remains under vacuum thereby drawing the molten metal into the preform.

Semi-solid casting (Compocasting): in this process [Lloyd 2000] an alloy is melted to obtain ~ 40 % solid primary particles of unreinforced alloy. To this partial melt is added reinforcing ceramic particles. As the ceramic is added the temperature of the melt is increased to ensure that the solid phase in the melt does not exceed ~ 40 %. This process behaves as a colloidal mixture and if the solid volume percent becomes too high then all solid phase will be rejected from the melt.

Spray deposition: this process involves atomising a metal and introducing reinforcing particles into the resultant spray, which is collected on to a suitable substrate [Lloyd 2000]. This method has a tendency to form a layered type structure due to the nature of deposition.

2.1.4 Strengthening Mechanisms in MMC Materials

Aluminium-based metal matrix composites using ceramic reinforcements have attracted research interest because of their potential advantages over traditional materials including weight reduction, increased specific strength and specific

stiffness, improved high temperature performance, improved creep and fatigue resistance and improved wear resistance [Harris 1999]. The improved strength of composites when compared to the monolithic alloy stems from two main mechanisms: (1) The reinforcing particles restrict the movement of the matrix around the particles with some of the applied stress being transferred to the particles [Callister 1994], which bear a fraction of the load. (2) The reinforcing particles restrict dislocation motion [Askeland 1998], also the increase in dislocation density around the particles [Varma 1996; Wang 1995] may lead to an increase in yield strength by restricting dislocation motion.

2.1.5 Examples of Current Engineering Applications for MMCs.

Two applications of MMC technology are discussed below. The first is aerospace applications, which effectively started the current research with the industry's demand for lightweight materials with a high structural integrity. As the cost of producing components fabricated from MMCs reduced, this resulted in their use becoming favourable to the automotive industry.

Aerospace: In a space (outside Earth's atmosphere) environment surface temperatures on a spacecraft can cycle between -150°C to +100°C [Dunn 2000]. This temperature cycling can lead to thermal fatigue. To counter the temperature variation, controlled expansion materials have been developed one of which is an aluminium alloy matrix containing between 50% to 80% SiC reinforcement.

In military aircraft Al-SiC MMCs are replacing titanium alloys as missile support structures [Hexemer 2000]. These MMCs are produced as near net shape, thus reducing cost, as titanium is an expensive material and requires extensive machining

to produce the component. The Al-SiC MMC is a viable alternative to titanium as it has a low coefficient of thermal expansion and high modulus.

A component made from Ti-SiC for use in jet engines exploits the lightweight and high compressive strength of MMCs. A hydraulic actuator for the thrust nozzle on a Pratt and Whitney F-119 engine experiences large compressive loads. The MMC provides increased compressive stiffness and strength resulting in a 40% weight reduction [Spowart 2000].

Other aerospace uses are engine fan exit guide vanes for Pratt and Whitney 4000 series engines, Iridium satellites for Motorola and F-16 aircraft ventral fins and fuel access covers [Johnson 2001].

Automotive: The Toyota Motor Company produced an MMC piston in 1983 consisting of Al-Al_2O_3 for diesel engines. This composite was used in the piston ring groove to reduce weight and improve wear resistance [Kevorkijan 1998]. The MMCs also have a low coefficient of thermal expansion, which results in finer tolerances between piston and cylinder resulting in increased cylinder pressures and, therefore, more efficient engines.

Al-SiC MMCs are being developed for military tank track shoes by Advanced Refractory Technologies, U.S. Weight saving of up to 25% have been achieved and wear performance is comparable to steel. Due to improved heat dissipation, shoe bush life has shown a potential 200% working life increase [Hexemer 2000].

Advances and usage of MMCs for automotive purposes are advancing continually. Other automotive uses are cylinder liners, connecting rods [Kevorkijan 1998], disc and drum brake components, drive shafts and torque tubes [Hexemer 2000], [Johnson 2001].

2.2 Powder Metallurgical (PM) Processing Technology

2.2.1 Introduction.

The pressing of metal powders to form solid objects of a specific shape is not a recent development and was known to have been used by ancient civilisations, for example the iron pillar in Delhi [Upadhyaya 1997]. The current research uses pre-alloyed aluminium metal powder and particulate ceramics. The types of aluminium based powders available fall into two categories - elemental and pre-alloyed. Elemental aluminium can be mixed with other metals e.g. copper, to produce an alloy during processing. Pre-alloyed powder is supplied with the alloying metals already present e.g. AA6061 containing Mg and Si, AA2124 containing Cu. Other and/or differing amounts of metals can be added to the powders to customize the alloys for particular properties.

The Powder Metallurgical (PM) route for the production of MMC's was introduced to reduce the problems of wetting and interfacial reactions often encountered with liquid processing, with an added benefit of improved spatial distribution of particulates in dis-continuously reinforced MMC's [Stone 1993]. The PM route also has net-shape or near net-shape production capability, thereby reducing machining and finishing costs [Liu 1993]. Liu also reports that MMC's with a high dislocation density, small grain size and limited re-crystallisation can be manufactured, resulting in improved mechanical properties.

2.2.2 Aluminium Alloys as Composite Matrix Materials

The reasoning behind MMC development is to produce a material with improved specific properties i.e. reduced weight and improved mechanical / physical properties

of the material. As reduction in weight is a priority for MMC development, the major research has concentrated on light metal alloy matrices e.g. alloys based on Aluminium (Al), Beryllium (Be), Magnesium (Mg) and Titanium (Ti). A comparison of these light alloys [King 1991] results in the following observations:-

Al - major disadvantage is its limited temperature capability. Age hardened alloys operating at temperatures ~190℃ can lead to precipitate coarsening and strength loss.

Be - major disadvantages are that it is brittle at room temperature, its oxide is toxic and it is very expensive.

Mg - major disadvantages are high chemical reactivity, poor corrosion resistance and high creep rate.

Ti - major disadvantages are chemical reactivity and oxide formation causing problems with powder forming and diffusion bonding.

The cost of materials is also a factor in the commercial exploitation of MMC's, with the current cost of the base metal for MMC materials being a significant part of the total cost. The current cost [Goodfellows 2000] of base alloy powders is given in Table 2.

Table 2. Comparative costs of metal powders.

Material	Quantity / grams	Size / μm	Cost / £ Sterling
Al	100	60	81.50
Be	100	75	339.00
Mg	100	50	130.00
Ti	100	45	186.00

From Table 2 the cost of aluminium can be seen to be significantly lower than any of the other light metals available. Aluminium has a slightly higher density when compared with Be and Mg, but has a lower density compared with Ti or traditional engineering metals such as copper (Cu), iron (Fe), nickel (Ni) or Tin (Sn). Table 3 displays density comparisons [Sharp 1990].

Table 3. Comparative densities of engineering metals.

Metal	Al	Be	Cu	Fe	Mg	Ni	Sn	Ti
Density / gcm^{-3}	2.70	1.85	8.92	7.87	1.74	8.90	7.30	4.50

From Table 3 aluminium is seen to be the third least dense material with only Be and Mg having a lower weight per unit volume.

Pre-alloyed aluminium is available in a variety of alloys. There are, currently, eight main categories of aluminium alloy, an example and chemical composition for each category is given below in Table 4 [Matweb 2001].

Table 4. Examples of main alloying elements of various aluminium alloys.

ASTM Alloy series designation	**Example alloy classification**	**Comments**
1000	1199	Al 99.99%
2000	2014	Al + Cu, Mg and Mn
3000	3003	Al + Mn, Fe and Si
4000	4032	Al + Si, Cu, Mg and Ni
5000	5052	Al + Mg and Cr
6000	6061	Al + Mg and Si
7000	7005	Al + Zn, Mg and Mn
8000	8090	Al + Li, Cu and Mg

Aluminium pre-alloyed powder is readily available from a selection of commercial suppliers. This availability results in reduced cost factors e.g. simplified sourcing and no or limited speciality manufacture (dependent upon the alloy required).

The alloying elements present in aluminium alloys affect the mechanisms, which give an alloy strength and hardness. The 1000, 3000, 5000 and most of the 4000 series alloys are not age hardenable (discussed in section 2.2.1.2 Precipitation) and rely on strain hardening, solid solution strengthening and grain-size control to achieve optimum mechanical properties [Askeland 1998]. The 2000, 6000, 7000 and 8000 alloys are age hardenable. Age hardening of aluminium alloys is the most effective way of improving their mechanical properties (e.g. strengthening) [Prangnell 2000]. Table 5 [Matweb 2001] displays the properties of a selection of age hardenable aluminium alloys in the aged condition and a comparison of their availability and cost.

Table 5. Comparison of physical properties and availability of aged aluminium alloys.

Example Aluminium Alloy	Density / gcm^{-3}	Tensile Strength / MPa	Hardness / VH number	Commercial Availability and Cost
2014	2.80	470	155	Good
6061	2.70	310	107	Excellent
7005	2.78	350	106	Poor
8090	2.55	440	137	Poor

2.2.2.1 Heat Treatment of 6061 Aluminium Alloy.

The improvement of strength and hardness in 6061 aluminium alloy is achieved by specific heat treatments. Age hardening is accomplished by two different heat treatments, solution heat treatment and precipitation hardening [Callister 1994]. In

6061 alloy the alloying elements are magnesium and silicon, which precipitate to form Mg_2Si. The sections below detail the theory of age hardening in the 6061 alloy.

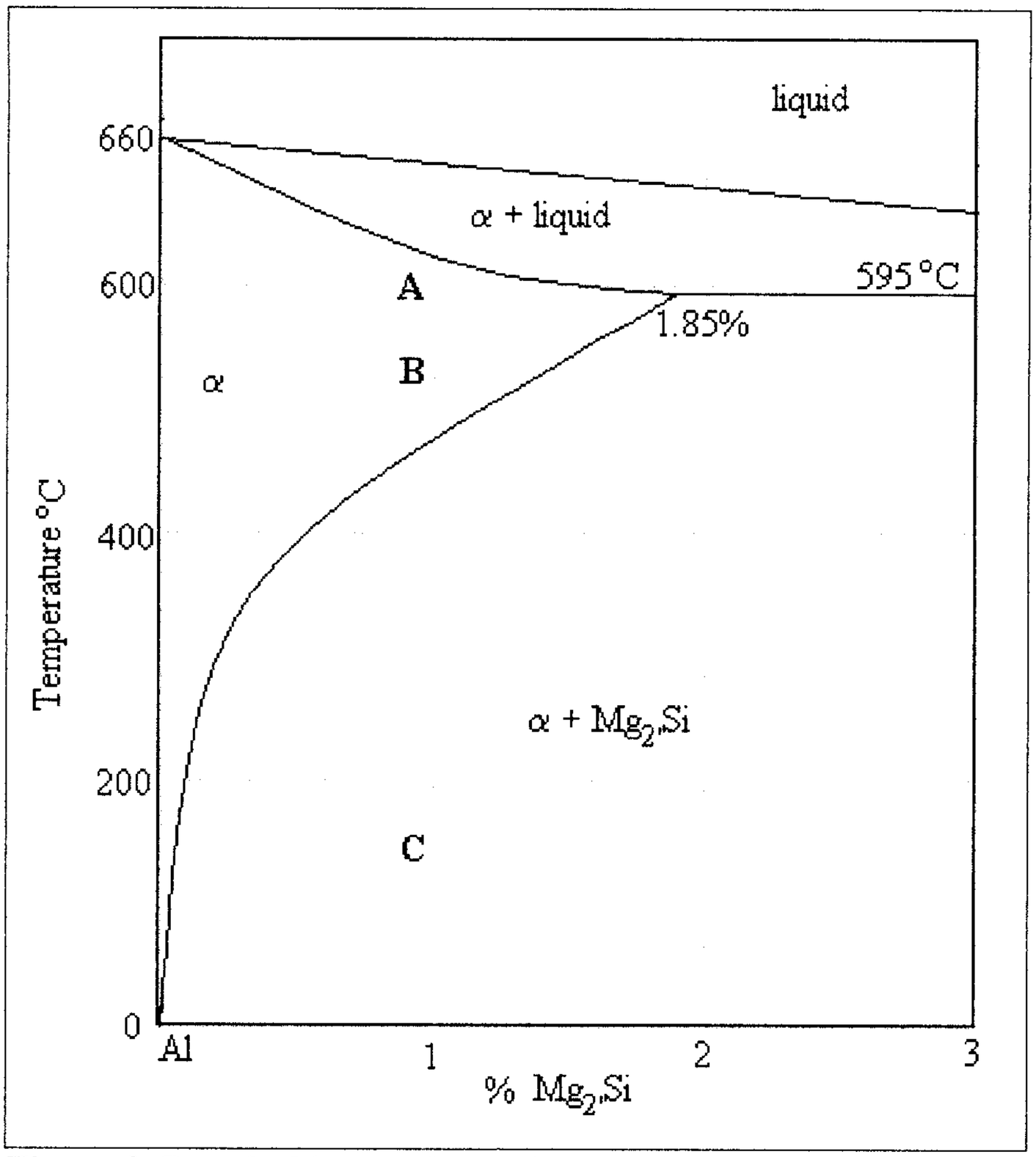

Figure 2. Pseudo-binary phase diagram for Al-Mg_2Si system [Polmear 1981]. (A) Sintering temperature 600°C, (B) Solutionizing temperature 530°C, (C) Precipitation temperature 175°C.

2.2.2.1.1 Solutionizing

The first heat treatment to the alloy is solutionizing. This treatment dissolves most of the solute to form a single-phase solid solution. The pseudo-binary phase diagram given in Figure 2 [Polmear 1981] shows that for an alloy containing ~0.8 wt% Mg_2Si, that heating the alloy to a temperature between ~500°C to ~600°C (position B on the phase diagram) all the Mg_2Si will be dissolved in the α phase region of the diagram. Enough time must be given at this temperature to ensure complete dissolution of these alloying elements. Rapid quenching in water at room temperature effectively freezes

the α phase and prevents any Mg_2Si formation. At room temperature the alloy is in a non-equilibrium state [Callister 1994] with a supersaturated α phase present.

2.2.2.1.2. Precipitation

The second heat treatment to the supersaturated alloy is precipitation or ageing. Precipitation may be accomplished by leaving the alloy at room temperature for many hours, days or weeks (natural ageing), or by artificial ageing whereby a higher temperature is applied to the alloy resulting in optimum precipitation in only a few hours. Natural ageing has the advantage of creating an alloy with a higher peak strength and no over ageing [Askeland 1998]. However, as allowing the alloy to age naturally takes a considerable amount of time, resulting in slow production times and higher costs, the accelerated ageing process is considered the most efficient and is described below.

The supersaturated α solid solution is heated to a temperature within the α + Mg_2Si phase region at which diffusion rates increase appreciably, point C in Figure 2. Mg_2Si begins to form as finely dispersed particles and these particles grow with time. There are four steps in a specific sequence for precipitate formation. (1) At the start of ageing the Mg_2Si begins to precipitate in small regions called Guinier-Preston zones (GP-I zones) [Askeland 1998, Callister 1994]. These GP-I zones are distributed throughout the α phase and are so small they are not considered as distinct precipitate particles [Callister 1994]. (2) As ageing continues more atoms diffuse to the GP-I zone and the precipitate thickens into thin discs, classified as GP-II zones. (3) As diffusion continues more Mg_2Si precipitate forms resulting in a greater degree of crystalline order and is classified as θ'. (4) The final stage is the formation of the

stable Mg_2Si precipitate, which is classified as θ. At the formation of θ precipitate the alloy is over aged.

The strengthening mechanism is the impediment of dislocations due to distortion of the crystal lattice around and within the precipitated particles. The distortion of the lattice is created by lattice mismatch strains for coherent particles [Calhoun 2000] within the lattice structure. Coherent particles are precipitates, which have a definite relationship with the surrounding crystal lattice. The structure of the precipitate must be related to, and even continuous with, the crystal structure of the surrounding matrix. This coherent relationship distorts the crystal lattice of the precipitate and the matrix which results in dislocation movement being impeded should the dislocation be near to the precipitate. Coherent precipitates exist during the formation of the stable θ precipitate. GP-I and GP-II are species which are coherent with the matrix, whilst θ' is semi-coherent. The stable θ is not coherent with the matrix and therefore does not have the distorting influence on the crystal structure that the pre-cursor species exhibit. The formation of θ phase results in larger precipitates with a reduction in strength and hardness of the alloy. The alloy is considered over aged when θ phase is present and heat treatment times must be carefully evaluated to produce the peak or optimum aged material.

Reinforcements have been shown to affect the precipitation behaviour in aluminium alloy based composites. Strangwood [1990, 1991] reported that solute super saturation (the driving force for nucleation) near to the interface may be due to segregation. Strangwood found solute enrichment at the interfaces of SiC reinforced aluminium alloys in which there was no interfacial reaction. Strangwood postulated that solute

enriched layers occur by non-equilibrium segregation due to the dragging of solute to interfacial regions by excess vacancies formed during quenching. Phases will nucleate preferentially at dislocations in order to relax their strain field with the matrix [Lorimer, 1981]. Within MMCs, the wide thermal property variation (e.g. the difference in coefficient of thermal expansion) between reinforcement and matrix can result in the increase in dislocation density in the matrix around the reinforcement. These dislocations form due to relaxation of thermal stresses during heat treatments [Prangnell, 2000]. Prangnell also states that the dislocations formed during quenching (quenching is part of the solutionising process) lower the quantity of *"quenched-in"* vacancies. The reduction in excess vacancies would contribute to the reduced growth of phases from solute clusters and GP zones. Interfacial reactions [Prangnell, 2000] may remove alloying constituents from the matrix resulting in a reduced driving force for precipitation due to a reduction in solute super saturation. This effect has been reported [Strangwood, 1991] in aluminium alloy 6061 reinforced with alumina. The magnesium from the matrix reacts with the reinforcement, resulting in magnesium depletion from the matrix and an increase in magnesium at the interface. Appendino [Appendino, 1991] states that artificial ageing is accelerated for the composite when compared to the monolithic alloy. This accelerated ageing is attributed to the high concentration of dislocations close to the alloy - matrix interface. Appendino also states that the dislocations only affect the artificial ageing and that natural ageing is dependent upon only the concentration of alloying elements in the supersaturated solid solution for the process's driving force.

In addition to thermal treatments, it is known that MMCs such as those based on 6061 can be pre-strained after solutionizing to encourage precipitation in the matrix but this additional variable was not investigated here.

2.2.3 Particulates as Reinforcing Phase in Composite Materials.

Particulates are chosen for the reinforcements as they give the composite isotropic properties, are not damaged during production and are commercially available at a lower cost than whiskers or fibres.

2.2.3.1 Alumina (Al_2O_3)

Commercial particulate alumina is primarily available as two structural types:

(1) α-Al_2O_3 has a rhombohedral crystal structure and displays good chemical inertness [Greenwood 1993]. The density of α-Al_2O_3 is 3.9 g cm^{-3} with a Vickers hardness of 1650 kgf mm^{-2} [Goodfellow 2000].

(2) γ-Al_2O_3 has a less compact cubic structure [Greenwood 1993] with a density of 3.4 g cm^{-3}. This type of alumina is called "activated alumina" which, when dehydrated, forms an open structured material.

The type of alumina chosen for investigation is the α type because of its chemical inertness, structural integrity, availability and cost (100g of 45μm powder costs £57.50 [Goodfellow 2000].

2.2.3.2 Silicon Carbide (SiC)

Silicon carbide is available in two principal forms, α-SiC and β-SiC. The α type has a hexagonal crystal structure and the β type has a cubic structure. The α-SiC is commercially available as black, dark green or purplish crystals. The colours are due to impurities such as iron being present [Greenwood 1993]. The α-type is the most stable of the two, displaying good chemical inertness, and is the most commercially available type of SiC. Therefore consideration will only be given to the α type. SiC has a density of 3.2 g cm^{-3} with a Vickers hardness of 2500 kgf mm^{-2}. The cost of SiC powder is £77.00 for 100g of 75μm sized powder [Goodfellow 2000]. The type of SiC powder chosen for investigation is α-SiC displaying a dark green colour.

2.2.4 Blending of Powder and Particulates.

The blending (or mixing) of the metal matrix powder and the ceramic reinforcement particulates is an important stage in the preparation of MMCs. Blending controls the distribution of the reinforcing particles and the green density of the pressed compacts, which, in turn, affects the mechanical properties of the MMC [Liu 1993].

Many variables have been identified in the powder mixing process [Hausner 1982], some which are listed below: -

1. Type of mixer
2. Volume of mixer
3. Geometry of mixer
4. Inner surface area of mixer
5. Constructional material of mixer
6. Surface finish of mixer
7. Volume of powder before mixing
8. Volume of powder after mixing
9. Volume ratio of component powders
10. Characteristics of powders

11. Rotational speed of mixer
12. Mixing time
13. Mixing temperature
14. Mixing medium (gas or liquid)
15. Humidity when mixing in air

There are various types of blenders available with the most common being the double cone mixer and the V-mixer [Upadhyaya 1997]. As the volumes of powder for this research are small and to reduce wastage a small-scale mixing technique is necessary. The method chosen to blend the powders is to use a planetary ball mill with air as the mixing medium and steel as the container material.

Prior to blending, the powders must be dried and de-agglomerated. The powder size, shape and density all have a part to play in the distribution of the powders. Generally, the larger the particles the better the distribution, larger particles rise to the top with the smaller particles concentrating at the bottom, spherical particles are more easily mixed than irregular shaped particles and heavier particles segregate on the top and lighter particles sink to the bottom [Liu 1993].

2.2.5 Compaction of Powder Blends.

Powder pressing to form a green billet can take many forms, some of which are listed below [Koerner 1978].

(a) single action unidirectional pressing
(b) double action unidirectional pressing
(c) isostatic pressing
(d) powder rolling
(e) stepwise pressing
(f) direct powder extrusion
(g) canned powder extrusion
(h) powder swageing
(i) explosive compacting
(j) powder forging

Cold pressing of the powders usually follows the blending stage. This cold compaction has four major functions [Upadhyaya 1997]: (1) To create the desired shape; (2) The control of dimensions; (3) Control of porosity; (4) To impart adequate strength for handling. Two common methods of cold compaction are single and double unidirectional pressing. Using unidirectional pressing to form compacts creates density gradients within the green billet. For example in a single action die compaction with an applied stress σ applied to the top of the powder results in only 0.25σ at the base during unlubricated pressing and 0.52σ at the base when using a die lubricant [Koerner 1978]. The density variations are increased when there is a large height to diameter (h/d) ratio [Smith 1983] and when single action pressing is used.

During compaction a lubricant is usually used, this may be mixed with the powder or applied to the walls of the die. The lubricant is necessary to reduce friction between the powder and the tooling surfaces, this permits higher effective pressures to be transmitted to the powder and thereby results in a higher green density being obtained. The pressure at which the powders are pressed has a large effect on the green density of the material. For aluminium and aluminium alloys relatively low pressures are needed to form a compact green billet as only small plastic deformation of the powder is necessary. Therefore any compacting pressure above the yield strength of the metal will form a coherent compact. Typical yield strengths [Matweb 2001] for aluminium and aluminium alloys in non-heat treated state are given in Table 6.

Table 6. Yield strengths for aluminium and two alloys in non heat-treated state [Matweb 2001].

Material	Yield Strength / MPa
AA6061-O	55
AA2014-O	95
AA1199-O (99.99% Al purity)	10

As compacting pressure is increased, so green density increases [Davis 1990] for aluminium alloys, see Table 7.

Table 7. Variation of density with compacting pressure for 601AB aluminium alloy (601AB alloy is similar to 6061 aluminium alloy [Davis 1990]).

Compacting Pressure / MPa	Green Density / % Theoretical
0	45
100	77
200	88
300	92
400	94
500	95

2.2.6 Sintering.

After the compaction stage the green billet is sintered to form a high density compact. Sintering is a high temperature (often solid state) process carried out at temperatures below the melting point or in the case of alloys below the solidus. Sintering is a diffusion process. The driving force is the reduction in surface area and hence reduction in surface energy which results in lower energy for the system. The powder particles coalesce which results in inter-particle pore shrinkage thereby increasing the density of the compact. Typical sintering temperatures for aluminium and aluminium alloys are 595 to 625°C [Davis 1990]. Sintering time and temperature have an effect on the strength (yield and tensile), elastic modulus and ductility of the material. These mechanical properties decrease with increasing porosity [Lawley 1978]. Increasing sintering temperature and sintering time results in an increase of sintered density [Upadhyaya 1997]. Therefore, generally, with increasing time and/or temperature the strength and ductility are increased as porosity is decreased. Aluminium sintering can be carried out in an inert atmosphere [Generous 1983] (e.g. nitrogen) or in vacuum. The method of sintering chosen for this work uses a vacuum furnace, as this is

potentially a more cost effective method with no gas to purchase, no controlled atmosphere to maintain and no separate de-gassing stage.

Theory of Sintering.

Sintering is the consolidation of small particles (powders) into a solid mass. The driving force for the consolidation is the excess surface free energy in the system [Upadhyaya 1997]. The consolidation of the particles is a diffusion process carried out at high temperature (the temperature being dependent on the material being sintered). The atoms within each particle diffuse to points of contact between powders [Askeland 1998].

The steps involved for the basic theory of sintering are described below [Askeland 1998], [Upadayaya 1997].

Step 1. The initial loose powder contact. The loose particles (powder) are brought intimately together, usually by pressing.

Step 2. The powder is brought to a specified elevated temperature, usually below the melting point of the major constituent.

Step 3. Diffusion of atoms is increased at the elevated temperature and a sinter bond forms between powder particles. This initial sinter bond where each bond is separate from the other, (i.e. there is no impinging between bonds) is termed the initial neck.

Step 4. The neck continues to crow, closing interconnecting pore channels.

Step 5. The pores become more rounded in shape.

Step 6. The continued consolidation results in a reduction of pore size.

Step 7. Continued consolidation gives further pore size reduction and leads to densification of the material.

Specific aluminium sintering complexities.

The sintering of aluminium has its own specific complexities. The formation of an oxide layer on the surface of aluminium particles creates a barrier between the aluminium particles and therefore aluminium is more difficult to sinter than materials, which have no inhibiting barrier coating [Okuma, 1987].

To facilitate sintering of aluminium and aluminium alloys the surface coating of the oxide layer must be disrupted to allow metal-to-metal contact. During the pressing stage the oxide layer can be broken to allow the aluminium metal of each particle to be in contact. Gutin [Gutin, 1972] states that in slightly oxidised aluminium powders, diffusion of aluminium atoms was found over the whole surface of the particles; however, in severely oxidised powders the diffusion was not uniform and took place only in regions free of oxide. During the initial pressing of the powders, Gutin found cracks to appear in the oxide and the particles seized together in areas containing low oxide formation.

The structure of the oxide layer alters at high temperature allowing aluminium metal to migrate through the oxide layer: Anan'in [Anan'in 1987] states *'Diffusive sintering of Al powder is preceded by the step of structural transformations occurring in the protective oxide film, the formation of through channels in it and thermal expansion-induced squeezing of the metal through the channels to the particle surfaces".*

Other researchers [Lumlev. 1999], [Kondoh, 2001] have reported the beneficial effect of magnesium during the sintering of aluminium. Lumley states that trace amounts of magnesium has been found to *"disrupt the passivating alumina layer through the formation of a spinel phase".* This disruption then allows solid slate sintering and the wetting of the aluminium metal. Kondoh states that the presence of magnesium has a *"de-oxidising effect".* This chemical change of the oxide was found to occur at temperatures above 397°C with holes observed in the oxide layer.

2.2.7 Summary

Considering all the points mentioned in this chapter, the following materials and methods were chosen to be investigated: -

- An age-hardenable aluminium alloy using aluminium 6061 as the principal alloy of investigation.
- Reinforcing the aluminium matrix with particulate ceramic material. α-Al_2O_3 and α-SiC being the materials chosen.
- To accomplish small scale powder blending using a rotational ball mill blender.
- Pressing of composites using cold uniaxial single and / or double compaction.
- Sintering of composites using a vacuum furnace method.

2.3 Wear

2.3.1. Introduction.

A definition of wear is: - *damage to a solid surface, generally involving progressive loss of material, due to relative motion between that surface and a contacting substance or substances* [ASTM 1999]. Wear occurs when material is removed or displaced from a solid surface. This can occur due to the mechanical or chemical action of a solid, liquid or gas, which is in contact with the material [Lansdown 1986 pp.21-22]. Engineering materials including Metal Matrix Composites can be subjected to surface interactions with other materials due to sliding motion. This motion may be intentional or unintentional. The motions of a piston against a cylinder liner or brake pad against a brake disc are cases of intentional motion. However the fretting wear of a joint is due to unintentional motion [Hutchings 2000]. When two solid surfaces move against each other frictional forces must be overcome to allow movement. Work must be done to overcome friction; therefore any reduction in friction will lead to greater efficiency (friction may be reduced by using a lubricant). However the reduction of friction is not always beneficial as in the case of brakes and clutches [Hutchings 1992]. A significant restriction in the use of aluminium alloys for weight saving applications has been their poor wear resistance, for example as engine blocks for internal combustion engines [Antoniou 1992]. Metal Matrix Composites are regarded as potential wear resistant materials because of the hard reinforcement (the reinforcement protecting the softer matrix) [Zhang 1996].

There are environmental and economic reasons for the development of wear resistant materials. In Table 8. the areas in which energy savings could be made from improved tribological management are given [Jost 1981].

Table 8.Methods by which savings of energy could be made through improved tribological practice in UK industry [Jost 1981].

Direct savings of energy:	
Primary:	saving of energy dissipated by friction
Secondary:	saving of energy needed to fabricate replacement parts
Tertiary:	saving of energy content of materials for replacement parts
Indirect savings of energy:	
savings consequential on direct savings, e.g. in investment in plant needed to compensate for frictional losses	

From Table 8, it is seen that energy wastage by friction only accounts for the primary energy saving. This energy saving may be accomplished by the use of improved lubrication. The secondary and tertiary energy savings would be accomplished by using wear resistant parts i.e. increase the time a part can be used in service.

Table 9. Methods by which financial savings could be made through improved tribological practices in UK industry. [UK Department of Education and Science 1966].

Reduction in energy consumption from lower friction	5%
Reduction in manpower	2%
Savings in lubricant costs	2%
Savings in maintenance and replacement costs	45%
Savings in losses resulting from breakdowns	22%
Savings in investment through greater availability and higher efficiency	4%
Savings in investment through increased life of plant	20%

Table 9 displays the potential financial savings, which could be made by improving the tribological practices in industry [UK Department of Education and Science 1966]. The percentages in Table 9. relate to a proportion of the annual savings, which is estimated at £515 million (as at 1965 values). From these potential savings (e.g. energy, raw materials, extended service life) it can be seen that the development and improvement of wear resistant materials would have a major economic impact on industry.

2.3.2 Theory of Sliding; Wear Archard Wear Equation [Archard 1953]

Sliding wear occurs when two solid surfaces slide over one another. There is therefore an interaction between the surfaces. The surfaces make contact at high points or asperities [Hutchings 1992], as any applied load is increased there is an increase in the number of asperitic contacts. The true area of contact, between surfaces, is then equal to the sum of the individual contacts between asperities. The contact area will be approximately proportional to the applied load. For metals any deformation of the asperities will be plastic. Assuming that the asperities are circular in their contact with each other (circular in plan view) with a radius of a, then at the maximum contact between two asperities the load, δW, supported will be given as

$$\delta W = P\pi a^2 \qquad \text{eqn. 4}$$

where P is the yield pressure for the plastically deforming asperity. P will have a value close to the materials indentation hardness H [Hutchings 1992]. As sliding continues the load supported by the asperity is gradually transferred to other asperity junctions, which form elsewhere across the surface. When the sliding is continuous there is the formation of and breaking of asperity junctions. Wear occurs when fragments (wear particles) of material are detached from the asperities. The volume of

the wear fragments depends on the size of the asperity junction from which the fragment was formed. An assumption is made that the volume of material removed is proportional to the cube of contact radius a. Therefore:

$$\delta V \propto a^3 \qquad \text{eqn. 5}$$

The volume of the displaced fragment is assumed to be that of a hemisphere with radius a. It is noted however that the shape of the fragment will not necessarily be hemispherical and the hemispherical shape is used to accommodate this model. This gives a displaced volume (volume of fragment) of:

$$\delta V = \frac{2\pi a^3}{3} \qquad \text{eqn. 6}$$

However not all asperity contacts will result in the formation of a fragment and a supposition of the proportion of fragments produced by asperity contact is made, this proportion is represented by κ. By including the proportion of fragments produced into equation 7 the average volume of material worn per unit sliding distance due to the sliding of one pair of asperities through a distance of the diameter of the circular contact area. The distance moved is therefore $2a$ and the average volume of material worn is represented by δQ, therefore the following can be deduced:

$$\delta Q = \frac{\kappa \delta V}{2a} = \frac{\kappa \pi a^2}{3} \qquad \text{eqn. 7}$$

The overall wear rate can be deduced by summation of all the asperity contacts over the entire real contact area. Representing the overall wear rate by Q equation 8 is deduced:

$$Q = \sum \delta Q = \frac{\kappa}{3} \sum \pi a^2 \qquad \text{eqn. 8}$$

By summation of equation 4 the overall normal load W can be deduced:

$$W = \sum \delta W = P \sum \pi a^2 \qquad \text{eqn. 9}$$

Combining equations 8 and 9 results in:

$$Q = \frac{\kappa W}{3P} \qquad \text{eqn. 10}$$

By combining the term κ with the $\frac{1}{3}$ term a more compact constant of proportionality is formed and called K. As P is approximate in value to the indentation hardness, assume $P=H$ the wear equation can be re-written as:

$$Q = \frac{KW}{H} \qquad \text{eqn. 11}$$

Archard's equation (eqn. 11) therefore relates the volume worn per unit sliding distance, Q, to the applied load, W, and the hardness of the softer surface, H. K is termed the coefficient of wear, is dimensionless and is less than 1. This is a simple equation for evaluating wear and can only be used in systems in which the asperities can be plastically deformed and the materials hardness can be evaluated

2.3.3 Types of Wear.

The type of wear which engineering materials may encounter can be categorised into four [Rabinowicz 1965] main forms; sliding, fretting, erosion and cavitation. The research investigates sliding wear, therefore only a brief explanation of the latter three types of wear will be given, with a more detailed description of sliding wear given below.

(1) Sliding wear occurs when two solid surfaces are moved over each other. The surfaces may be lubricated. There are four main types of lubrication [Hutchings 1992]:

(a) Hydrodynamic lubrication is where the surfaces are separated by a fluid film. The fluid film may be oil, grease, water, air or other liquids or gases. This film is usually thick compared to asperity height.

(b) Elasto-hydrodynamic lubrication is where the pressure between surfaces is very high resulting in a thin film of lubricant separating the surfaces. The lubricant is usually an oil or grease.

(c) Boundary lubrication occurs when surfaces are separated by an adsorbed film. Repulsive forces between the adsorbed films prevent or limit asperity contact. The lubricant may be an adsorbed carboxylic acid, which has polar end groups which results in like polar groups repelling each other.

(d) Solid lubrication is a method by which a solid interfacial film of low shear strength separates the sliding surfaces. Common solid lubricants are graphite, molybdenum disulphide and polytetrafluoroethylene (PTFE).

When a lubricant is present wear is classified as lubricated sliding wear and when no lubricant is present wear is classified as dry sliding wear.

Sliding wear can be further sub-divided into four further wear regimes [Rabinowicz 1965]:

(i) Adhesive wear. When two surfaces are slid over each other fragments from one surface adheres to the other and is pulled from its original position. This type of wear occurs when the atoms on two surfaces come into intimate contact and a strong adhesive bond is formed. During the sliding process there is a probability that when

the contact between two adhering asperities is broken the fracture will not occur at the original interface resulting in a transfer of material from one surface to another.

(ii) Abrasive wear. This type of wear can again be sub-divided into two categories - two-body abrasion and three-body abrasion, see Figure 3. [Hutchings 1992]:

(*a*) Two-body abrasion is caused by hard protrusions from one of the surfaces or a rough hard surface sliding over a softer surface. The harder material ploughs grooves into the softer surface.

(*b*) Three-body abrasion occurs when hard particles are free to move between two sliding bodies resulting in removal of material from the surfaces.

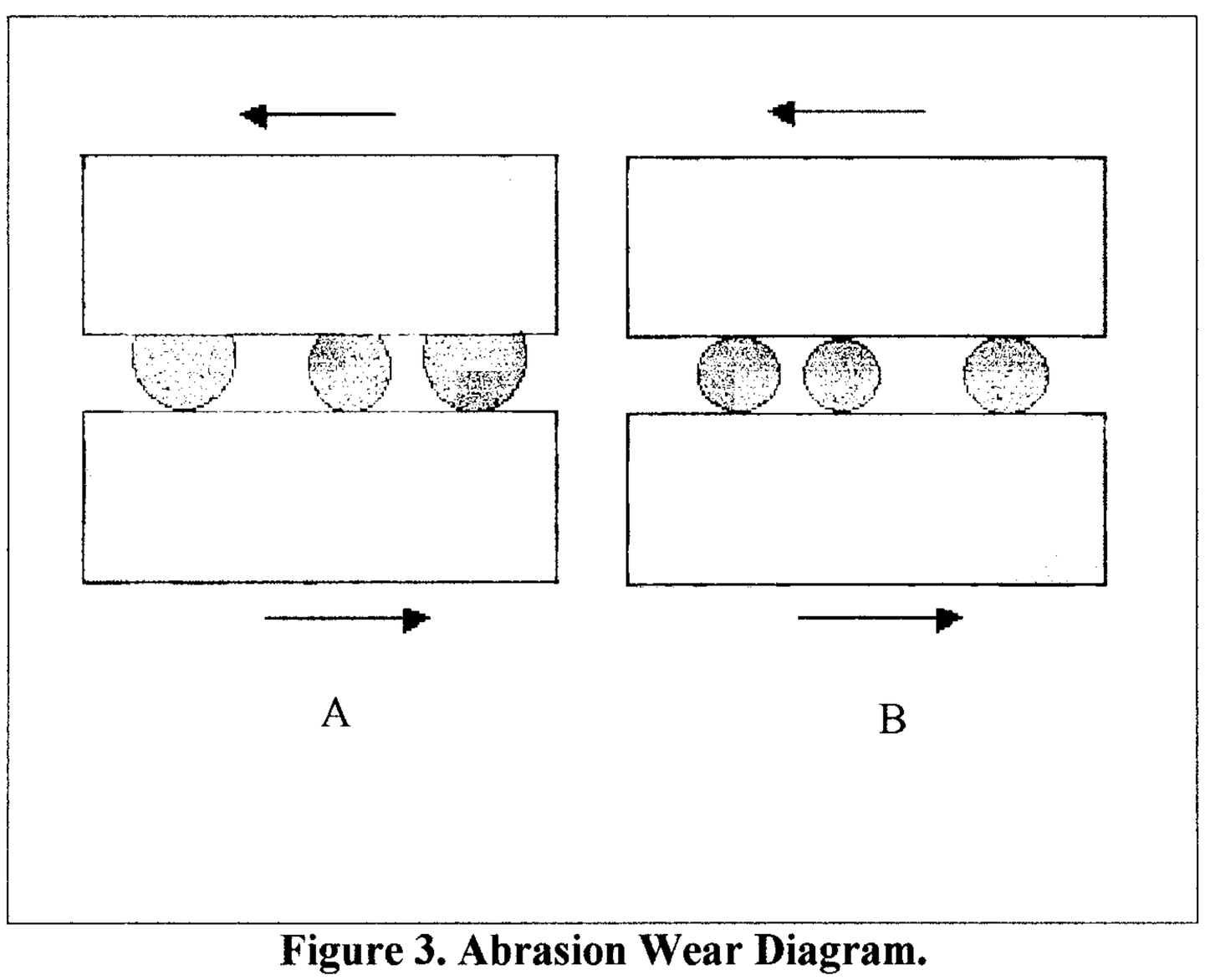

Figure 3. Abrasion Wear Diagram.
(A) Two-body abrasion (B) Three-body abrasion

(iii) Corrosive wear occurs when two surfaces are slid over each other in a corrosive environment. When the surfaces are at rest (no sliding is taking place) then the act of corroding would form a film on the surfaces, either slowing the rate of corrosion or preventing any further corrosion from taking place. However when the surfaces are

sliding the film of corrosion is worn away revealing un-corroded material and allowing the corrosion to continue. The formation of loose hard oxide particles would now also enter the wear regime.

(iv) Surface fatigue occurs when there is repeated sliding or rolling of one surface over another. The continual cyclical loading and unloading of the materials may create surface or sub-surface cracks. The formation of these cracks leads to the destruction of the surface with the forming of large fragments resulting in deep pits in the surface.

(2) Fretting is a form of wear which arises when two surfaces in contact with each other *undergo oscillatory tangential displacement of small amplitude* [Rabinowicz 1965]. An example given by Rabinowicz is the steel teeth in a splined out-of-line shaft coupling which have a small to and fro movement tangentially to, and for every revolution of, the shaft. This movement results in adhesion between steel particles which then oxidise producing iron oxide, which is abrasive. The type of wear seen in fretting is not simplistic but involves three wear types; adhesive, corrosive and abrasive.

(3) Erosion can occur to due the interaction of liquid jets or drops on to a solid surface [Hutchings 1992], however erosion of engineering materials is accelerated when hard particles are carried in a moving fluid i.e. a gas stream or flowing liquid. This type of hard particle wear is distinguished from fluid erosion by qualifying it as solid particle erosion or solid impingement erosion [Hutchings 1992]. The impingement of hard particles on to a solid surface causes damage closely analogous to abrasion [Rabinowicz 1965]. Solid particle erosion differs from abrasion in that the impinging particle may remove material from a low point on the solid surface which

may increase the surface roughness (e.g. sand blasting) [Rabinowicz 1965] compared to abrasion (e.g. surface polishing) which may reduce the surface roughness.

(4) Cavitation is a process in which a liquid may boil due to applied stresses forming a bubble in the liquid. The bubble may collapse suddenly producing a shock-wave through the liquid, any solid surface close to the collapsing bubble could be damaged due to the shock and thereby lead to the removal of a particle from the solid surface [Rabinowicz 1965]. Cavitation is similar in process to surface fatigue wear.

2.3.4 Wear Mechanisms in MMC's.

Wear of particle-reinforced composites is complex with four possible mechanisms involved [Antoniou 1992].

(1) Particle protection of the matrix. During a running in period the matrix will wear leaving the reinforcing particles protruding from the matrix surface. These protuberances will protect the matrix from further wear.

(2) Particle pull-out. The particles are pulled out of the matrix due to de-bonding (possible poor interfacial bond) causing the matrix to come into contact with the sliding material and if the particles are between the composite and the sliding material abrasive wear can occur.

(3) Particle fracture. The reinforcing particles are fractured during wear causing compaction of small reinforcing fragments in the surface of the composite. Wear is now dependent on the fragmented surface layer.

(4) Delamination. This occurs due to fatigue causing fracture along particle-matrix interfaces, which generate debris between the contact surfaces, see Figure 4.

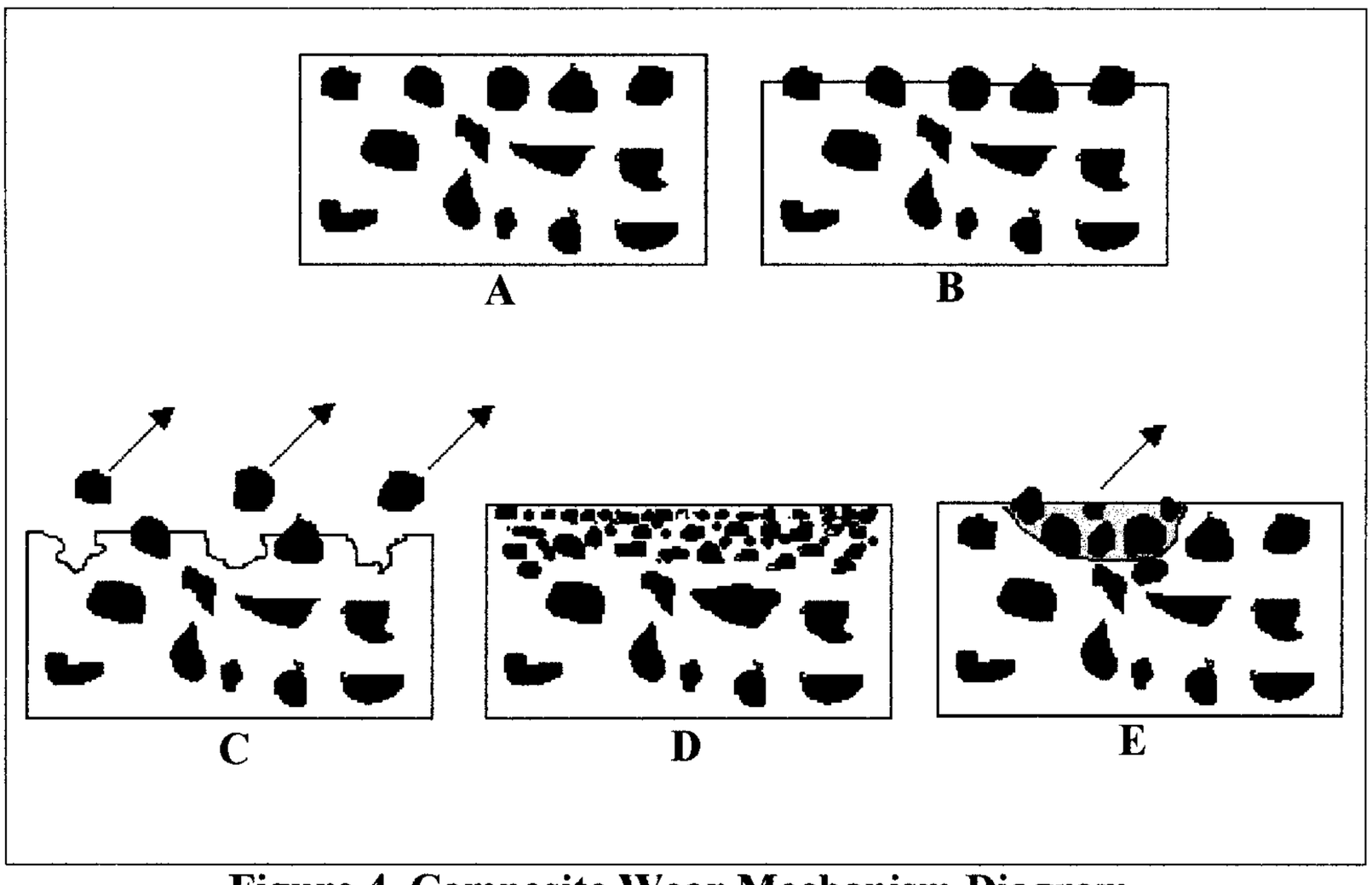

Figure 4. Composite Wear Mechanism Diagram.
(A) Composite prior to wearing. (B) Composite after run-in period with particles protecting matrix. (C) De-bonding of particles. (D) Fracture/compaction of particles. (E) Delamination caused by fatigue.

In particulate reinforced composites particulate size and volume fraction are found to influence the wear rate of the composites. Chung [Chung 1994] investigated the wear of aluminium with SiC particles and states that for a fixed size of SiC particle, the resistance to wear improved with increasing SiC content and for a fixed content of SiC particles composites containing coarser particles are more wear resistant than composites containing fine particles. Chung also states that the main mechanism of wear is the detachment of aluminium layers with SiC particles buried away from the surface; Chung reported no evidence of pull-out or brittle fracture of the SiC particles. Chung's research findings are in contrast to the results published by Zhang [Zhang 1996]. Zhang reports that composite wear increases with SiC particle size and decreases with particle volume fraction. Both results were obtained using a pin on disc method of wear testing; however, Chung used identical materials for both pin and disc while Zhang used a steel disc and composite pins. Their results give an indication

that wear performance cannot be easily classified and that the whole wear test regime must be considered. Alahelisten states that the tribological behaviour of a composite depends on the micro structural properties of the material and type of loading-contact situation (the tribo-system) [Alahelisten 1993].

Narayan reports that the heat treatments of aluminium alloys containing particulate reinforcement may also affect the wear properties of a composite [Narayan 1995]. Narayan reports that the Al 2024-15vol%Al_2O_3 composite displays better seizure resistance than the monolithic alloy in the peak aged condition and that in the as extruded condition, the wear resistance of the monolithic alloy is better than that of the composite. Recent research by Hong using an Al-Mg-Si matrix with 10 vol% Al_2O_3 particulate reinforcement [Hong 1999] states that the peak-aged composite is more wear resistant than the under-aged composite.

A report by Li states that wear resistance of as-cast Al-Si/SiC_p composites can be slightly increased by a T6 heat treatment although the increase in wear resistance is not significant when compared to the increase in hardness due to the heat treatment [Li 1997]. Inference from these results is that in age hardenable aluminium alloy based composites, the peak aged state is the preferred state for wear resistance. Research by Gurcan revealed that aluminium 6061 reinforced with 20 vol% Saffil (short fibre 10μm in length Al_2O_3) had an inferior wear resistance when compared to aluminium 6061 reinforced with 20 vol% SiC particles (7μm diameter) in pin on disc tests against SiC grit and steel counterfaces [Gurcan 1995]. However research by Baptista reports that alumina reinforced AA6061 composites show less wear loss than SiC containing composites in block on steel ring lubricated wear tests [Baptista 1993].

From the previous results quoted above it is shown that there is no definitive way to predict wear performance and that many results are contradictory. At present the only effective way of identifying and classifying wear is by practical testing and examination.

2.3.5 Wear Measurement and Testing.

The parameters to be considered when wear testing are many [Lansdown 1986 pp.111-117] with the six principal factors being: (1) the materials mechanical properties e.g. hardness, strength and ductility. (2) The materials surface finish e.g. two highly polished surfaces would be expected to initially wear less than two rough surfaces. (3) The operating temperature, as temperature alters the mechanical properties of the materials. (4) Atmospheric conditions, high humidity can lead to corrosion, which will affect the wear properties. (5) The velocity at which the surfaces are moved against each other, with higher speeds causing greater temperatures to be generated and higher surface areas worn for a given timescale. (6) The loading applied to the wear surfaces, higher applied pressures usually (velocity dependent) cause higher wear rates.

There are various methods of measuring wear using test rigs. These test rigs are briefly described below as given in the 1996 Donald Julius Groen Prize Lecture [Alliston-Grenier 1996].

Group 1 machines. These machines have a stationary point of contact with respect to one of the wearing specimens and are subject to constant speed unidirectional sliding, see Figure 5 below. The test specimen is subjected to continuous rubbing and the contact temperature is self-regulating and cannot be controlled.

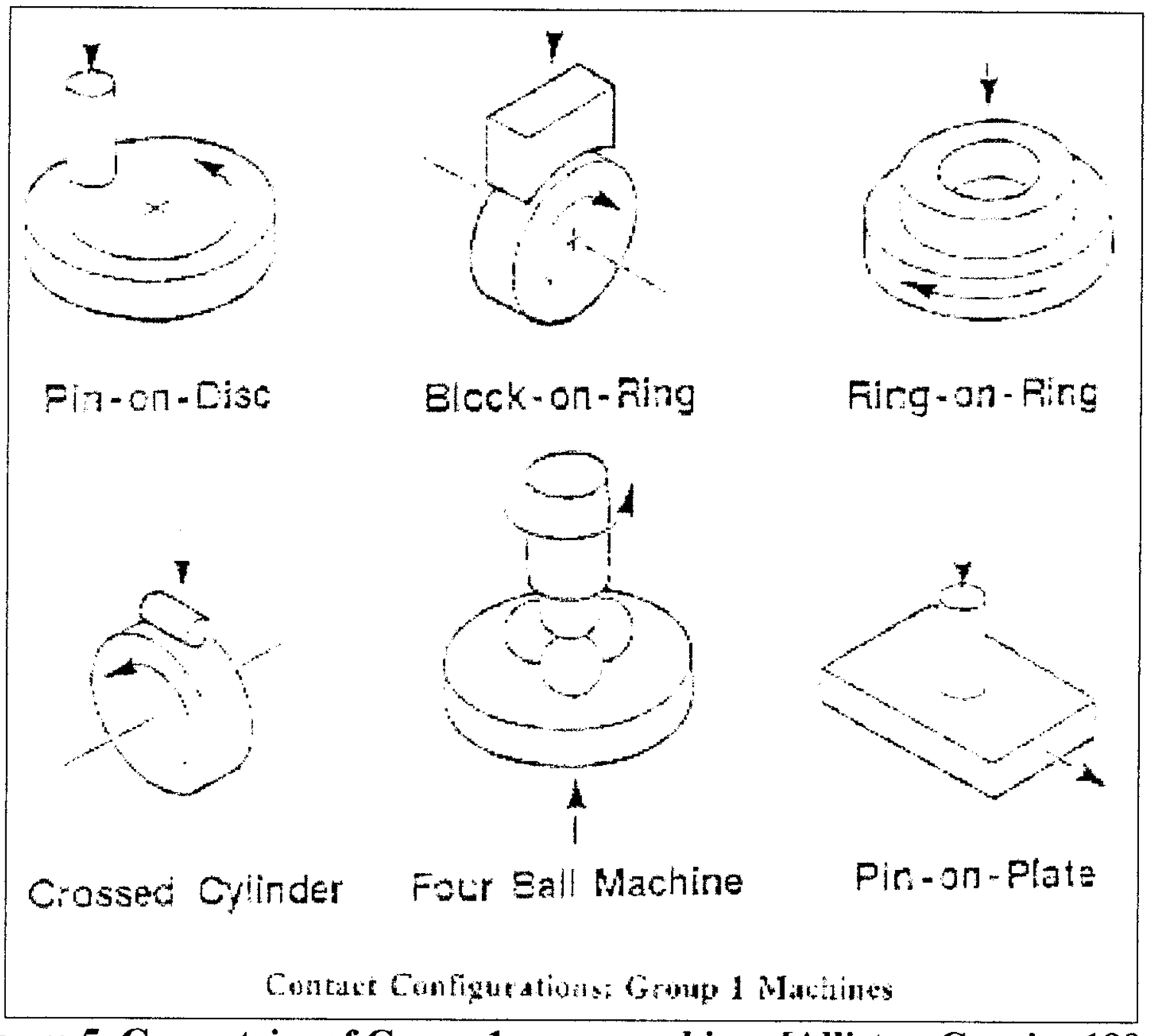

Figure 5. Geometries of Group 1 wear machines [Alliston-Grenier 1996].

Group 2 machines. These machines have the point of contact moving over both surfaces. These include using idealised or standardised components such as gears, cam/follower and other slide/roll devices. These machines are very similar to machinery found in actual situations and are essentially full scale test rigs. Again the contact temperature cannot be regulated with the temperature being self-regulating.

Group 3 machines. These machines operate at low sliding velocities to minimise frictional heating and are short stroke reciprocating rigs. Compared to Group 2

machines these test rigs do not attempt to be the same as the real contact under investigation. They try to simulate the intimate contact between surfaces in a controllable and accessible manner and come closest to achieving the requirements of an effective bench test. Some examples of group 3 test geometries are shown in Figure 6 below.

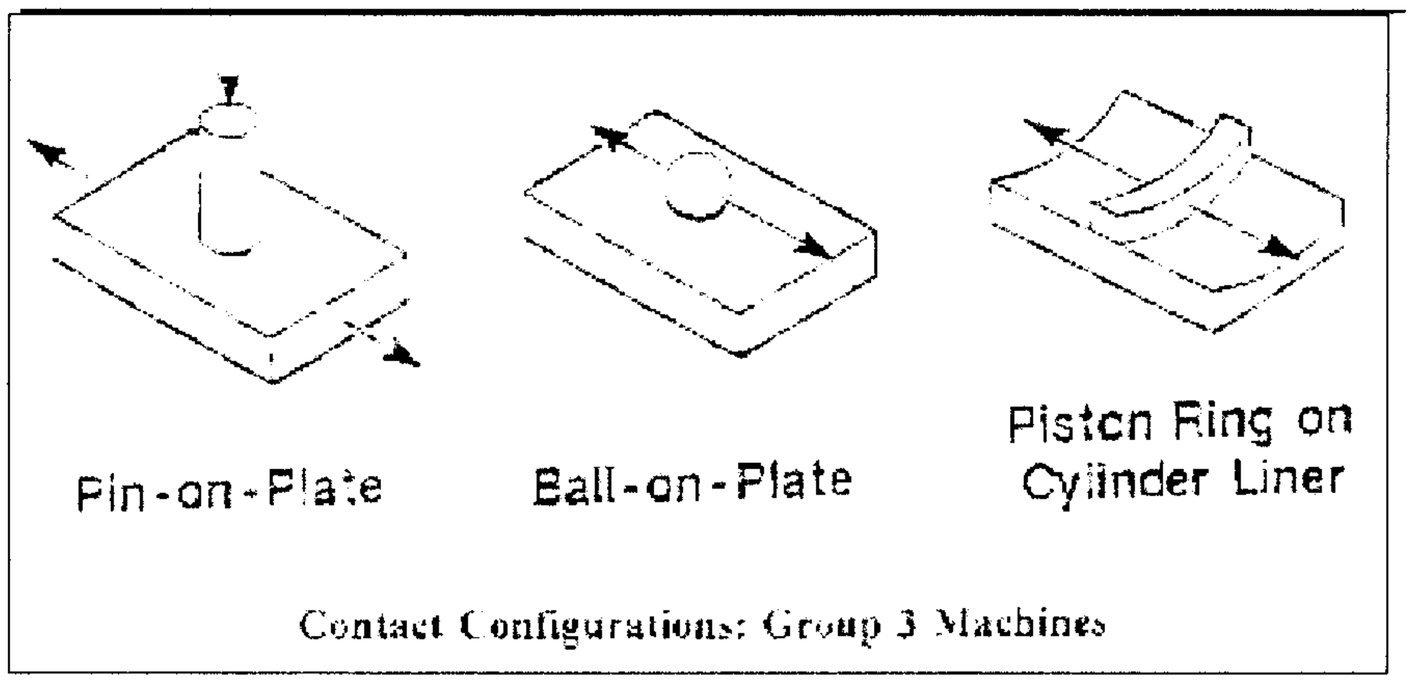

Figure 6. Geometries of Group 3 wear machines.

2.3.6 Summary of Section 2.3

Wear of materials is a phenomenon, which cannot easily be predicted. Test methods vary and wear regimes are dependent on many variables. Any wear analysis, if comparison between different materials wear performance is to be carried out, must be done under constant, reproducible test conditions. It is also obvious by comparing other research that a material cannot simply be said to be wear resistant. The production method, the tribo-system and other variables (e.g. humidity, ambient temperature) all must be taken into account and the only declaration that can be made is that a given material displays good or poor wear resistance for that given set of circumstances.

2.4 Matrix - Reinforcement Interfaces

2.4.1 Introduction

The interface between the reinforcement and the matrix is important [Harris 1999; Foo 1994; Arsenault 1995] to the final properties of the composite as through the interface load transference occurs. The fundamental role of the interface is to transfer load (restrain movement of the matrix phase in the vicinity of the reinforcement [Callister 1974]) between the matrix and the reinforcement and the interface must retain structural integrity for all types of loading and for the life of the composite [Metcalfe 1974 pp.1-30]. Metcalfe proposed a classification scheme for the different types of matrix-reinforcement interface behaviour. Three classes are suggested and given below: -

Class I, reinforcement and matrix mutually nonreactive and insoluble.

Class II, reinforcement and matrix mutually nonreactive but soluble.

Class III, reinforcement and matrix react to form compound(s) at interface.

Metcalfe also refers to a pseudo-Class I interfacial behaviour. This class of composite appears free from any interfacial reaction however the thermodynamic data suggest that a reaction should take place. Aluminium-stainless steel is given as an example. When the fabrication route is solid state then no reaction is seen; however, if the aluminium is melted then aluminium-iron compounds are observed at the interface. When the solid-state processed aluminium-stainless steel composite is subjected to additional processing, e.g. cold rolling and annealing, aluminium iron compounds are found at the interface. The initial non-reactivity of aluminium-stainless steel is explained by the preservation of an oxide layer (Al_2O_3) between the reinforcement

and matrix. Any breakdown of this oxide layer, by melting or further processing, results in reaction between the matrix and reinforcement.

The types of bonds between matrix and reinforcement have been classified into six distinct types [Metcalfe 1974 pp. 65-123]. The types of interfacial interaction according to Metcalfe are given and discussed below: -

(1) Mechanical bonding. For a purely mechanical bond to exist there must be no sources of chemical bond available. This of course is impossible as there is always some form of chemical reaction, for example there is always the weak attraction of Van der Waals forces in all materials. As Metcalfe states: *a better definition of the mechanical bond would be one where the mechanical interactions predominate*. The effects of mechanical bonding were investigated by Hill [Hill 1969]. Hill used aluminium reinforced with tungsten wires to measure the effect of mechanical interlocking on the strength of the composite. The experimentation used tungsten wires of length 0.1in with a diameter of 0.008in. A proportion of the wires were etched to produce a reduced diameter of 0.0065in. Composites were fabricated containing: (a) smooth 0.008in tungsten wires; (b) smooth 0.008in tungsten wires which were coated with graphite; (c) etched 0.0065in tungsten wires coated with graphite. The composite consists of 12% tungsten wire in an aluminium matrix, produced by vacuum infiltration of molten aluminium. Aluminium and tungsten react at temperatures > 450°C to form the intermetallic WAl_{12} [Tsukada 1995]. The graphite coating was used to prevent the reaction between Al and W occurring. Hills results compared the measured strength of the composites to the theoretical strength, and the results achieved were: -

(a) Smooth tungsten wires	95% theoretical strength
(b) Smooth tungsten wires coated with graphite	35% theoretical strength
(c) Etched tungsten wires coated with graphite	91% theoretical strength

In (a), the intermetallic (WAl_{12}) formed resulted in a chemical bond with a strength approaching theoretical. In (b) the Al-W reaction was prevented; there was no strong chemical bond and poor mechanical interaction between matrix and reinforcement resulted. In (c) there was no strong chemical bond (the graphite prevented any strong chemical Al-W interaction) and there was strong mechanical interlocking (due to the etch causing roughening of the W surface), which resulted in the strength approaching the value obtained for (a) the strong chemical bond.

These findings illustrate the possible value of mechanical bonding and the possible deleterious effect coating of reinforcements may have. Other research has shown that Al and C (graphite) react via dissolution, resulting in the formation of a phase change at the interface with the reactant product Al_4C_3 produced [Eremenko 1974; Maruyama 1986; Lu 2000], with Al_4C_3 production being time and temperature dependent.

(2) Dissolution (including wetting) bonding. In liquid (molten matrix) production methods of composites, the liquid-solid contact angle must be less than 90° for wetting to occur. This contact angle limit allows the adherence of liquid on to the solid surface [Sears 1987]. Metcalfe assumes that some dissolution (irrespective of amount) occurs when wetting takes place. Therefore to achieve wetting, and thereby dissolution bonding, the removal of adsorbed gases and contaminants from the surface must be accomplished to allow element-to-element contact. An example given by

Metcalfe is the non-wetting of graphite by liquid aluminium until the graphite has been pre-treated to remove contaminants from the surface [Pepper 1970].

(3) Reaction bonding. This type of bonding relates to the reaction between matrix and reinforcement resulting in the production of a new chemical species (a *class III* type interface). The reaction between constituents involves transfer of atoms, from one or more of the constituents, to the reaction site, with the transfer process controlled by diffusion. When a new compound is formed at the interface it results generally in a degradation of properties of the composite. The general argument presented by Metcalfe is that the strength of the reaction compound will be lower than the strength of the reinforcement, and when the reaction compound is brittle, its strain to fracture will be lower than that of the reinforcement. However when the reaction at the interface results in the formation of a solid solution there may be enough ductility within the interfacial species, so that failure will initiate through the more brittle reinforcement. Ochiai [Ochiai 1994] stated evidence to support that excessive and minimal interfacial reactions are detrimental to the strength of metal matrix composites. Ochiai studied the strength of boron fibre-aluminium matrix composites for various processing times and temperatures. He showed that at low processing temperatures with a short pressing time, the composite strength was low with extensive fibre pull out. In these processing conditions there was little interfacial reaction. When the processing temperature was high with a moderate pressing time, a slight interfacial reaction was observed resulting in a moderately strong interface and a high composite strength. The interfacial reaction resulted in AlB_2 formation. Ochiai found that there was an optimum processing condition and when these conditions were exceeded, an excessive reaction occurred at the interface resulting in a reduction

in strength below that obtained for a weak interfacial bond. It was concluded that it was desirable to have an interfacial reaction, but the reaction layer should be thin to achieve optimum composite properties.

(4) Exchange reaction bonding. This is a type of reaction bond in which there may be two or more reactions occurring. An example given by Metcalfe is the reaction between aluminium-titanium solid solution and boron. This is described as being a two-step reaction.

$$Ti(Al)_{ss} + B \rightarrow (Ti, Al)B_2 \qquad \text{eqn. 12}$$

$$Ti + (Ti, Al)B_2 \rightarrow TiB_2 + Ti(Al)_{ss} \qquad \text{eqn. 13}$$

This exchange reaction causes a change in the composition of the matrix adjacent to the reinforcement. The matrix becomes deficient in the element, which is involved, in the interfacial reaction and rich in the element(s), which take no part in the reaction. The reaction rate is then controlled by the rate of diffusion at which the element(s), which take no part in the reaction, can be diffused away. Blackburn [Blackburn 1966] found that in the system Ti-8Al-1Mo-1V / B, aluminium was rejected from the TiB_2 phase and aluminium accumulated in the matrix ahead of the growing TiB_2. Metcalfe also stated that there will be an improvement in interface stability due to the overall reduction in reaction rate during exchange reactions.

(5) Oxide bonds. This type of bond includes composites where an oxide is used as a reinforcement and/or there are oxide films present. Metcalfe quotes the work by Sutton and Feingold [Sutton 1966] as an example of oxide / matrix interaction. A

model proposed by Sutton and Feingold relates the interaction between sapphire and nickel. The observed bond strength has little variation as the interface thickness increases from 100 to 5000 nm. This suggests that to achieve a good interfacial bond a small amount of reaction is required. Moore [Moore 1969] has shown that the formation of the spinel $NiAl_2O_4$ in a nickel / alumina system only occurs when there is access to oxygen.

(6) Mixed bonding. This bond occurs in pseudo-Class I systems when there is a breakdown from a Class I to either a Class II or Class III system. Metcalfe gives an example described by Klein and Metcalfe [Klein 1971]. In the study by Klein, boron fibres were in an aluminium matrix. An aluminium oxide film was identified at the interface and breakdown of the interface occurred with the formation of AlB_2. Diffraction patterns obtained from the reaction and interface zones showed AlB_2, Al and Al_2O_3 to be present. The absence of any boron oxides being present was explained by the reduction of any boron oxides by aluminium to form alumina.

2.4.2 Aluminium Alloy - Ceramic Interface.

This section examines the reported interfacial reactions / phenomena which occur or may occur at aluminium 6061 alloy interfaces with silicon carbide and alumina. Reactions of aluminium 6061 with silicon carbide and alumina are specifically examined as these are the chosen matrix and reinforcement targeted for investigation in this thesis.

2.4.2.1 AA6061 - Silicon Carbide (SiC) Interface.

Zhao [Zhao 1993] investigated the reaction and the reaction kinetics between silicon carbide and aluminium. Aluminium was deposited on to silicon carbide using a physical vapour deposition technique to form reaction couples. The investigation was carried out at temperatures ranging from 570 - 900°C with times ranging from 20 - 3000 seconds. The experiments were carried out in a non-reactive noble gas, argon, atmosphere. Zhao stated that investigations by X-ray diffraction analysis produced results, which identified aluminium carbide (Al_4C_3) and alumina (α-Al_2O_3) as an interfacial product when the Al - SiC couple is heated at or below 750°C. The quantity of reaction products increased with raising the temperature and / or increasing the reaction times. Zhao also identified that the reaction products nucleated at local sites, grew gradually and did not form an interface with uniform thickness. It is noted that Zhao stated the interfacial products had been identified at or below 750°C, thereby inferring that Al_4C_3 and α-Al_2O_3 reaction products had been found at experimental temperatures of between 570 and 750°C. Zhao also stated that the SiC / Al system is consistent with the characteristic of a pseudo-class I composite system.

Suery [Suery 1993] detailed reactions, which can occur in aluminium based composites reinforced with ceramic particles. He stated that silicon carbide is prone to attack by molten aluminium and reacts according to the following equation:-

$$4\ Al + 3\ SiC \rightarrow Al_4C_3 + 3\ Si \qquad \text{eqn. 14}$$

This reaction equation shows that aluminium carbide is formed with the formation of silicon, which is rejected into the aluminium matrix. This reaction leads to a degradation of the composite as the Al_4C_3 is a brittle intermetallic and the formation of Al_4C_3 leads to degradation of the SiC reinforcement. Suery also stated that the

formation of Al_4C_3 occurs at temperatures above 650°C (i.e. the aluminium alloy is in the molten state), which is contradictory to the results published by Zhao who inferred that Al_4C_3 was found in the temperature range 570 - 750°C. Suery stated that when an alloy of aluminium contains magnesium, the free silicon can react with Mg to form the hardening phase Mg_2Si. This alteration in the Si content will affect the age hardening behaviour and characteristics of the alloy matrix. The rejection of Si from the reinforcement has been found to increase the hardness of the matrix when SiC particles are in an aluminium-1%magnesium matrix. Suery showed that hardness increased with increasing re-melt times. For example, Figure 7 displays the increase in hardness when the fabricated composite is re-melted for various times at 800°C.

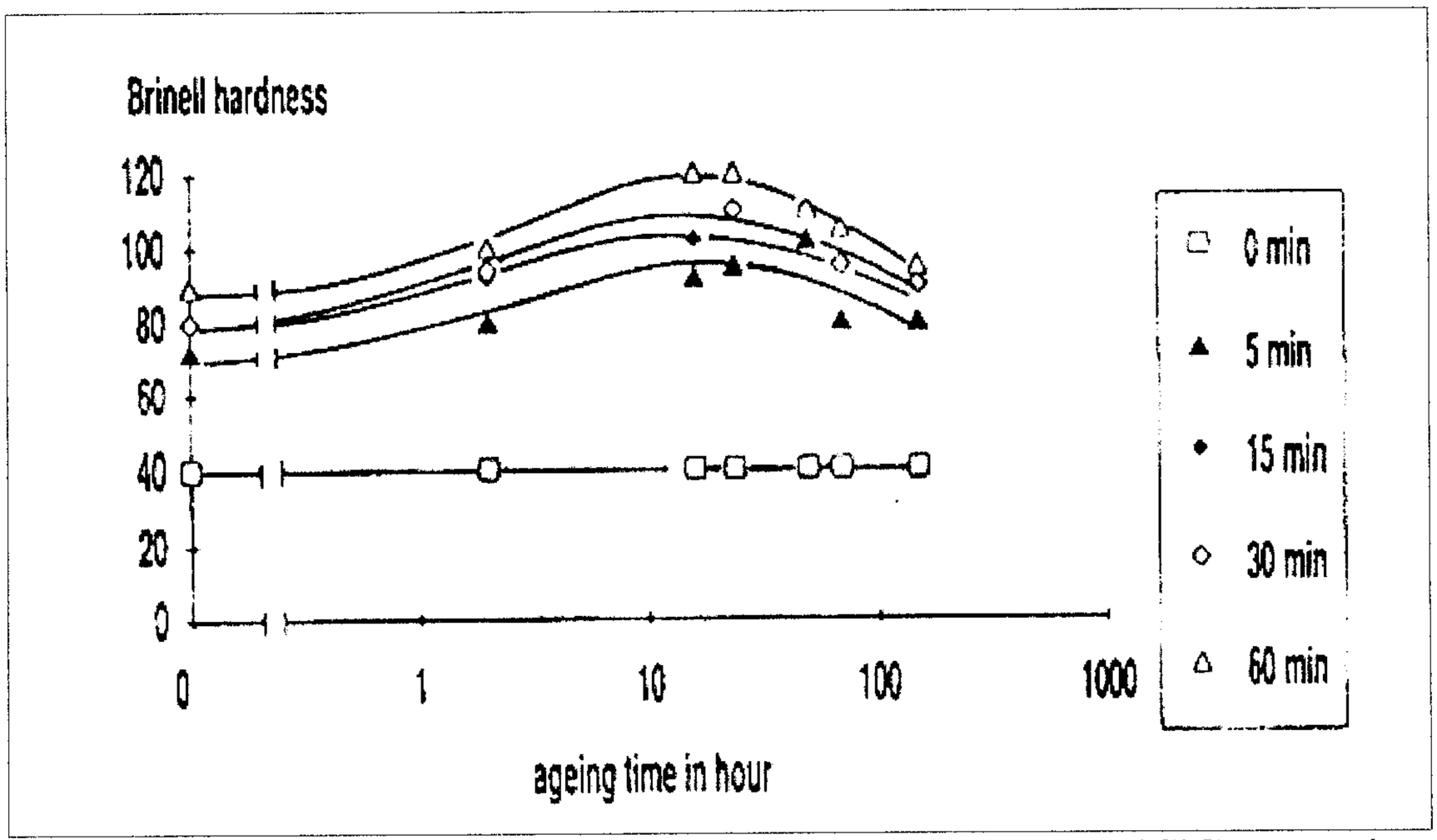

Figure 7. Brinell hardness versus ageing time for Al-1%Mg / SiC composites with as-received particles re-melted for various times at 800°C [Suery 1993].

Foo [Foo 1994] investigated interfacial phenomenon observed between silicon carbide particulates and aluminium 6061 alloy matrix. The production route for the composites involved a powder metallurgy, liquid phase sintering process. Foo's experimental processing procedure unfortunately gives no indication of the

temperature or time involved for sintering. The production process did not involve any heat treatments - no solutionizing or ageing - to the sintered composites. Foo identified facets that had developed on the SiC to produce a mechanically interlocking interface resulting in a strong bond. This faceting has also been reported by Janowski [Janowski 1990] and is attributed to the preferential attack of liquid aluminium on the SiC particulates. Examination of reaction products, by Foo, at the interface gave no indication of Al_4C_3 particles forming, but other intermetallics, Mg_2Si and $FeSiAl_5$, were found in the interface region. These interfacial reaction products were demonstrated by Foo as being deleterious to the composite strength as they could act as crack initiation sites. This phenomenon was observed by Foo as de-cohesion at the matrix - reinforcement interface.

It is reported by Appendino [Appendino 1991] that at the interface between SiC particulates and aluminium 6061 alloy there is a high density of dislocations present which affects the heat treatments when comparing composite with monolithic alloy. Appendino stated that the achievement of the solutionized state is more difficult in the composite than in the monolithic alloy, suggesting a temperature of 557°C for two hours to achieve complete dissolution. However, the artificial ageing of the composite is recorded as accelerated for the composite when compared to the monolithic alloy for peak hardness. Appendino commented that the areas of high dislocation density resulted in zones of high deformation, which acted as nucleation sites for precipitation growth and accelerated the formation of the Mg_2Si precipitate. The monolithic alloy showed a broad hardness peak occurring between 4 - 10 hours ageing, with the composite showing a sharp hardness peak at 4 hours ageing.

Teng [Teng, 1994] agreed with Suery and stated that in a composite comprising 99%

pure aluminium reinforced with SiC particulates, produced at 700^0C, $A1_4C_3$ and Si were observed in the interface region.

From these papers it can be stated that the production of aluminium 6061 - SiC particulate composites at a temperature around 600^0C should produce a strong material with good interfacial properties. However the increase in dislocation density around the SiC particles results in preferential precipitation of Mg_2Si in these areas resulting in an increase of precipitate free zones (PFZ's) throughout the matrix. It is thereby considered that a SiC reinforced aluminium 6061 composite would be a satisfactory datum to gauge composite performance for other materials.

2.4.2.2 AA6061 - Alumina (Al_2O_3) Interface.

Janowski [Janowski 1990] studied the interfacial regions of Al_2O_3 particulate reinforcement in an aluminium 6061 alloy matrix. The processing procedures used were: 400°C de-gas for 30 minutes in N_2 atmosphere; 620°C liquid phase sinter for 120 minutes in N_2 atmosphere; hot isostatic press at 510°C for 120 minutes in air; solutionize at 525°C for 45 minutes in air then water quench; age for 14 hours at 175°C in air. Janowski states that a glassy silicon-rich amorphous phase was observed at the Al_2O_3-matrix interface. It is suggested that silicon-oxide-based glassy phases form from the high silicon concentration around the reinforcement reacting with oxygen remaining in the powder compact or from oxygen supplied by the reduction of Al_2O_3; however, although the Al_2O_3 particles may have reacted with the molten matrix to provide a source for oxygen to form the glassy Si phase, there was no evidence of faceting on the Al_2O_3 particles as had been previously described for SiC.

Janowski noted that sub-micron particles of $MgAl_2O_4$ were found in the interfacial region and attributed them to a *partially reacted remnant of the oxide "skin" on the aluminium particles.* It is noted here that Janowski found the yield strength of SiC-containing composites to be higher than for Al_2O_3-containing composites.

Suery [Suery, 1993] stated that Al_20_3 reacts with Mg to form the spinel $MgA1_2O_4$ in the solid state during solution heat treatment. He showed the Mg content in the matrix reduced during processing (compocasting) and during solution treatment. Suery demonstrated that strength and age hardening decreased with time when exposed to a solution treatment temperature of 560^0C. Suery stated: *"The explanation for this loss of the properties is spinel formation at the matrix/A 1203 interface which removes Mg from the matrix and as a result there is loss of Mg_2Si precipitation and less hardening".* The presence of spinel, $MgA1_2O_4$ at the interface may lead to decohesion and therefore lower the strength of the composite.

Hallstedt [Hallstedt, 1993] conducted experiments using $A1_20_3$ fibres in a magnesium matrix. It was reported that at high temperatures, 600^0C, extensive reaction between the $A1_20_3$ fibres and the Mg matrix occurs, in which MgO was formed and Al was dissolved into the matrix. No spinel, $MgA1_2Q_4$ was found. It was suggested, theoretically, that spinel would form along with MgO. As spinel has been reported as forming in Mg-containing aluminium alloys, this suggests a complex reaction mechanism in the $6061/A1_20_3$ composites takes place, resulting in the formation of $MgAl_2Q_4$.

An investigation into interfacial reactions has been carried out by Horng [Horng 1992] using an aluminium-4wt% magnesium alloy, processed in the molten state, with Al_2O_3 particles as reinforcement. The composites were subjected to various temperatures, 700 - 850°C, for various lengths of time, 0 - 20 hours. The following results were determined by Horng:

$MgAl_2O_4$ is the unique interfacial reaction product for Al_2O_3- (Al-Mg) composites at temperatures between 700 to 850°C; the spinel, $MgAl_2O_4$, was not only found at the interfaces but also on the surface of the composites; the formation of $MgAl_2O_4$ crystals started as fine crystals on the surface of the Al_2O_3 particles then grew rapidly to form bulges on the surface; Suggested reactions of formation of $MgAl_2O_4$ at the stated temperatures are –

$$Mg\ (l) + 2\ Al\ (l) + 2\ O_2\ (g) \rightarrow MgAl_2O_4\ (s) \qquad \text{eqn. 15}$$

$$3Mg\ (l) + 4\ Al_2O_3\ (s) \rightarrow 3\ MgAl_2O_4\ (s) + 2\ Al\ (l) \qquad \text{eqn. 16}$$

Horng suggested that both of these reactions are equally important.

An investigation into the microstructure of an Al-Mg-Si alloy reinforced with Al_2O_3 particulates was undertaken by Hong [Hong 1996], in which the processing of the composites was carried out by a molten metal method. The composite was solutionized for 2 hours at 550°C, and then peak aged at 178°C for 8 hours. Hong observed that in the peak aged composite, needle-shaped Mg_2Si precipitates were found throughout the matrix with a higher population found nearer the interface region, yet not at the interface. Hong reported that a PFZ (precipitate free zone)

existed along the Al_2O_3 / matrix interface at a width of 90 nm; also at this interface, *noticeable reaction products* were noted and inferred to consist of some $MgAl_2O_4$. The high density of Mg_2Si precipitates around the reinforcements were attributed to the high dislocation density surrounding the particulates (as previously mentioned for SiC particulates).

Interfacial reactions involving Al-Mg and Al_2O_3 have been discussed and evaluated by Zhong [Zhong 1995]. Zhong's paper presents the possible reactions in an aluminium-magnesium-alumina system:

Note equation 15 is previously quoted, but is given here again as Zhong also quotes it.

$$Mg\ (l) + 2\ Al\ (l) + 2\ O_2\ (g) \rightarrow MgAl_2O_4\ (s) \qquad \text{eqn. 15}$$

$$Mg\ (l) + 4/3\ Al_2O_3\ (s) \rightarrow MgAl_2O_4\ (s) + 2/3\ Al\ (l) \qquad \text{eqn. 17}$$

$$MgO\ (s) + Al_2O_3\ (s) \rightarrow MgAl_2O_4\ (s) \qquad \text{eqn. 18}$$

$$2\ Al\ (l) + 3/2\ O_2\ (g) \rightarrow Al_2O_3\ (s) \qquad \text{eqn. 19}$$

$$2\ Mg\ (l) + O_2\ (g) \rightarrow 2MgO\ (s) \qquad \text{eqn. 20}$$

$$3Mg\ (l) + Al_2O_3\ (s) \rightarrow 3\ MgO\ (s) + 2\ Al\ (l) \qquad \text{eqn. 21}$$

Also quoted are suggested reactions in the saffil (Al_2O_3 / SiO_2) - Al - Mg system:

$$SiO_2\ (s) + 2\ Mg\ (l) \rightarrow 2\ MgO\ (s) + Si\ (s) \qquad \text{eqn. 22}$$

$$Mg\ (l) + 2\ Al\ (l) + 2\ SiO_2\ (s) \rightarrow MgAl_2O_4\ (s) + 2\ Si\ (s) \qquad \text{eqn. 23}$$

The composites for Zhong's investigation were processed using a compo-casting technique in the temperature range 600 - 640°C. The composites were re-melted at 800°C for 30 minutes in an argon atmosphere; the main reaction product found was fine MgO crystals and the main reaction route is shown in equation 21, although the

reactions shown in equations 15, 17, 18, 19 and 20 may also occur. By comparing the results of Horng and Zhong it is suggested that interfacial reactions are system specific.

Lee [Lee, 1998] produced composites using a pressureless infiltration method at 700^0C using Al-3wt%Mg - Al_2O_3 particulates. Lee found $MgAl_2O_4$ at the interface and at the surface of the composite. MgO was also found at the interface region.

Using aluminium alloy 6061 and Al_20, particulates to produce composites will probably result in the formation of $MgAl_2O_4$ and/or MgO at the interface resulting in Mg depletion from the matrix and subsequent reduction in hardness/strength. The phenomenon of reduction in hardness with the addition of Al_20_3 to 6061 alloys and the increase in hardness when SiC is added was shown by Gurcan [Gurcan, 1995]. It is clear that if $A1_20_3$ is to compete with SiC as reinforcement in Mg-containing Al alloys then the processing route and heat treatment regimes must be optimised to reduce temperatures and/or heat treatment times.

2.4.3. Improving Interface Characteristics

As previously mentioned, the interface between the reinforcement and the matrix is of vital importance in the overall performance of the composite material. Previous researchers [Abraham. 1992], [Rajan, 1998] acknowledge the importance of the interface and state that the main problems are with chemical reaction, improper wetting and degradation. Both Abraham and Rajan suggest that coating the reinforcement with another metal may overcome these problems.

As this thesis investigates the use of Al_20_3 particulates as the reinforcement in aluminium 6061 alloy matrix, it is considered a viable study to determine if a metal, in this case copper (Cu), could be effectively deposited on to the surface of Al_20_3 particles in a cost efficient manner and thereby potentially reduce any deleterious interfacial phenomena.

Electroless deposition was chosen as potentially the most effective and lowest cost method. As $A1_20_3$ is a non-conductor of electricity, conventional electrolytic deposition is not an option. It has been shown previously that brittle intermetallic interfaces are deleterious to a composite's performance. Also, localised growth of reaction products may act as crack initiation sites. The migration of magnesium to the interface site has been shown to weaken the strength and hardness of the composite. A possible way of preventing elemental migration to the interface and prevent the production of unwanted interfacial material may be to coat the reinforcement with another metal to act as a barrier to elemental migration. The electroless coating of ceramic material is discussed below in section 2.4.3.1. The coating of the reinforcements in MMCs can have multifunctional beneficial effects on the composite as stated by Rajan [Rajan 1998]. Rajan states that:

(1) A coating may act as a promoter of wetting for ceramic reinforced composites fabricated using a liquid matrix phase;

(2) Ceramic coatings may act as a diffusion barrier, preventing reaction between matrix and reinforcement;

(3) In-situ hybridisation may occur when the coating reacts with the matrix to form an intermetallic phase; for example, if the coating dissolves into the matrix to form a second hybridised reinforcement e.g. $Al/A1_2Cu$;

(4) When a coating dissolves into the matrix this has an in-situ alloying effect.

2.4.3.1. Electroless Coating of Reinforcement

Electroless or autocatalytic [for example, Deckert 1994] deposition is a method by which a metal is deposited on to a substrate using a non-electrolytic process of deposition from a solution. Deckert states that, for electroless copper plating, *copper plates uniformly over all surfaces, regardless of size and shape, demonstrating 100% throwing power, and it may he plated on to non-conductors.* This method of coating would therefore appear ideally suited to the deposition of a metal on to a non-conducting ceramic substrate. There are various procedures available for the electroless coating of ceramic substrates and the basic theory for a commonly used technique is reviewed here.

The basic theory of electroless copper coating given below is extracted from two standard publications [Deckert, 1994] and [Leonida, 1989]. The actual experimental methods are described in the experimental section of this thesis. The two essential components for electroless deposition are a metal salt and a suitable reducing agent.

The plating procedure is carried out in a plating bath (size of bath is dependent on size of material to be plated - a glass beaker is adequate for small scale laboratory work). The copper is provided from simple copper salts e.g. copper sulphate, chloride or nitrate. There are many possible reducing agents: formaldehyde, dimethylamine borane, borohydride hypophosphite, sugars (glucose, sucrose), hydrazine and

dithionite. However, formaldehyde is the most widely used commercial electroless solution.

The main steps and the chemistry of the copper plating process, using formaldehyde as reducing agent, are given below:

Step 1. Degrease and clean the substrate.

Step 2. Sensitising. This involves the immersion of the substrate into an acidic solution containing Sn^{2+} (tin II) ions. The Sn^{2+} ions are adsorbed on to the surface of the substrate.

Step 3. Activation. The substrate with adsorbed Sn^{2+} ions is immersed into an acidic solution containing Pd^{2+} (palladium II) ions. At this stage the Pd^{2t+} ions are reduced to Pd^{o} (palladium metal) by the Sn^{2+} ions, according to the equation:

$$Sn^{2+} + Pd^{2+} = Sn^{4+} + Pd^{o} \qquad \text{eqn. 24}$$

The Pd now forms a thin cover on the substrate which acts as a catalyst for electroless copper deposition.

Step 4. Copper deposition. As this example uses formaldehyde (HCHO) as the reducing agent, a high pH (above 12) is necessary. Therefore the bath is maintained at high pH by addition of sodium hydroxide (NaOH).

The overall plating equation (i.e. the reduction of copper from Cu^{2+} to copper metal Cu^{o}) is:

$$Cu^{2+} + 2HCHO + 4OH^{-} = 2HCOO^{-} + Cu^{o} + H_2 + 2H_2O \qquad \text{eqn 25}$$

The substrate is now coated with a uniform layer of copper.

Several researchers have reported successful methods of electroless coating ceramic substrates, which may be used for composite production [Bhatgadde, 1983], [Garg, 1993], [Abraham, 1992], [Liu, 1997] and [Mel'nikov, 1980].

2.4.3.2. Alternatives to Electroless Coating

A sol-gel technique has been reported [Kindl. 1994] for the coating of SiC particulates with alumina and zirconia. This process appears to use more energy (long drying times and high temperature firing) than for the relatively simple electroless process.

Rajan [Rajan, 1998] discusses techniques for the coating of carbon, SiC and Al_2O_3. The methods discussed include chemical vapour deposition (CVD), physical vapour deposition (PVD), thermal spraying, electrolytic, and cementation processes. When these techniques are compared to electroless deposition, they all appear to have higher cost implications e.g. higher temperatures, longer times and high capital equipment costs.

Chapter 3

Experimental Apparatus and Procedures

3.1 Introduction

This chapter details the materials, apparatus and procedures used in the production, testing and examination of metal matrix composites manufactured during the course of the research. The powder types and sizes used are stock materials held by Napier University School of Engineering with the exception of the Mg, Si, tabular Al_2O_3 and spherical shaped Al_2O_3 powders, which were acquired specifically for the MMC research.

Materials and Equipment

Below is listed all chemicals and apparatus used during the experimental investigations. A full COSHH assessment (in the form of Materials Safety Data Sheets) for all chemicals used is given in Appendix 2.

Aluminium powder	10μm, 63μm maximum diameter
Aluminium 6061 powder	45μm, 75μm maximum diameters
Silicon carbide (αSiC) powder	7μm, 23μm average diameters, tabular shaped particles
Alumina (αAl_2O_3) powder	2.1μm, 6μm, 12μm average diameters, irregular shaped particles
Alumina (αAl_2O_3) powder	13μm average diameter, rounded (spherical) shaped particles
Alumina (αAl_2O_3) powder	8μm average diameter, tabular shaped particles

Copper powder	50μm maximum diameter
Magnesium powder	44μm maximum diameter
Silicon powder	44μm maximum diameter
Formaldehyde (HCHO)	
Tin (II) chloride ($SnCl_2$)	
Palladium (II) chloride ($PdCl_2$)	
Hydrochloric acid (HCl)	
Ammonium chloride (NH_4Cl)	
Potassium sodium tartrate ($C_4H_4KNaO_6 \cdot 4H_2O$)	
Sodium hydroxide (NaOH)	
Copper sulphate ($CuSO_4$)	
Hydrazine (N_2H_2)	
Cupric acetate ($Cu(OOCCH_3)_2 \cdot H_2O$)	
Die wall lubricant	
Fritsch planetary ball mill / mixer	
Presses, hydraulic	
Double action die, 40 mm diameter	
Single action die, 12.7 mm diameter	
Oven	
Vacuum furnace	
Surface preparation equipment (grinding and polishing)	
Weighing scales, accurate to 0.1 mg	
Optical microscopes	
Scanning electron microscope / EDXA	
XRF analyser	

Vickers hardness tester

Wear testing apparatus

3.2 Selection of Materials

The reasons for selecting the materials used in this research are given below.

3.2.1 Matrix

Since age hardening of aluminium alloys is considered the most effective method of improving their strength, it was decided that an alloy from the 2000, 6000, 7000 or 8000 series be selected as the principal matrix material. In deciding on the exact alloy for investigation other parameters were taken into consideration:

1. Matrix alloys used in previous relevant research (aluminium alloys containing magnesium)
2. Commercial availability and cost effectiveness
3. Specific properties of alloy e.g. strength and hardness.

The 6061 aluminium alloy was chosen as the principal matrix material due to its availability, cost and good specific properties. Later sections detail the heat treatments for aluminium 6061 alloy.

3.2.2 Reinforcement

The primary reinforcement material selected for investigation was particulate alumina ($A1_20_3$). Silicon carbide particulates were also used, but these were selected primarily as a method of comparing $A1_2O_3$ performance. Additional reasons for selecting $A1_2O_3$ particles as the reinforcement were:

1. Commercial availability and low cost of $A1_2O_3$ particulates, and

2. The high hardness values for $A1_2O_3$ (although not as hard as SiC) would be expected to provide good wear protection for the matrix.

3.3 Blending of Powders

The first stage in blending the powders was to dry them in an oven at 110°C to remove any moisture. The reinforcing powders were sieved through a 38μm mesh (smallest available) to assist in the break up of any agglomerates. The powders were weighed to produce a mix, which would result in a composite containing the correct volume or weight ratios of reinforcement to matrix. The powders were then dry blended using a Fritsch planetary ball mill/mixer at a cup rotation speed of 585 r.p.m. for eight minutes.

The above blending regime was satisfactory for SiC-containing composites but the Al_2O_3-blended composites showed some agglomeration. An investigation of methods in which the agglomerated Al_2O_3 particles may be dispersed was carried out. This employed the use of hardened steel balls in the ball mill cups, but with this method came excessive iron contamination of the particles. Energy Dispersive X-Ray Analysis (EDXA) revealed no contamination of the powders when mixing was carried out without the steel balls being present - even after up to three hours mixing, see Figures 8 and 9.

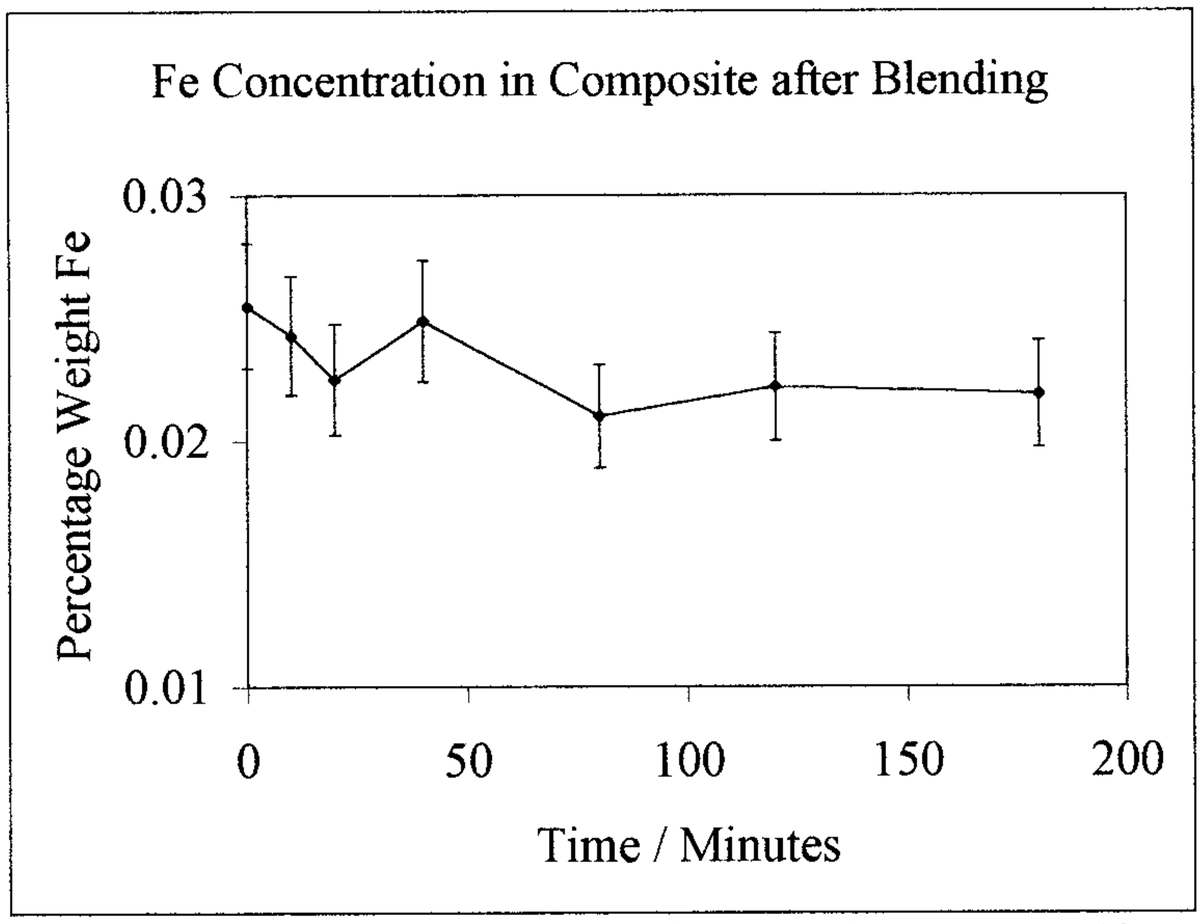

Figure 8. Iron contamination during blending without grinding balls.

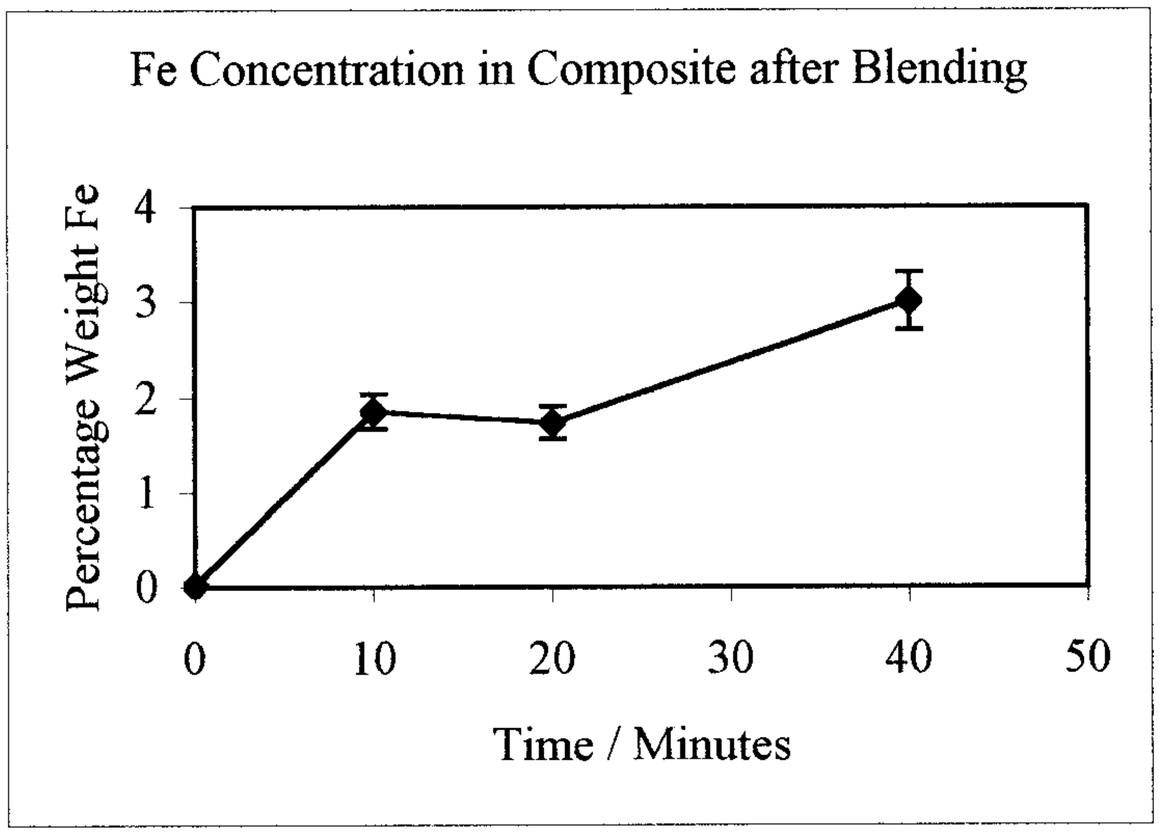

Figure 9. Iron contamination during blending with grinding balls.

The Al_2O_3 particles were found to be less agglomerated when they had been subjected to a more rigorous cleaning and moisture protection regime. The regime was as follows:-

1. ultrasonic cleaning of Al_2O_3 in propan-2-ol,
2. drying of particulates in oven at 80°C,
3. sieving of particulates,

4. weighing the Al_2O_3 and aluminium alloy powders when hot (straight from oven),
5. mixing powders when hot and storing mixed powders in a desiccator to protect from moisture contamination.

3.4 Compaction (Pressing) of Powders.

The composites were pressed using double and single action pressing, with pressures of 275 and 400 MPa being used. The billets produced were of the shape and dimensions as displayed in Figure 10.

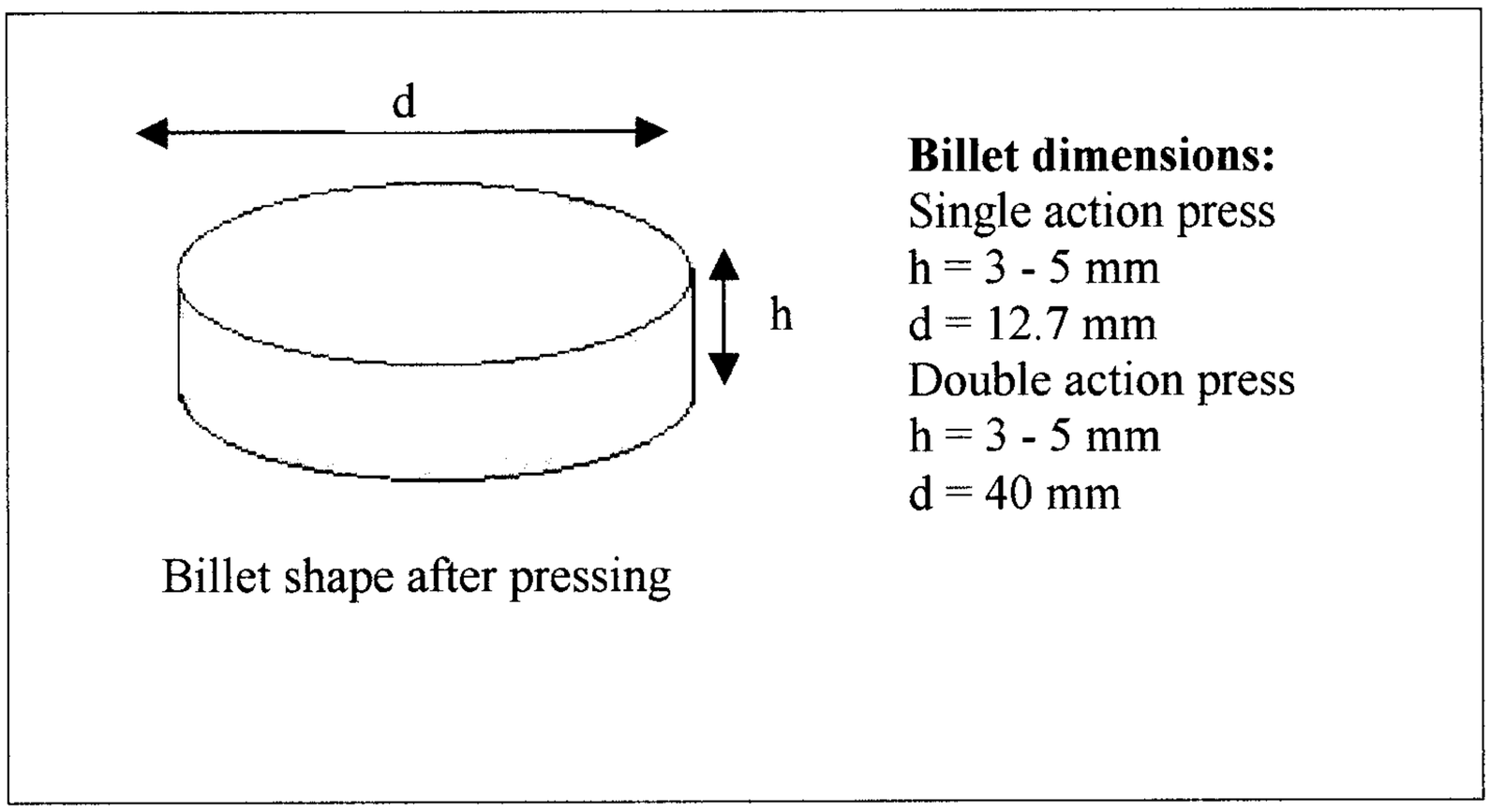

Figure 10. Billet shape and dimensions.

Although the height to diameter ratios were different, the billet dimensions should give a uniform density throughout the green composite by keeping the h/d ratio low, (as discussed previously, section 2.2.5). A silicone lubricant was used on the punch and die walls before each pressing operation.

3.5 Sintering of Green Compacts.

Sintering was carried out at 600°C +/- 10°C (see Figure 2) for times ranging from 30 minutes to 5 hours. Theoretically, improved densification (pore closure) should occur with increased sinter times. The temperature of 600°C [Davis 1990] was chosen because it is below the melting point of aluminium and below the solidus of the alloys used [Polmear 1981], ensuring little or no melting of the metal.

3.6 Heat Treatments.

To obtain optimum hardness levels, various heat treatments were carried out. Solutionising was performed at 530°C for thirty minutes and one hour followed by precipitation heat treatment at 175°C for a range of times between two hours and 24 hours. Results for the optimum heat treatments are presented in Chapter 4.

3.7 Density Measurement Procedure.

Densities of the composites were measured using the Archimedes Method [British Standards Institution (15 June 1993) BS EN 23369:1993] of weighing in air and then in liquid (water), see Figure 11. The density was calculated using the following equation (equation 26):

$$\rho = \frac{m_1 \rho_1}{m_2} \qquad \text{eqn. 26}$$

ρ = composite density

ρ_1 = density in air of liquid (water)

m_1 = mass of composite measured in air

m_2 = mass of liquid displaced by test piece (subtract apparent mass from mass of test piece determined in air)

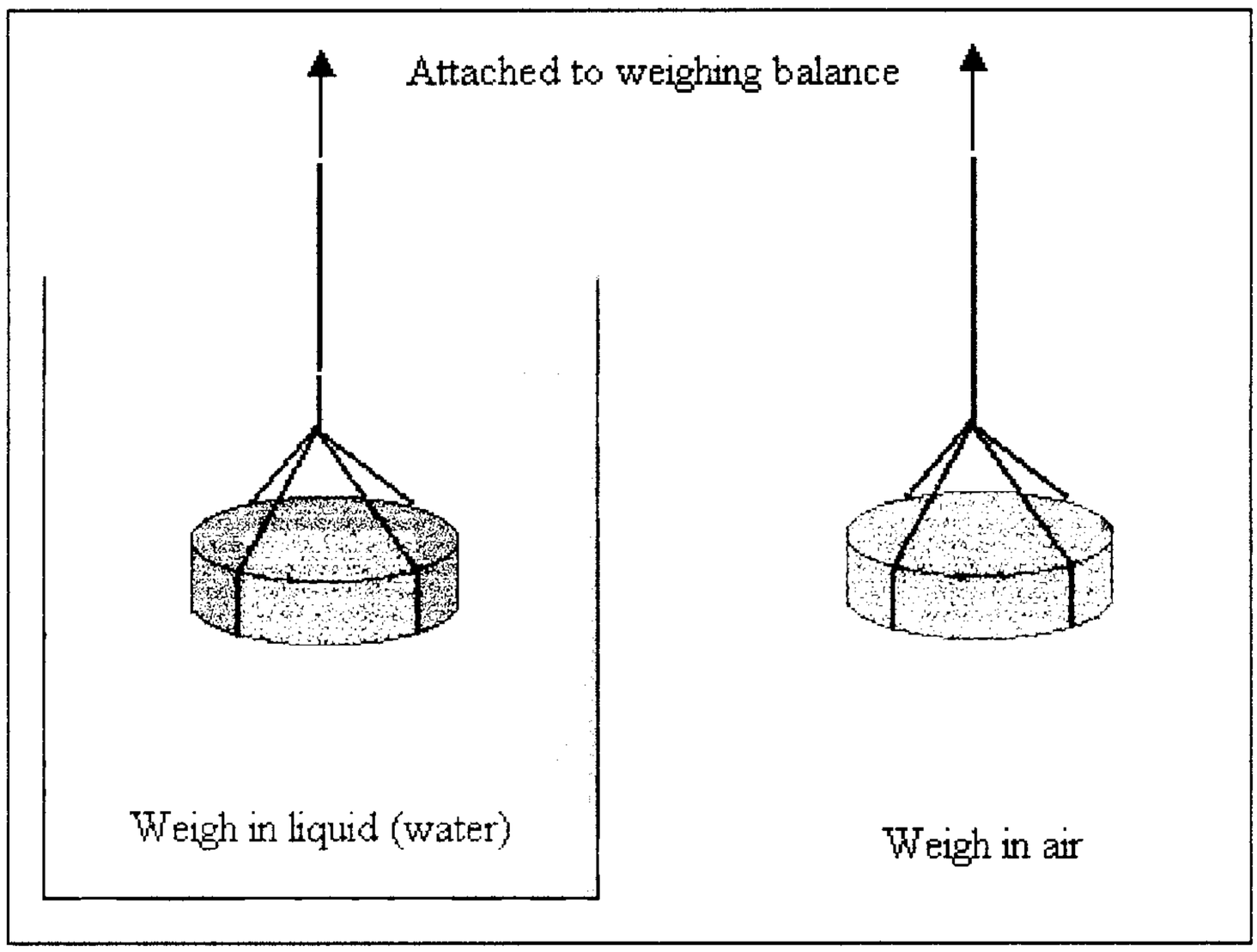

Figure 11. Density determination using the Archimedes Method.

Theoretical ideal densities were calculated using the Rule of Mixtures [Askeland, D.R. 1998]. Using equation 27, below, the theoretical densities of the composites can be deduced:

$$\rho_c = V_m \rho_m + V_r \rho_r \qquad \text{Eqn. 27.}$$

ρ_c = composite density

ρ_m = matrix density

ρ_r = reinforcement density

V_m = matrix volume fraction

V_r = reinforcement volume fraction

By dividing equation 26 by equation 27 and multiplying by 100 the percentage of theoretical density obtained in the actual composite samples produced can be obtained from equation 28, below:

$$\frac{m_1 \rho_1}{m_2 (V_m \rho_m + V_r \rho_r)} \times 100 \qquad \text{Eqn. 28}$$

Equation 28 expresses the measured density (measured using the Archimedes method) as a percentage of the ideal density (calculated using the Rule of Mixtures). This percentage density will be used in the forthcoming results section to determine how close to ideal density the processed composites are.

3.8 Method of Hardness Determination.

The hardness of the samples was measured using a Vickers Hardness Tester using a 10 kg load with a $^2/_3$ objective lens and using a square based diamond pyramid indenter. This form of testing gives a value for the bulk hardness of a material. A minimum of five hardness values were measured for each sample ensuring a variation of no more than 10 HV numbers between each of the five measurements. Should a variation of more than 10 H_V numbers occur, then the test was repeated until five consecutive measurements within a 10 H_V number range was obtained.

3.9 Tribological (Wear) Measurement.

The wear performance of the processed composites was determined by the weight loss from the composite and comparing different composite weight losses and monolithic alloy weight loss.

3.9.1. Swansea Wear Test Rig.

Wear testing was carried out using a test rig designed and built at the Swansea Tribology Centre. The rig uses a rotating cone of mild steel against which three test samples are simultaneously worn with an applied load of 200 g. The test cone has a

Vickers Hardness value of 222 H_V numbers. The wear samples were machined from the processed billets to the following dimensions: 10 x 6 x 2 mm.

The cone rotates at a speed of 100 r.p.m. for times of up to 27 hours. Mass loss from the wear samples was measured at set time intervals during the test, typically at 3, 9, 15 and 27 hours. The samples were removed from the test rig, cleaned, and then weighed to measure mass loss. See Figure 12 for a schematic view of the wear test rig operation.

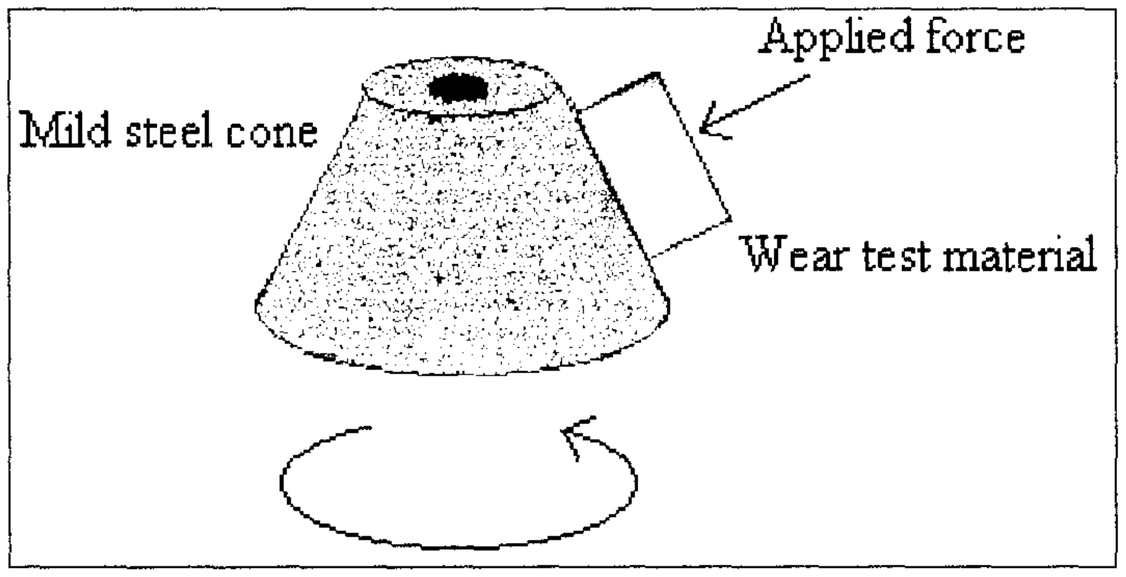

Figure 12. Schematic diagram of the wear testing principle for the Swansea Test Rig.

One problem with the efficacy of the wear test rig was that while the angular velocity of the cone was constant, the actual velocity at the surface of the cone varied. Near to the apex of the cone, the circumference was 29.9 mm, while at the base the circumference measures 62.2 mm; this gave a mean cone circumference of 46.0 mm. Over a 27 hour wear regime the wear test samples were subjected to different sliding distances over the contact surface of each sample, see Table 10.

Table 10. The variation of distance travelled at different positions on a cone incline for a test of 27 hours at a rotation speed of 100 r.p.m.

Position on cone	Circumference / mm	Sliding distance / m
Apex	29.5	4779
Mid (mean)	46.0	7452
Base	62.2	10076

This form of wear testing effectively sets up a sliding velocity gradient over the surface of any tested sample, thereby no two points over the surface of the sample are subjected to the same wear regime. If the sample surface wears unevenly, a change in the load applied over the sample surface may occur.

In addition, three samples were simultaneously tested, all running on the same wear track around the cone. Therefore any debris or deposits from one sample may affect the wear of another. Even with all samples cut from the same original material there may be differences between them, such as particle distribution and density which can give different wear properties e.g. pull out or delamination.

The set up for this test rig was a precise process, which, if not done correctly, could result in the wear surfaces not being in full contact. This was also identified as a problem when the samples were removed for weighing and then replaced. If they were not replaced in the position they were removed from, any gouging or scoring from previous testing may result in the sample having to be run-in again.

3.9.2 Napier Wear Test Rig.

To overcome the problems associated with the Swansea Wear Rig, a new test rig has been designed, built and commissioned, see Figure 13. The new design uses a rotating steel drum of constant circumference with a larger diameter than the previous cone to reduce running-in time. The new rig can take up to six samples each wearing independently with separate applied loads. The machining of the test samples is also easier than previously to reduce error and speed up the testing process.

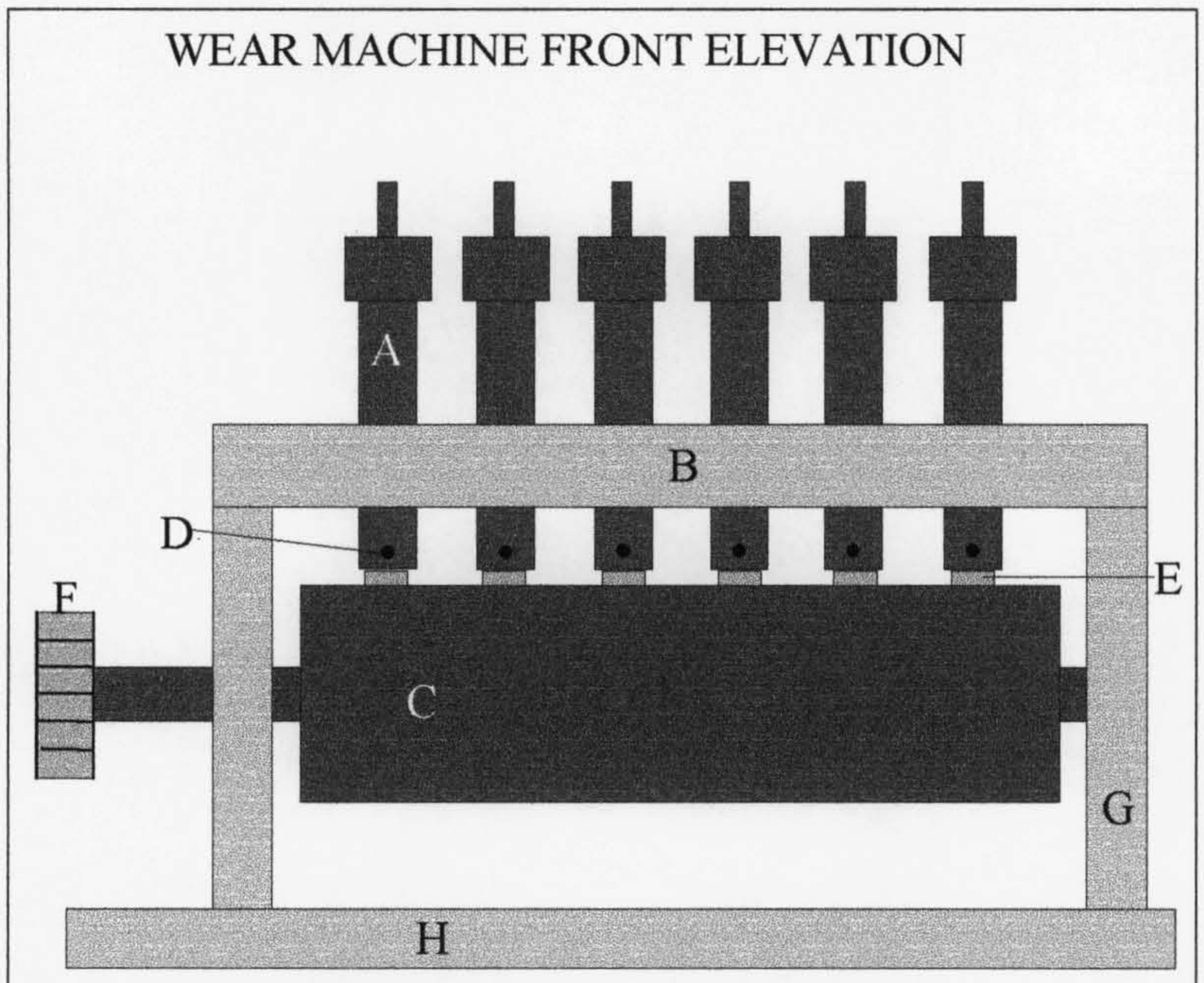

Figure 13. Diagrammatic representation of the Napier Wear Test Rig.

The Napier wear machine is proving successful in its operation. However to keep the power at the motor within acceptable levels the wear test rig can only operate with four samples when maintaining maximum rotational velocity of 70 rpm.

3.10. Electroless Copper (Cu) Coating of $A1_2O_3$ Particulates

This investigation was carried out to evaluate if electroless copper coating would be a viable method of depositing a layer of copper on to Al_2O_3 particulates, which may provide a beneficial interface layer. For example the copper layer may prevent or reduce any deleterious interaction between matrix constituents and the reinforcement. Two forms of α-Al_2O_3 were employed to test the success of copper coating by electroless methods: Tabular, Photographic Plate 1 (see appendix I) with an average

diameter of 8 μm; Spherical Al_2O_3, Photographic Plate 2, with an average diameter of 13μm.

The following cleaning regime was used for all the Al_2O_3 particulates used in the copper coating experiments:

The particulates were first ultrasonically cleaned for ~ 15 minutes.

The particulates were then cleaned using an agitated nitric acid solution. The acid solution contained 25 ml de-ionised water and 2.5 ml concentrated nitric acid. The solution containing acid and particulates was stirred (magnetic stirring) for ~ 15 minutes. The solution was decanted/filtered and the particulates dried.

3.10.1. Process using Formaldehyde (HCHO) as Reducing Agent

The conventional method for electroless plating normally has the sensitisation and activation stages as separate steps, which involves rinsing between these steps; however it is documented that a combined sensitisation and activation stage may be employed [Leonida 1989]. To reduce the process time (thereby reducing cost) for the copper deposition, the combination method was employed.

The solution for the catalyst contains both tin II (Sn^{2+}) and palladium (Pd^{2+}) ions, which are stabilised in the solution by a high acid concentration and an excess of tin II ions. Three grams of Al_2O_3 particulates was immersed in the solution for approximately two minutes.

The following processes are adaptations of the process described by Leonida [Leonida 1989]. The mixed catalyst solution consisted of: 3g of Al_2O_3 particulates, 7.5 g tin II chloride ($SnCl_2$), 0.125g palladium chloride ($PdCl_2$), 25.0 ml hydrochloric acid (37%) (HCl), 0.5g ammonium chloride (NH_4Cl) made up to a total solution volume of 125 ml with de-ionised water. The solution was magnetically stirred (slowly) for approximately two minutes at room temperature, 26°C. The solution was then filtered and the Al_2O_3 particulates were gently rinsed with de-ionised water. The rinsing is a critical step as it is necessary to remove any remaining chemicals adhering to the surface, however the rinsing must not be too vigorous, as too vigorous a rinse may remove the palladium catalyst from the substrate surface. Once the particulates are filtered and rinsed they are ready for copper plating.

Copper bath: The copper bath solution consisted of the following chemicals ~ 12.5 g potassium sodium tartrate ($C_4H_4KNaO_6.4H_2O$), 2.5 g sodium hydroxide (NaOH), 2.5 g copper sulphate ($CuSO_4$), 2.5 g formaldehyde (HCHO) made up to 125 ml with de-ionised water. The experimental procedure was carried out as follows: Sodium hydroxide solution was added to a beaker containing Al_2O_3 particulates, which were being magnetically stirred in a minimal amount of de-ionised water. To ensure the bath is maintained at the correct pH, 12-14, a pH meter was used for pH monitoring and a standby solution of sodium hydroxide was prepared to adjust pH if needed. The potassium sodium tartrate and the copper sulphate were added. Finally the formaldehyde was added which brought the solution to ~ 125 ml. The plating bath was left for 30 minutes and results noted. The copper coated particulates were then filtered and dried then stored in a desiccator.

3.10.2 Process using Hydrazine Hydrate ($N_2H_4.H_20$) as Reducing Agent

In this method there is no catalyst involved [Bhatgadde 1983] and therefore no sensitising or activation steps are required. With the removal of expensive chemicals (e.g. palladium chloride) and the reduction in time (e.g. removal of catalyst deposition and rinsing steps), this method would be expected to be more economical than the previous process, which used formaldehyde.

The following processes are based on the process described by Bhatgadde [Bhatgadde 1983]. Copper bath procedure: All solutions are magnetically stirred. 1 g cupric acetate was dissolved in 100 ml of de-ionised water. To this 3 g of Al_2O_3 particulates were added. Finally 6.25 ml of hydrazine hydrate was added. The final ratio of cupric acetate solution to hydrazine hydrate was 16:1. The temperature of the bath was measured at ~ 25°C. The pH of the solution was measured at 9.6. The solution was continually stirred for 30 minutes, then filtered and rinsed. The copper coated particulates were then dried and stored in a desiccator.

Chapter 4

Results

4.1 Introduction

All results were collected at Napier University, Edinburgh except for some composite SEM examinations, which were collected at the Otto-von-Guericke Universitat, Magdeburg, Germany, under the author's supervision.

4.2 Density Measurements.

Densities are expressed in the following tables as a percentage of the ideal density, in which 100% dense is rated as ideal. The ideal density is determined from the rule of mixtures, and the actual density was measured using the Archimedes method. These are described in section 3.7. Processed samples densities were measured ten times for each composite and alloy material. The average of the ten measurements was used to determine the percentage density achieved. Due to the variance in the measured densities there is a confidence limit of ±3%.

Table 11 details the variation in density with composite using AA6061 45μm powder, SiC 23μm, Al_2O_3 12μm, pressed at 275 MPa, sintered at 610°C for 5 hours, solution heat treated at 530°C for 40 minutes and age hardened at 175°C for 8 hours.

Table 11. Measured density expressed as a percentage of ideal density compared to composite constituents for 6000 series aluminium alloy containing SiC and Al_2O_3 reinforcements.

Composite Composition	Percentage Density
AA6061	99
AA6061 + 5%SiC	98
AA6061 + 10%SiC	99
AA6061 + 15%SiC	98
AA6061 + 20%SiC	98
AA6061 + 5%Al_2O_3	98
AA6061 + 10%Al_2O_3	95
AA6061 + 15%Al_2O_3	95
AA6061 + 20%Al_2O_3	92
AA6061 + 5%Al_2O_3 + 15%SiC	95
AA6061 + 10%Al_2O_3 + 10%SiC	94
AA6061 + 15%Al_2O_3 + 5%SiC	94

From the results in Table 11 it can be seen that there is a trend for decreasing density with increasing Al_2O_3 volume fraction. Table 12 details the variation in density using Al powder 63μm, Cu 50μm, AA6061 45μm, SiC 23μm, Al_2O_3 μm, pressed at 400MPa, sintered at 600°C for 30 minutes, solution heat treated for 30 minutes and age hardened at 175°C for 7 hours.

Table 12. Measured density expressed as a percentage of ideal density compared to composite constituents using 2000 series aluminium alloy (containing Cu) and 6000 series alloy (containing Mg and Si).

Composite Composition	Percentage Density
Al + 4%wt Cu	98
Al + 4%wt Cu + 10%SiC	96
Al + 4%wt Cu + 10%Al_2O_3	92
AA6061	98
AA6061 + 10%SiC	95
AA6061 + 10% Al_2O_3	93

In Table 12 again there is a trend of decreasing density with increasing reinforcement volume, in particular the Al_2O_3 containing composites perform poorly with densities below 95%. Table 13 details density variation of various combinations of Al 10μm powder, Al_2O_3 12μm, SiC 7μm, Cu 50μm, Si 44μm and Mg 44μm. The materials

were pressed at 400 MPa, sintered for 5 hours at 600°C and solution treated at 530°C for 30 minutes with no ageing treatment given.

Table 13. Density variation with composite composition using aluminium with Si, Mg or Cu additions.

Composite Composition	Percentage Density
Al + 1.5%wtSi + 10%Al_2O_3	92
Al + 4%wtMg + 10%Al_2O_3	89
Al + 4%wtCu + 10%Al_2O_3	93
Al + 10%Al_2O_3	95
Al + 1.5%wtSi + 10%SiC	86
Al + 4%wtMg + 10%SiC	93
Al + 4%wtCu + 10%SiC	98
Al + 10%SiC	98
Al + 4%wtMg	93
Al + 1.5%wtSi	91
Al + 4%wtCu	92
Al	99

In Table 13 it can be seen that the SiC containing composites have better densities when compared to Al_2O_3 containing material except where Si is used as an addition.

Table 14 tabulates the results obtained for AA6061 containing 10%vol Al_2O_3 with fixed mass additions of Mg and/or Si. The heat treatments given were - sintering for 5 hours at 600°C, solutionizing at 530°C for 1 hour and ageing at 175°C for 8 hours. The density results are all poor for the composites with densities below 95%. The monolithic alloy performed well with 99% of theoretical density being measured.

Table 14. Density variation with composite composition using AA6061 with Mg and/or Si additions.

Composite Composition	Percentage Density
AA6061	99
AA6061 + 10%Al_2O_3	94
AA6061 + 10%Al_2O_3 + 0.002g Mg	94
AA6061 + 10%Al_2O_3 + 0.004g Mg	94
AA6061 + 10%Al_2O_3 + 0.006g Mg	93
AA6061 + 10%Al_2O_3 + 0.002g Si	95
AA6061 + 10%Al_2O_3 + 0.004g Si	94
AA6061 + 10%Al_2O_3 + 0.006g Si	94
AA6061 + 10%Al_2O_3 + 0.002g Mg + 0.002g Si	93
AA6061 + 10%Al_2O_3 + 0.004g Mg + 0.002g Si	94
AA6061 + 10%Al_2O_3 + 0.002g Mg + 0.004g Si	94

Addition of 5 wt% silicon to aluminium 6061 alloys to attempt the retention of magnesium in the matrix of 10 vol% alumina reinforced MMCs and examination of density variation.

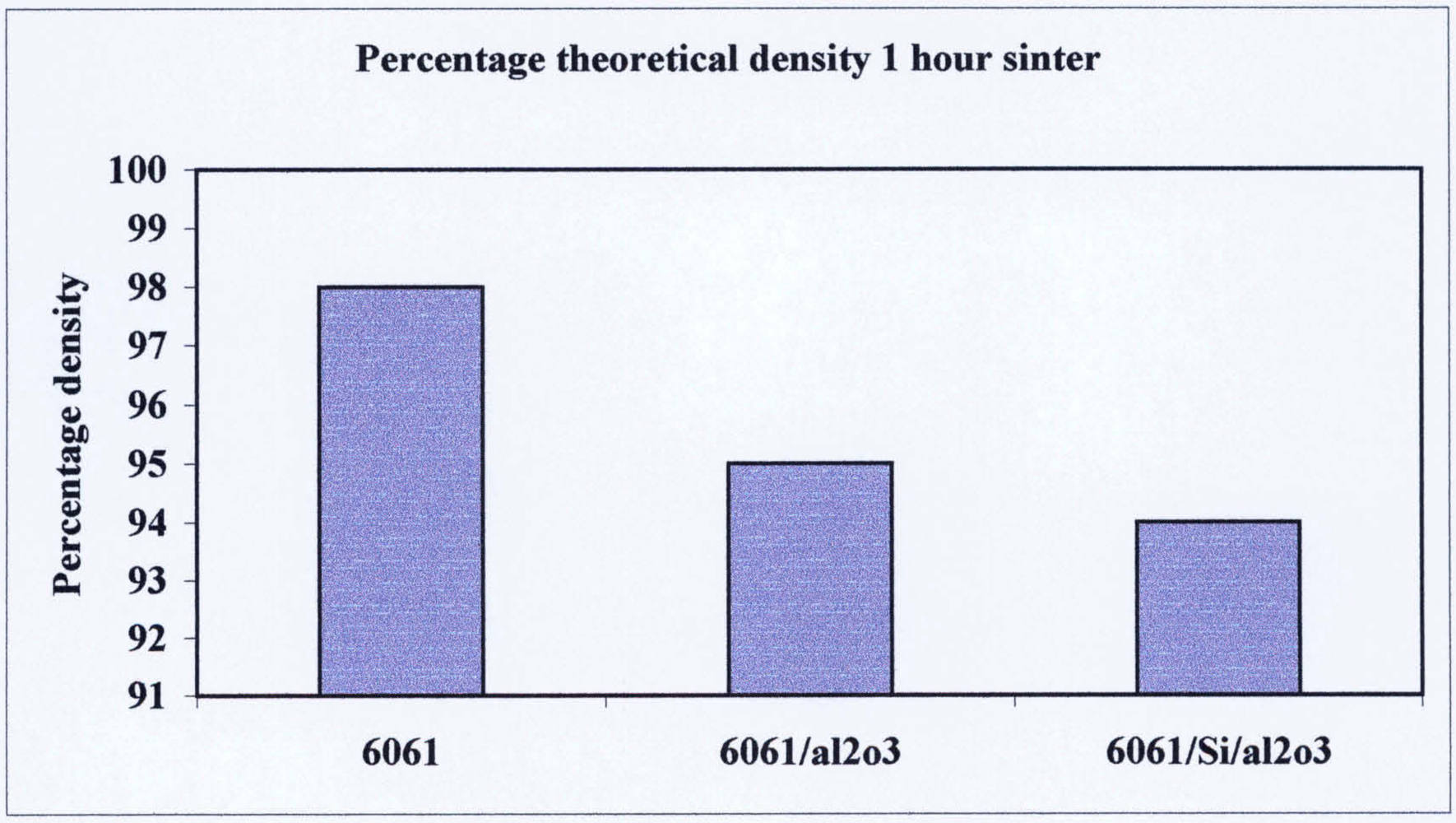

Figure 14. Bar graph displaying that the monolithic alloy has superior density when compared to the Al_2O_3 containing MMC's after1 hour sinter.

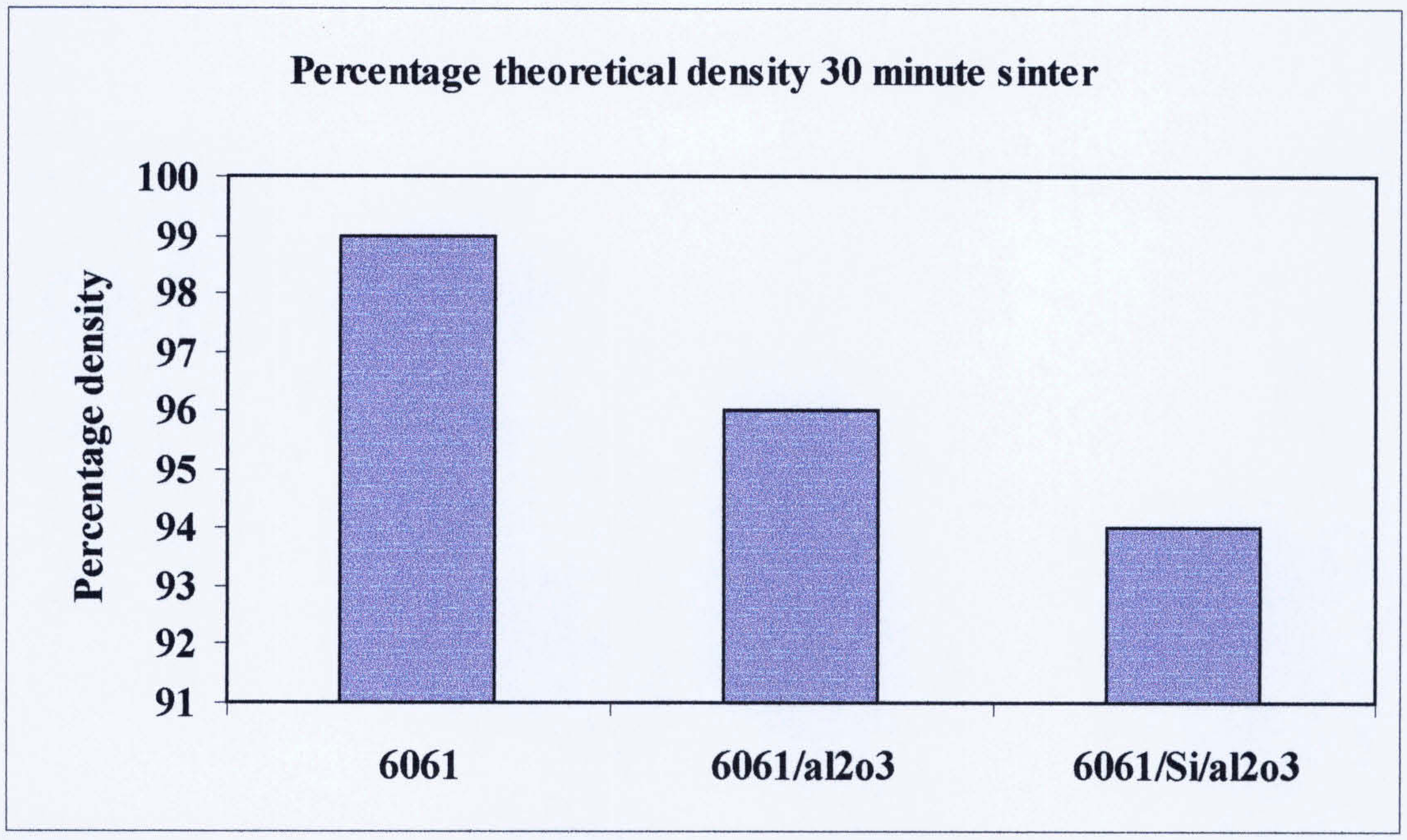

Figure 15. Bar graph displaying that the monolithic alloy has superior density when compared to MMCs after 30 minute sinter, with the density of the 6061/Al_2O_3 composite showing a slight improvement when compared to the one hour sintered composite from Figure 14.

4.3 Hardness Measurements.

The hardness values were determined from the average value obtained from twenty measurements, ten on each side of each sample tested. The error range was found to be ten HV numbers giving confidence limits of ±5 HV numbers.

Table 15 presents the Vickers Hardness values for composites using AA6061 45μm powder, SiC 23μm, Al_2O_3 12μm, pressed at 275 MPa, sintered at 610°C for 5 hours, solution heat treated at 530°C for 40 minutes and age hardened at 175°C for 8 hours.

Table 15. Aluminium 6061 composite composition hardness comparison after pressing at 275 MPa, sintering at 610°C for 5 hours, solution heat treated at 530°C for 40 minutes and age hardened at 175°C for 8 hours.

Composite Composition	Vickers Hardness
AA6061	85
AA6061 + 5%SiC	107
AA6061 + 10%SiC	111
AA6061 + 15%SiC	113
AA6061 + 20%SiC	113
AA6061 + 5%Al_2O_3	79
AA6061 + 10%Al_2O_3	49
AA6061 + 15%Al_2O_3	52
AA6061 + 20%Al_2O_3	51
AA6061 + 5%Al_2O_3 + 15%SiC	52
AA6061 + 10%Al_2O_3 + 10%SiC	56
AA6061 + 15%Al_2O_3 + 5%SiC	62

In Table 15, the SiC reinforced composites all performed well achieving hardness values in excess of 30% greater than the monolithic alloy. The Al_2O_3 containing materials all showed poorer hardness's than the monolithic alloy. Table 16 presents the hardness values obtained for various ageing times for composites, which were given the initial heat treatments of 30 minutes sinter at 600°C and solutionizing at 530°C for 30 minutes. The ageing temperature was 175°C. The results in Table 16 show that there was no appreciable increase in hardness for the composites or the alloy after ~ 8 hours ageing. Again the Al_2O_3 containing composites gave measured hardness values less than the SiC composites or the alloys.

Table 16. Hardness variation with ageing time following 30-minute solution treatment.

Composite Composition	Hardness at 2hrs	Hardness at 4hrs	Hardness at 8hrs	Hardness at 13hrs	Hardness at 18hrs	Hardness at 24hrs
Al + 4%wt Cu	84	79	98	100	97	102
Al + 4%wt Cu + 10%SiC	74	80	101	95	95	93
Al + 4%wt Cu + 10%Al_2O_3	69	88	87	91	90	90
AA6061	77	73	113	100	105	115
AA6061 + 10%SiC	98	113	111	114	106	113
AA6061 + 10%Al_2O_3	85	89	90	92	91	90

Table 17 presents the hardness values obtained for various ageing times for composites, which were given the initial heat treatments of 30 minutes sinter at 600°C and solutionizing at 530°C for 60 minutes. The ageing temperature was 175°C. The results shown in Table 10 show the Al_2O_3 composites having lower hardness values than the SiC composites or the alloys. Comparing the values between the 30minute and the 1-hour solutionizing there is little to be gained from the extra 30 minutes heating, with peak values being obtained at both solution temperatures at ~ 8 hours ageing.

Table 17. hardness variation with ageing time following 60-minute solution treatment.

Composite Composition	Hardness at 2hrs	Hardness at 4hrs	Hardness at 8hrs	Hardness at 13hrs	Hardness at 18hrs	Hardness at 24hrs
Al + 4%wt Cu	75	83	97	103	98	106
Al + 4%wt Cu + 10%SiC	84	82	101	102	107	99
Al + 4%wt Cu + 10%Al_2O_3	70	70	92	90	87	88
AA6061	85	105	114	110	117	94
AA6061 + 10%SiC	96	107	116	110	110	95
AA6061 + 10%Al_2O_3	78	86	88	87	90	87

Table 18 displays the hardness results for various composites containing 10% Al_2O_3 particulates in a AA6061 matrix with Si and Mg additions. The heat treatment regime consisted of sintering at 600°C for 30 minutes, 1 hour, 3 hours and 5 hours. The sintering was followed by solutionizing at 530°C for 30 minutes and ageing at 175°C for 7 hours.

Table 18. Variation of hardness with sinter time and Mg/Si additions.

Composite Composition	Hardness 30 minutes sinter	Hardness 1 hour sinter	Hardness 3 hours sinter	Hardness 5 hours sinter
AA6061	119	112	104	105
AA6061 + 10%Al_2O_3	114	87	47	56
AA6061 + 10%Al_2O_3 + 5%wt Mg	54	64	52	56
AA6061 + 10%Al_2O_3 + 5%wt Si	111	120	90	62
AA6061 + 10%Al_2O_3 + 2.5%wt Mg + 2.5%wt Si	65	62	67	47

The results displayed in Table 18 show that sintering time has a marked effect on the hardness of Al_2O_3 containing composites and that Si additions have a role to play in maintaining composite hardness with increasing sinter time. Figure 16 displays the results in a graphical format below.

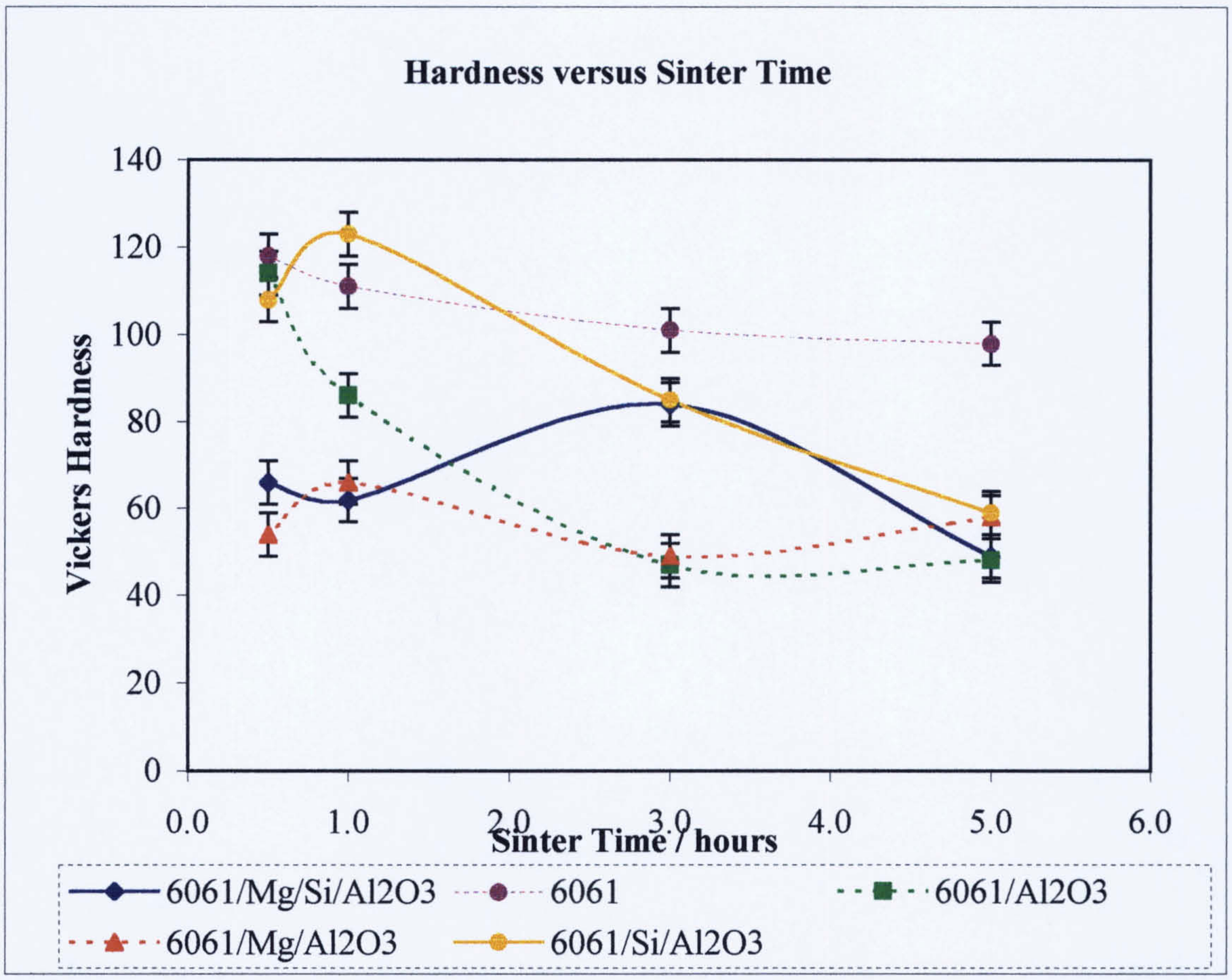

Figure 16. Graphical interpretation of the variation of hardness with sinter time for composites containing Al_2O_3 with additions of Si and Mg, showing error bands for ±5 HV values.

Addition of 5 wt% silicon to aluminium 6061 alloys to attempt the retention of magnesium in the matrix of 10 vol% alumina reinforced MMC's and examination of hardness compared to sinter time and Si addition..

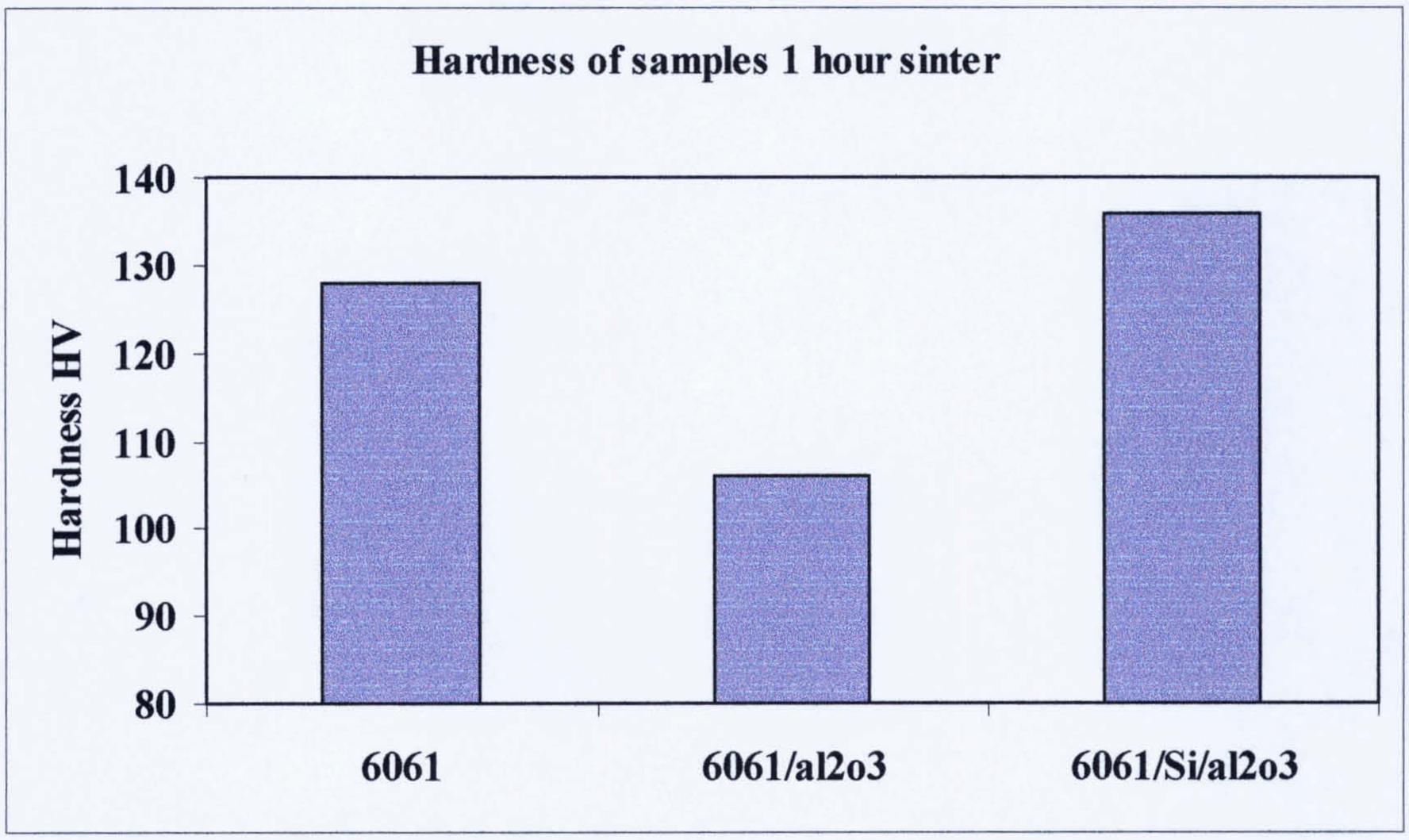

Figure 17. The addition of silicon has improved the hardness of the MMC after one hour sinter. The MMC without added silicon performs the poorest when compared to the Si added MMC and the monolithic alloy.

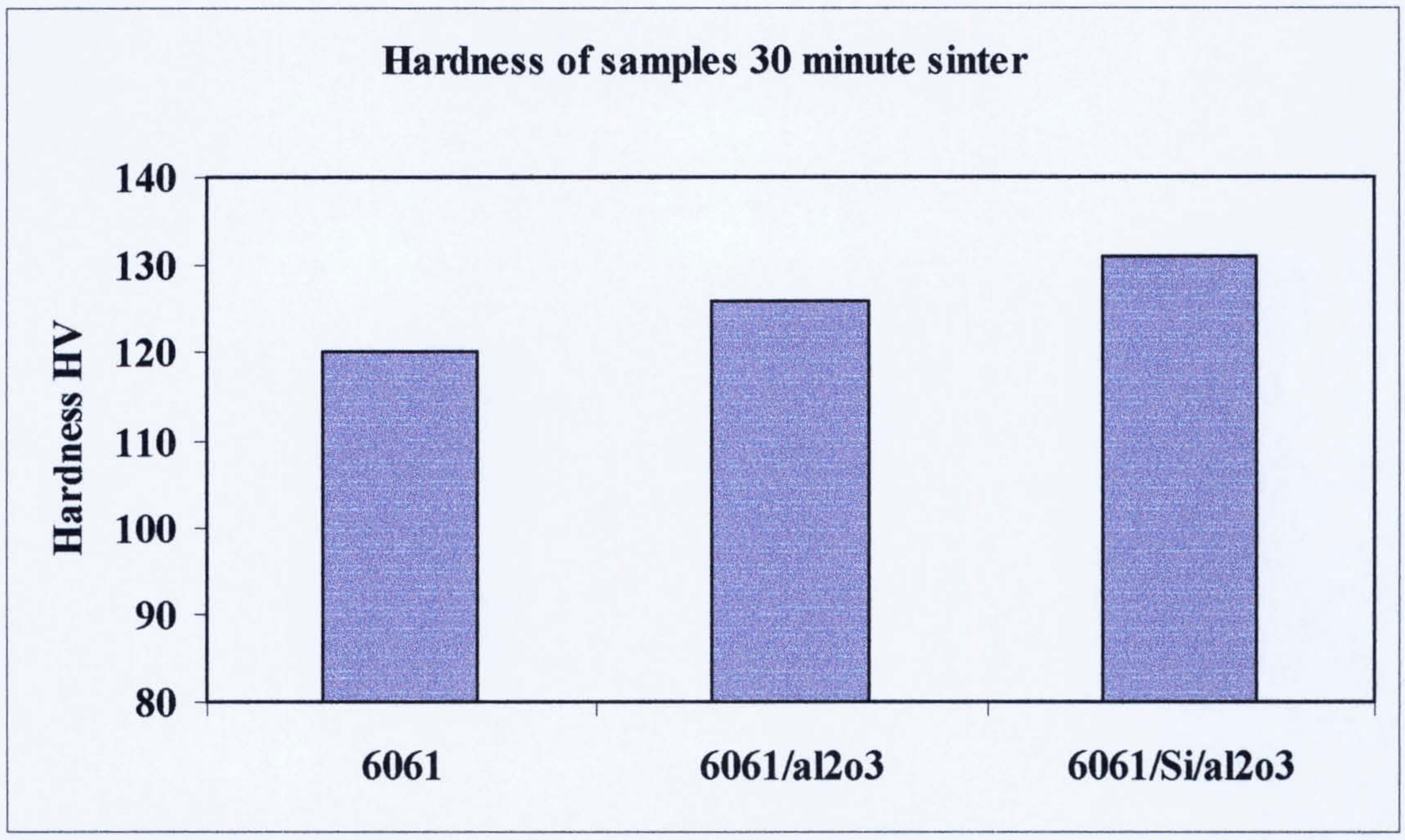

Figure 18. The addition of silicon has improved the hardness of the MMC, however the non-silicon added MMC has improved hardness after 30 minutes sinter when compared to the monolithic alloy.

4.4 Wear Test Results.

Figures 19, 20 and 21 give graphical analysis of the wear for AA6061 alloy and composites using AA6061 as the matrix. These materials were pressed at 275 MPa, sintered at 600°C for 5 hours, solution treated for 30 minutes at 530°C and aged at 175°C for 8 hours.

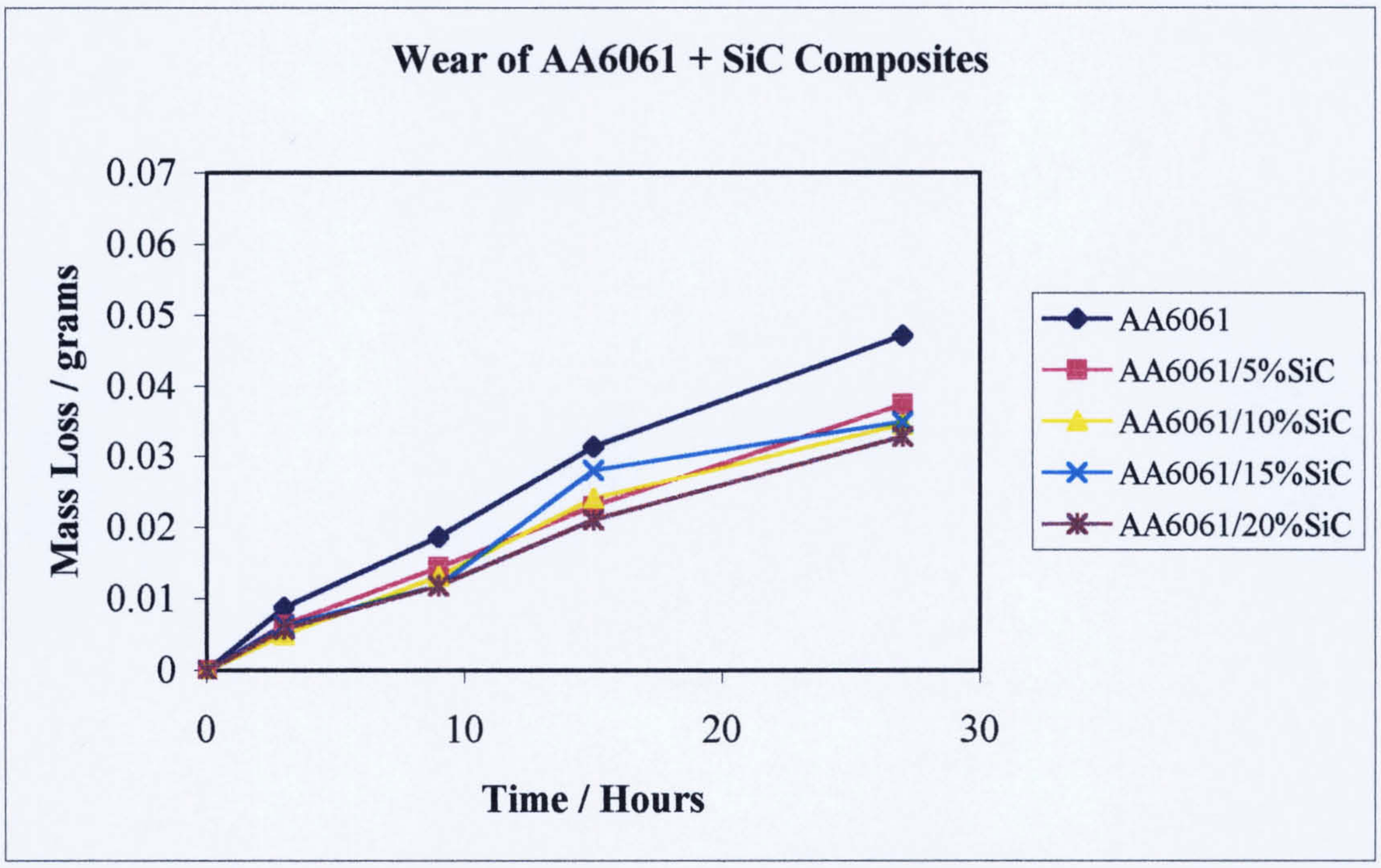

Figure 19. Wear of SiC containing composites compared with monolithic AA6061 alloy.

Figure 19 displays the wear performance of SiC containing composites. The wear performance of the composite materials show an improvement over the monolithic alloy. The wear performance is improved with increasing volume percent of SiC particulates.

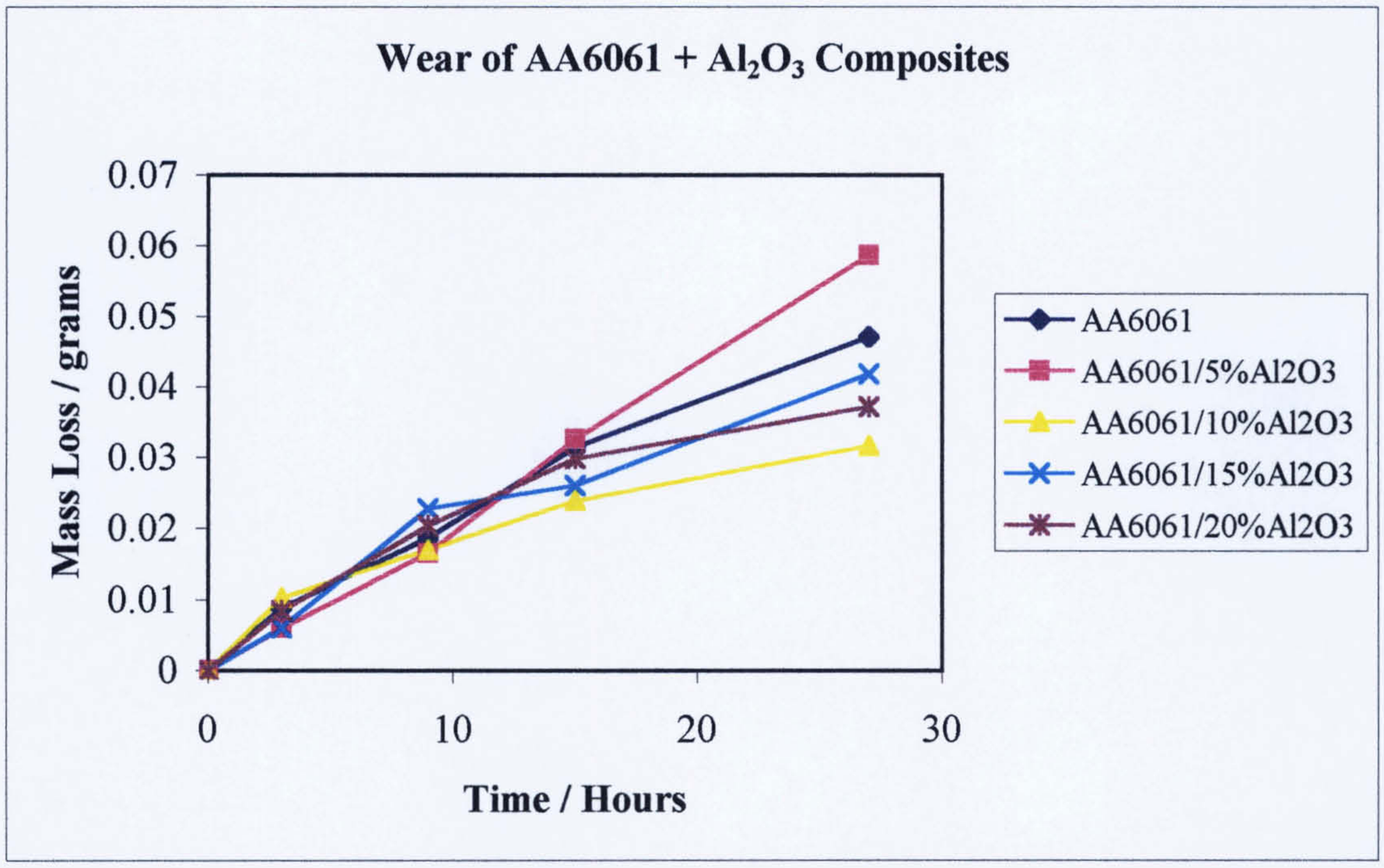

Figure 20. Wear of Al_2O_3 containing composites compared with monolithic AA6061 alloy.

Figure 20 displays a general improvement of wear performance of the Al_2O_3 containing composites over the monolithic alloy. However the 5% Al_2O_3 composite showed poorer wear resistance than the alloy. There is no definite trend displayed that increasing volume percent reinforcement would improve wear resistance.

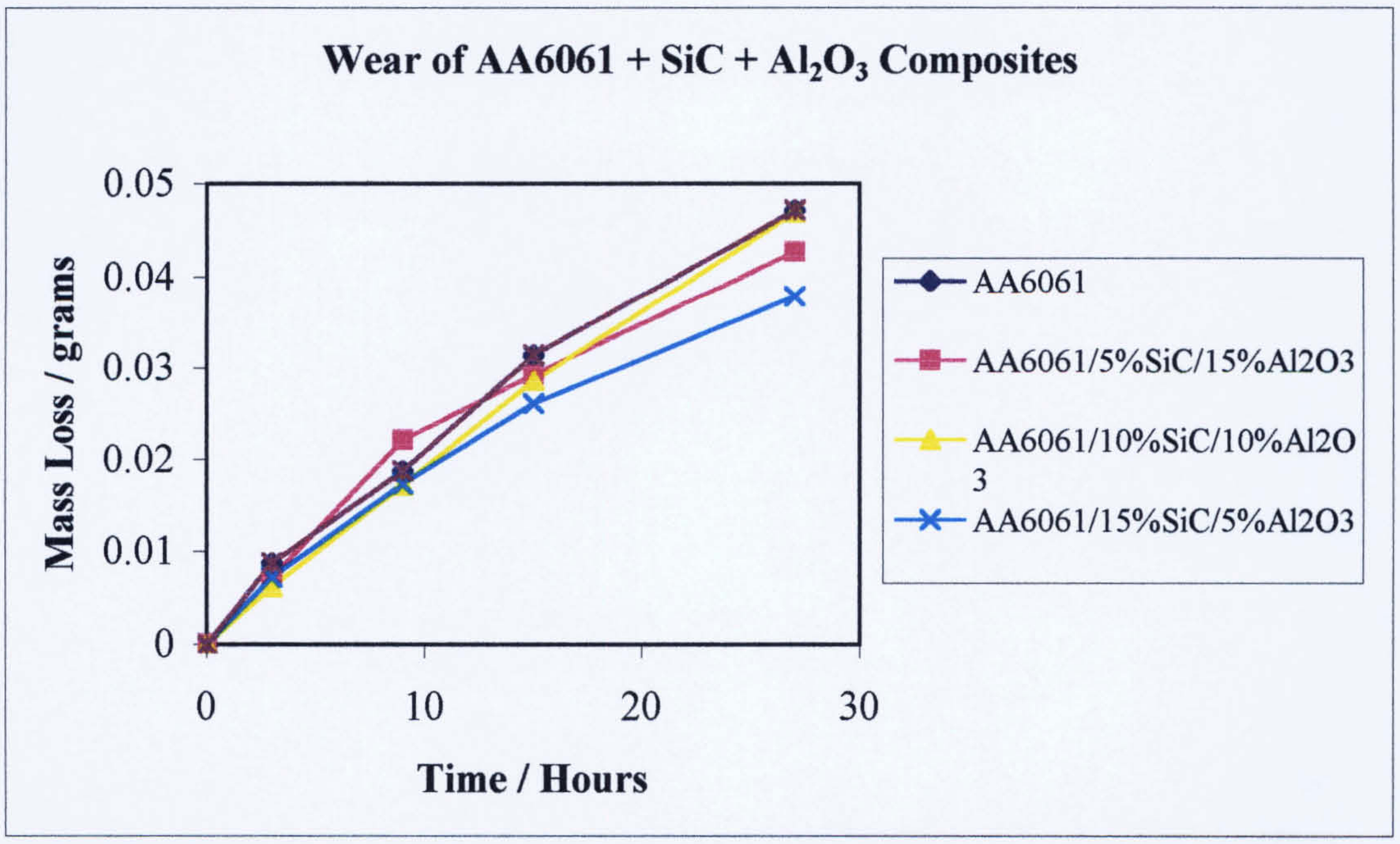

Figure 21. Wear of SiC and Al_2O_3 containing composites compared with monolithic AA6061 alloy.

Figure 21 shows the hybrid SiC/Al_2O_3 containing composites matched or surpassed the monolithic alloy for wear resistance. No trend is evident that altering the reinforcement quantities improves wear resistance.

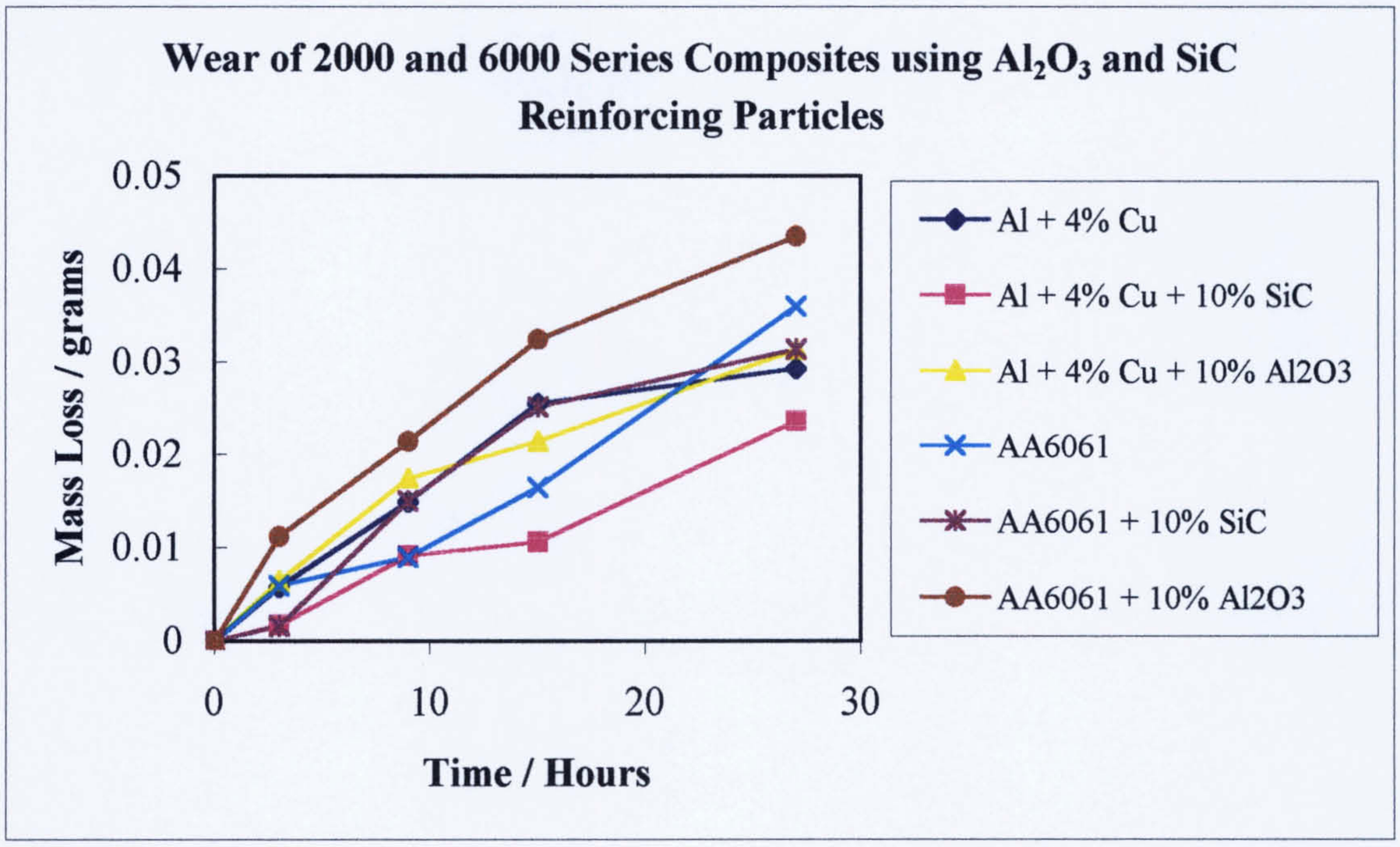

Figure 22. Graph of mass loss due to wear for 2000 and 6000 alloys containing 10 vol% reinforcement.

The results obtained in Figure 22 are for composites produced from a 30 minute sinter at 600°C, solutionized at 530°C for 30 minutes and aged at 175°C for 8 hours. The 2000 series materials out-performed the 6000 composites for wear resistance. The composites containing Al_2O_3 have the poorest wear resistance when compared to the SiC and monolithic alloy with respect to each alloy series. The SiC composites have the greatest wear resistance with respect to each alloy series.

Wear test graphs for composites containing added Si.

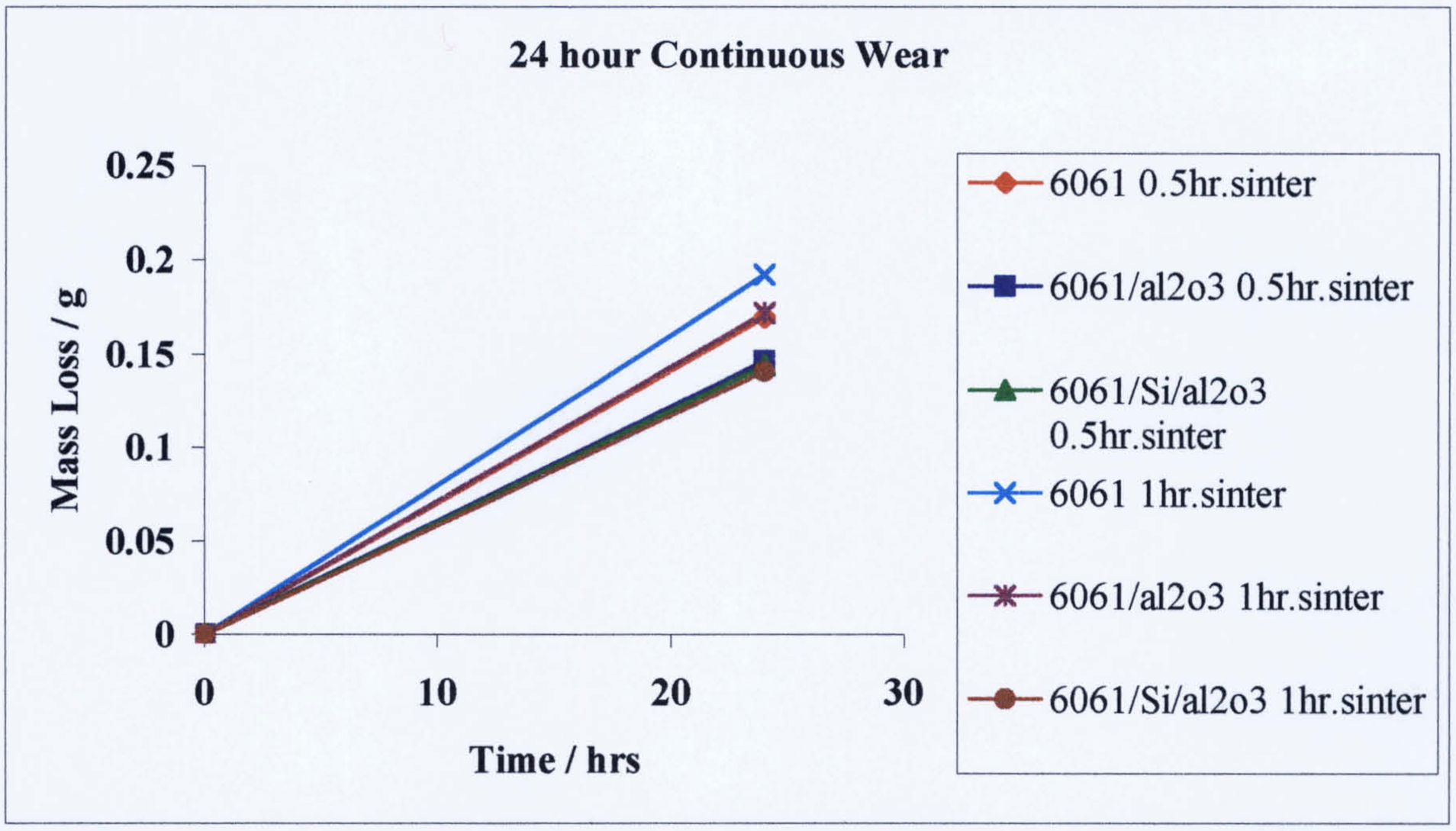

Figure 23. Graph displaying that monolithic 6061 after 1 hour sinter performs the poorest in a continuous 24 hour wear test. 6061 30 minute sinter and MMC with no added silicon after 1 hour sinter are similar in wear performance. The 30 minute sinter MMC's with and without added silicon perform similarly to the MMC 1hour sinter with added silicon.

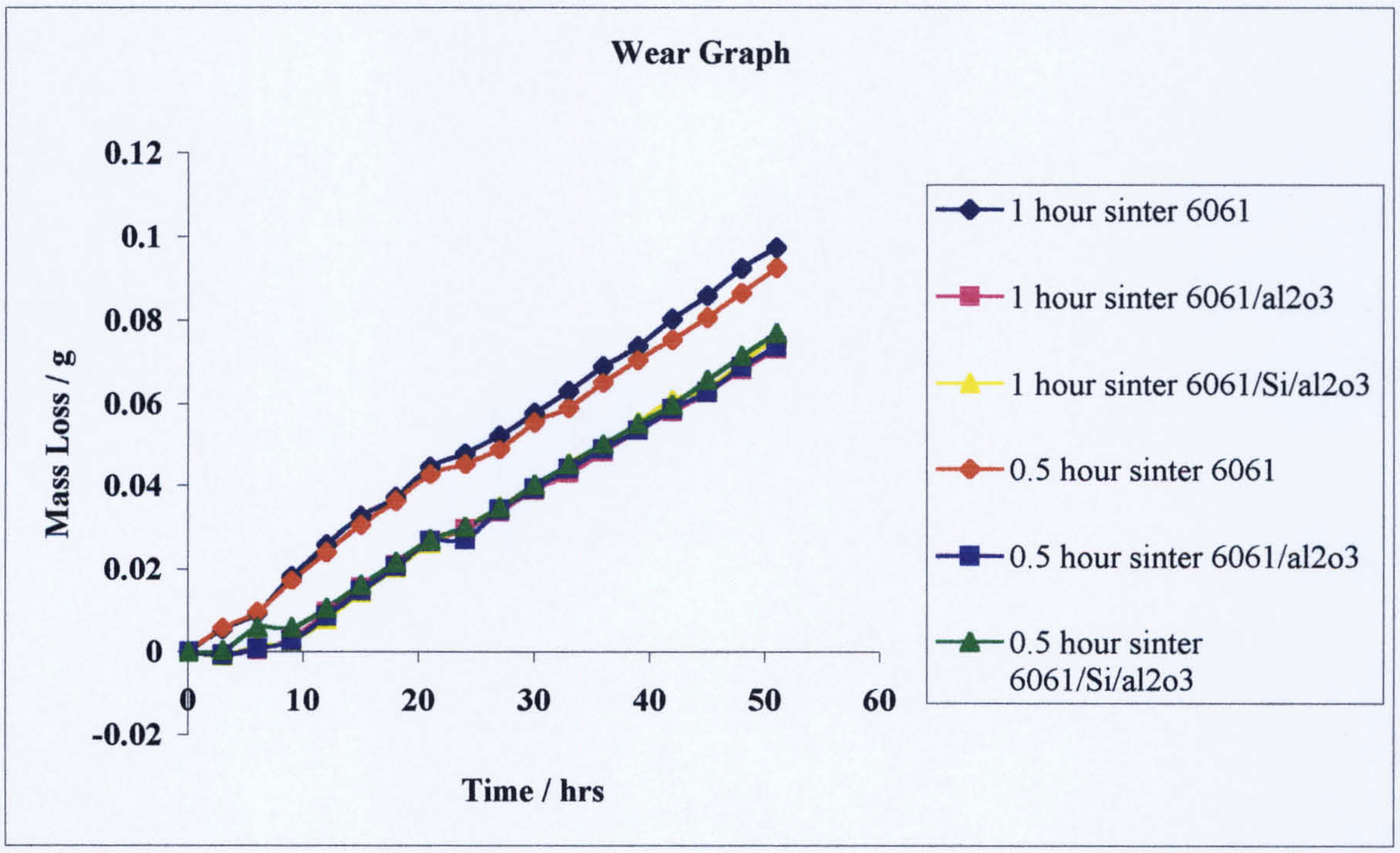

Figure 24. graph displaying that the monolithic alloys after 30 minute and 1 hour sinter regimes perform similarly after 51 hour wear testing , with the 1 hour sintered alloy performing slightly poorer. All MMCs performed similarly, with all outperforming the monolithic alloys.

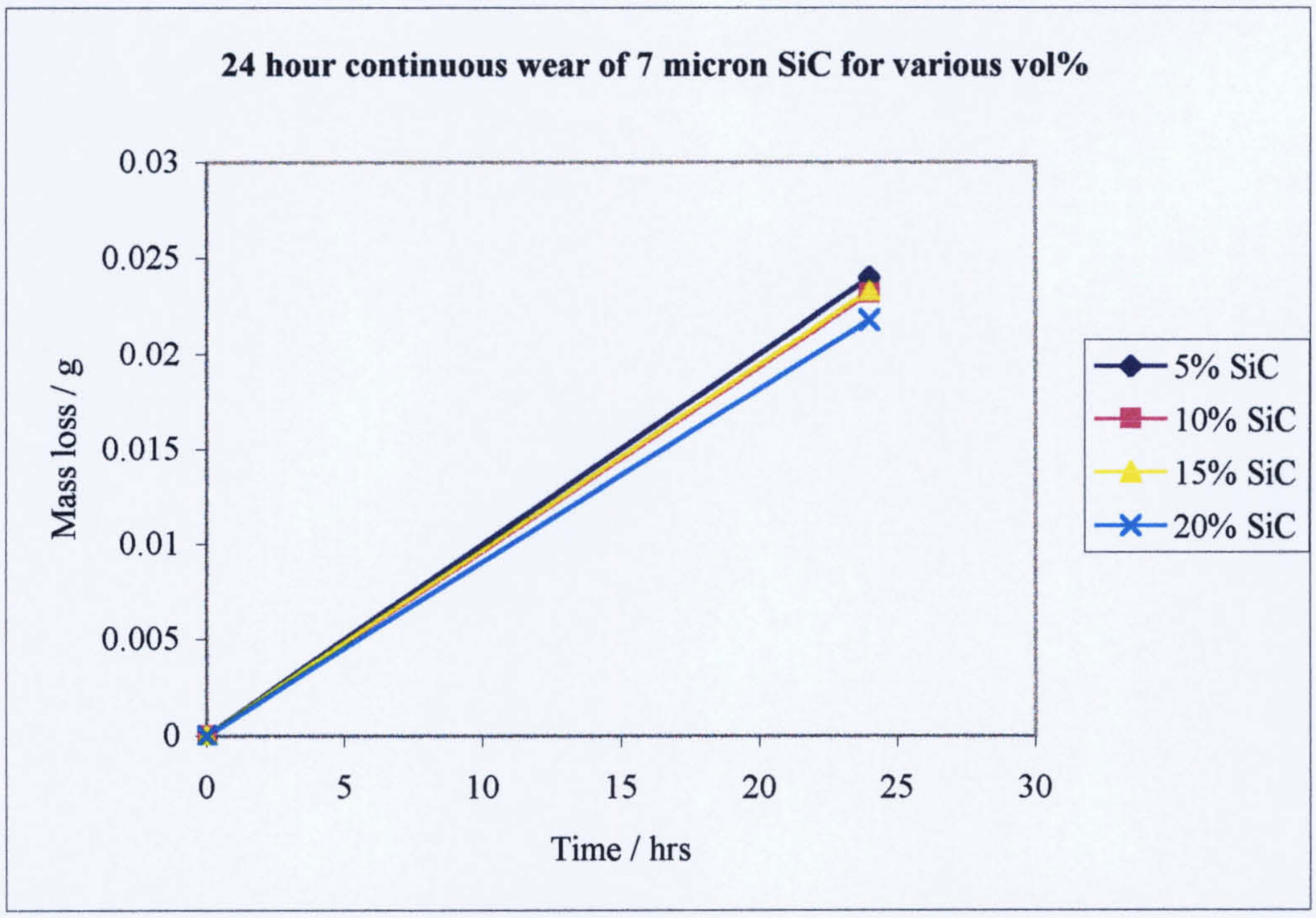

Figure 25. Graph showing that as percentage SiC is increased then wear resistance increases for 7 μm reinforcement.

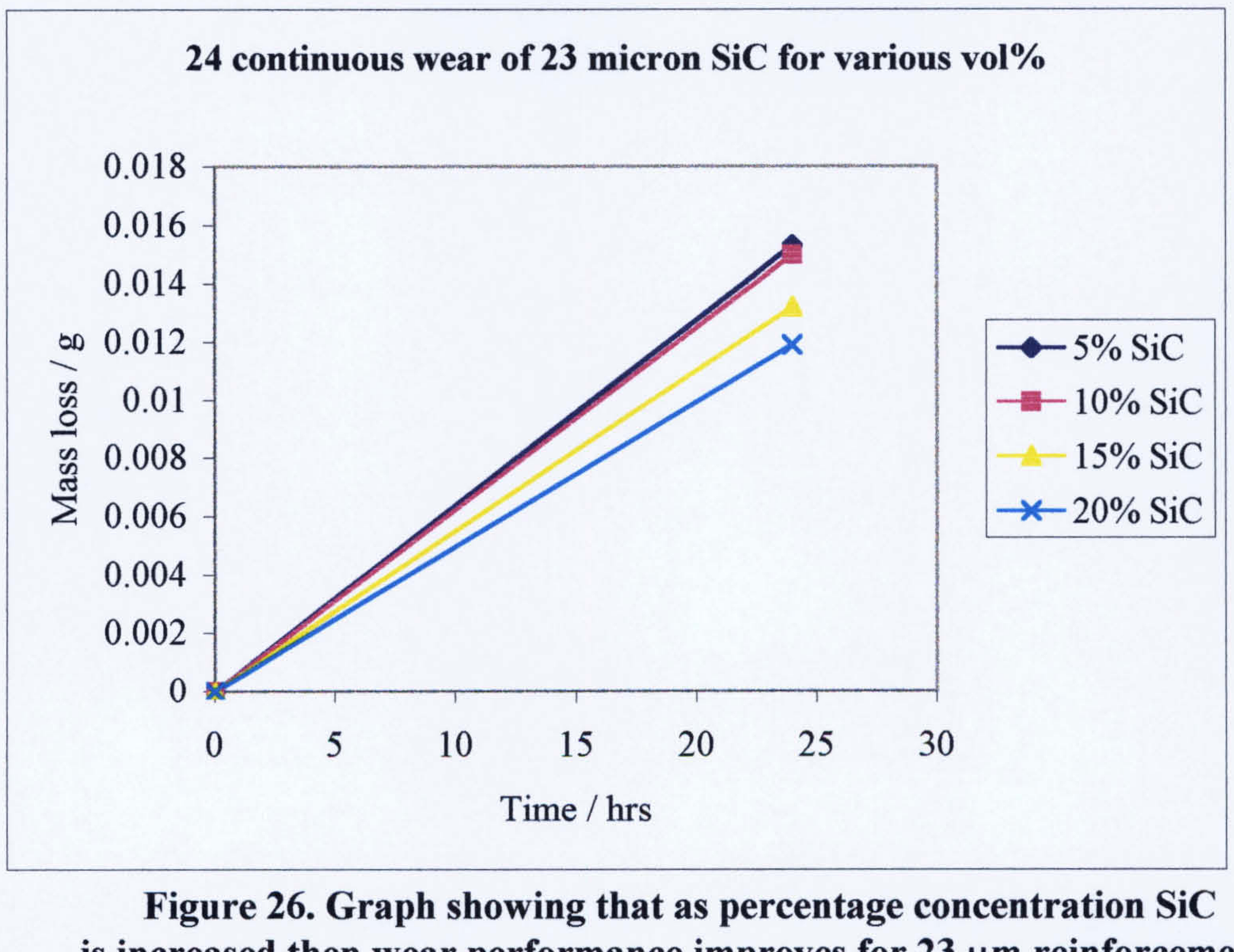

Figure 26. Graph showing that as percentage concentration SiC is increased then wear performance improves for 23 μm reinforcement.

By comparing graphs Figures 25 and 26 it is seen that particle size has an effect on the wear performance of these composite materials. The large 23μm particle composites out perform the 7μm containing composites for wear resistance.

4.5 Electroless Cu Coating of Al_2O_3 Particulates Results.

Copper coating of alumina particles.

The copper coating of the alumina particles is to attempt to create a barrier coat of copper to reduce any reaction between alumina and magnesium present in the alloy.

Formaldehyde versus hydrazine as reducing agent.

The formaldehyde (HCHO) method, based on a method described by Leonida [Leonida 1889], requires sensitisation and activation steps to achieve Cu deposition on to a ceramic surface. Sensitisation uses tin (II) chloride, ($SnCl_2$) and activation uses a catalyst palladium (II) chloride ($PdCl_2$). Hydrochloric acid (HCl) and a stabiliser ammonium chloride (NH_4Cl) are required for the activation / sensitisation procedure. The copper bath procedure requires potassium sodium tartrate ($C_4H_4KNaO_6 \bullet 4H_2O$), sodium hydroxide (NaOH), copper sulphate ($CuSO_4$) and formaldehyde for the necessary reactions to take place.

The hydrazine (N_2H_4) method, based on a method described by Bhatgadde [Bhatgadde 1983], does not require any sensitisation or activation pre-cursor to the Cu bath. Cupric acetate and hydrazine are the only chemical required and the Cu bath is the only procedure necessary. The hydrazine method appeared to be a quicker, and more efficient method of copper deposition on to the alumina particulates.

4.6. Metallographic Examinations.

4.6.1. Optical Microscopic Analysis.

- In terms of wear, optical microscopy revealed severe ductile deformation in the monolithic alloys (appendix 1. Plate 3). The image shows material from the wear surface has been displaced (curled at the edges of the wear sample). The composite wear samples did not show this severe displacement of attached material (appendix 1. Plate 4). Optical microscopic analysis also revealed that the wear surfaces displayed similar patterns of wear for both monolithic and composite materials (appendix 1. Plates 5 and 6).
- The addition of Mg and Si to the 6061-Al_2O_3 composites resulted in changes to the surface morphology for each sample tested. it was observed that an addition of 5wt% Mg to the 6061-10 wt%Al_2O_3 composite resulted in severe blistering on the surface of the material after a 1-hour sinter (appendix 1. Plate 7). The monolithic 6061 alloy and the composite containing 10 wt% Al_2O_3 both displayed a moderate surface roughness with no severe blistering evident (appendix 1. Plates 8 and 9). The composite which contained 5 wt% Si displayed a low surface roughness with no visible blistering.
- From optical microscopic analysis of copper coated Al_2O_3 spherical and irregular tabular particulates the images were difficult to interpret as both showed a large amount of copper coloured material. An example of an image is shown in appendix 1. Plate 11.

4.6.2. Scanning Electron Microscopic (SEM) Analysis.

- SEM analysis of Al_2O_3 tabular shaped particles coated with Cu using formaldehyde as reducing agent identified that there was extensive agglomeration of the particulates (appendix 1. Plate 12). SEM analysis of Al_2O_3 spherical shaped particles coated with Cu using formaldehyde as reducing agent showed that there was reduced agglomeration. There are however very small discrete particles present (appendix 1. Plate 13). Analysis of Al_2O_3 tabular shaped particles coated with Cu using hydrazine as reducing agent identified some agglomeration of the particulates (appendix 1. Plate 14). The SEM micrograph of Al_2O_3 spherical shaped particles coated with Cu using hydrazine as reducing agent (appendix 1. Plate 15) presents an image showing there is little agglomeration with no discrete small particulates present.

- Porosity in the sintered MMC's was evident in the Al_2O_3 reinforcement regions (appendix 1. Plate 16). This would account for the lower density measurements reported elsewhere in section 4.2. This level of porosity was not evident in the monolithic alloy (appendix 1. Plate 17) - again supporting the density observations.

- With respect to wear, SEM analysis identified that the principal type of wear was "gouging" (appendix 1. Plate 18). From analysis of the grooves in the wear tested Al_2O_3 containing composites, there was evidence of Al_2O_3 fragmentation within areas of pitting which may result in the formation of the grooves (appendix 1. Plate 19).

- With increasing sinter time, scanning electron microscopy revealed increased surface roughness - see appendix 1. Plates 20 and 21. Plate 20 represents the surface after sintering at 600°C for 5 hours and plate 21 represents the surface at identical sinter temperature for 30 minutes.

- SEM micrograph observations for Al_2O_3 particulate distribution throughout the matrix showed a good distribution with little agglomeration (appendix 1. Plate 24).

4.6.3. Energy Dispersive X-ray Analysis.

- EDX analysis obtained from copper coated Al_2O_3 particulates. From the spectra presented below it is shown that the method using formaldehyde gave higher copper peaks than the spectra obtained from the hydrazine method. The amount of copper observed is similar when the two shapes of particulates are considered for each method. For example copper content for Figure 27 is comparable to Figure 28. Similarly copper content for Figure 29 is comparable to Figure 30. Figure 31 displays the spectra for small discrete particles, which were previously reported in section 4.6.2. The EDXA identifies these small discrete particles as elemental copper.

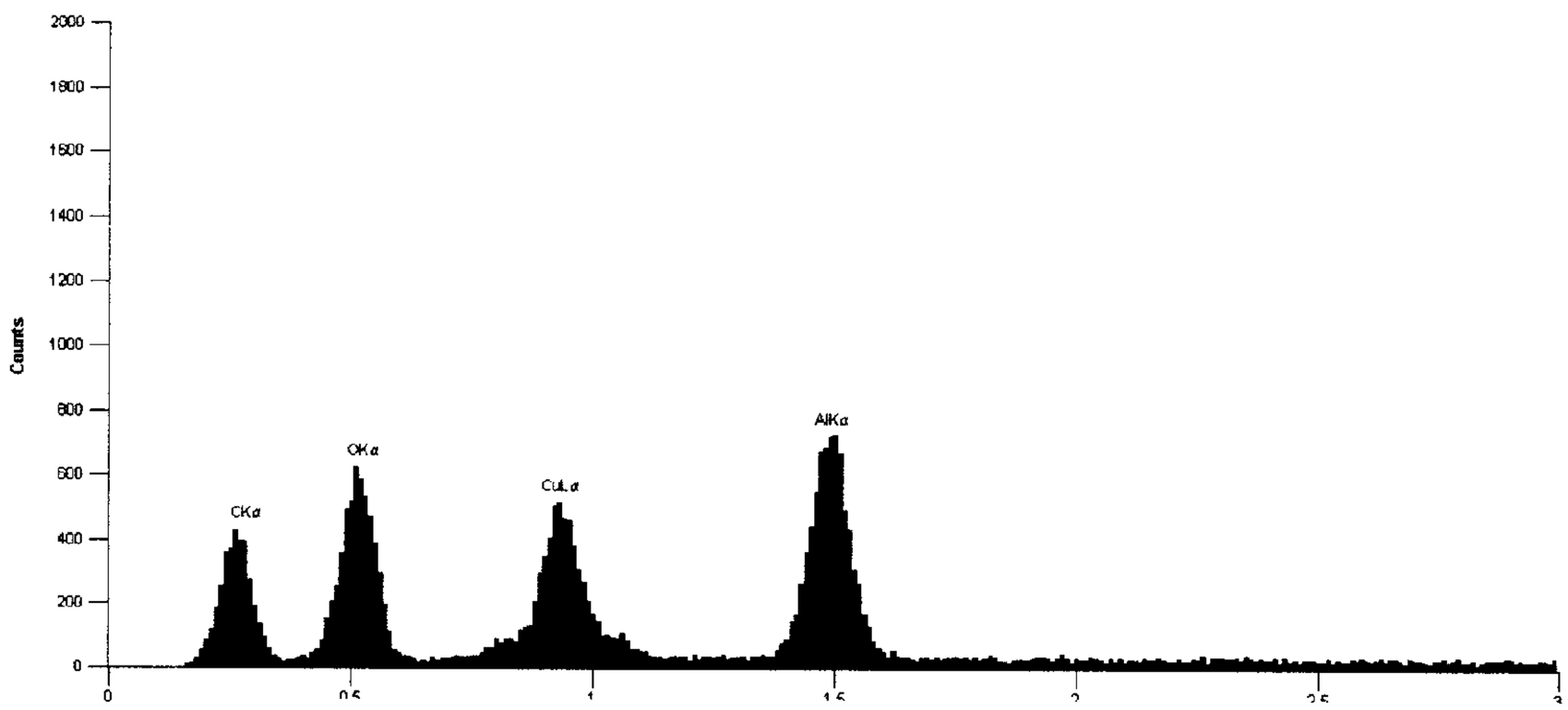

Figure. 27. EDX spectra of tabular shaped Al_2O_3 particles coated with Cu using formaldehyde as reducing agent.

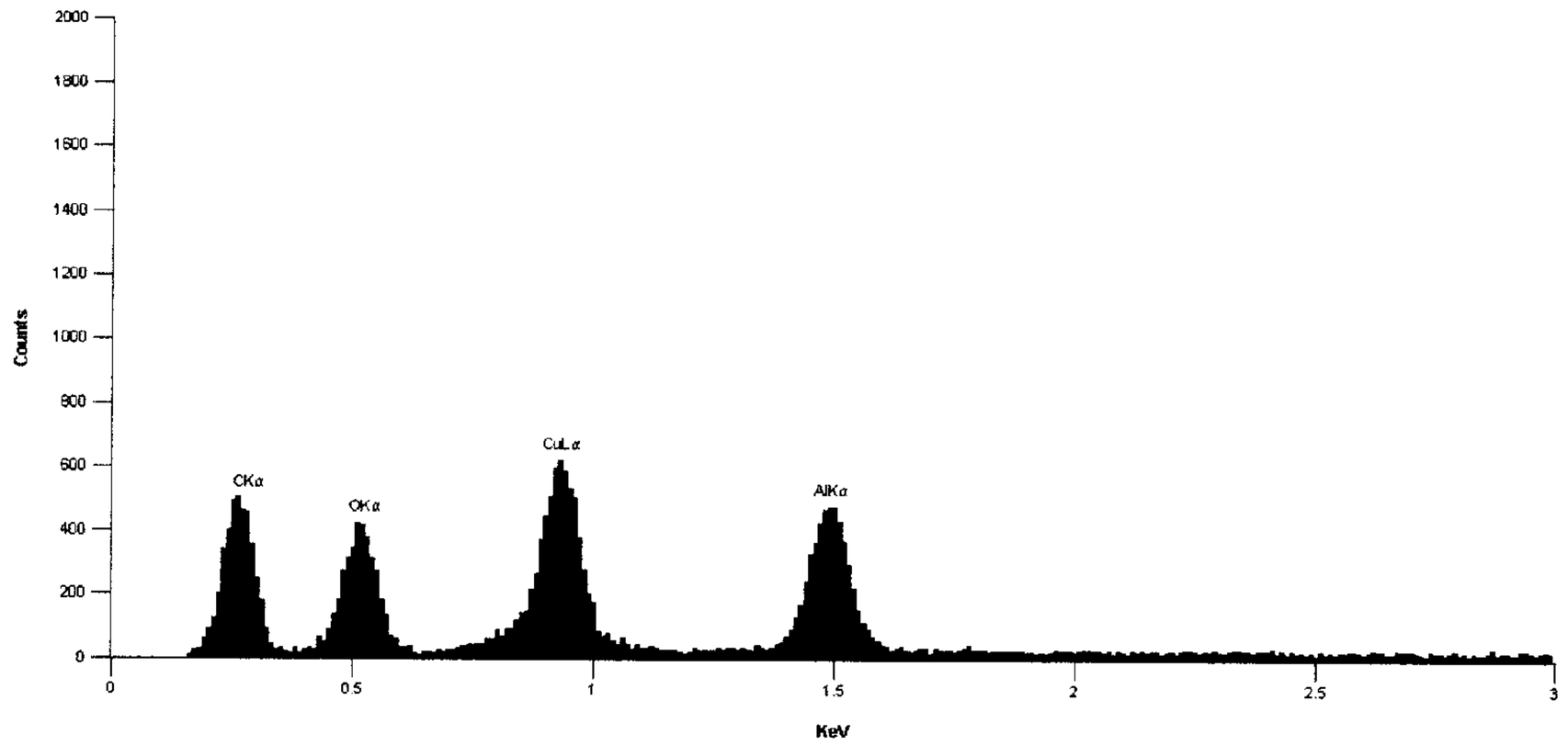

Figure 28. EDX spectra of spherical Al_2O_3 particles coated with Cu using formaldehyde as reducing agent.

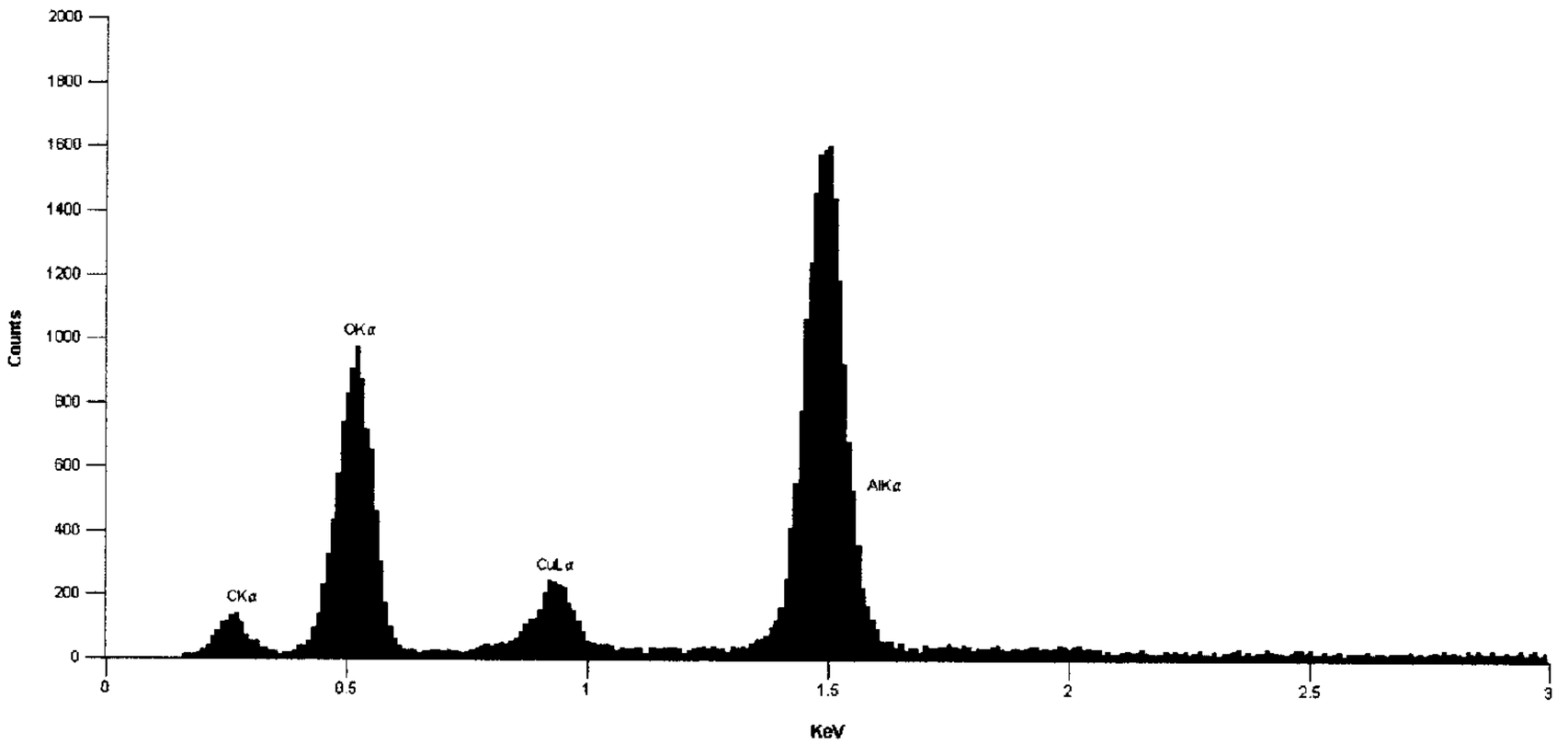

Figure 29. EDX spectra of spherical Al_2O_3 particles coated with Cu using hydrazine as reducing agent.

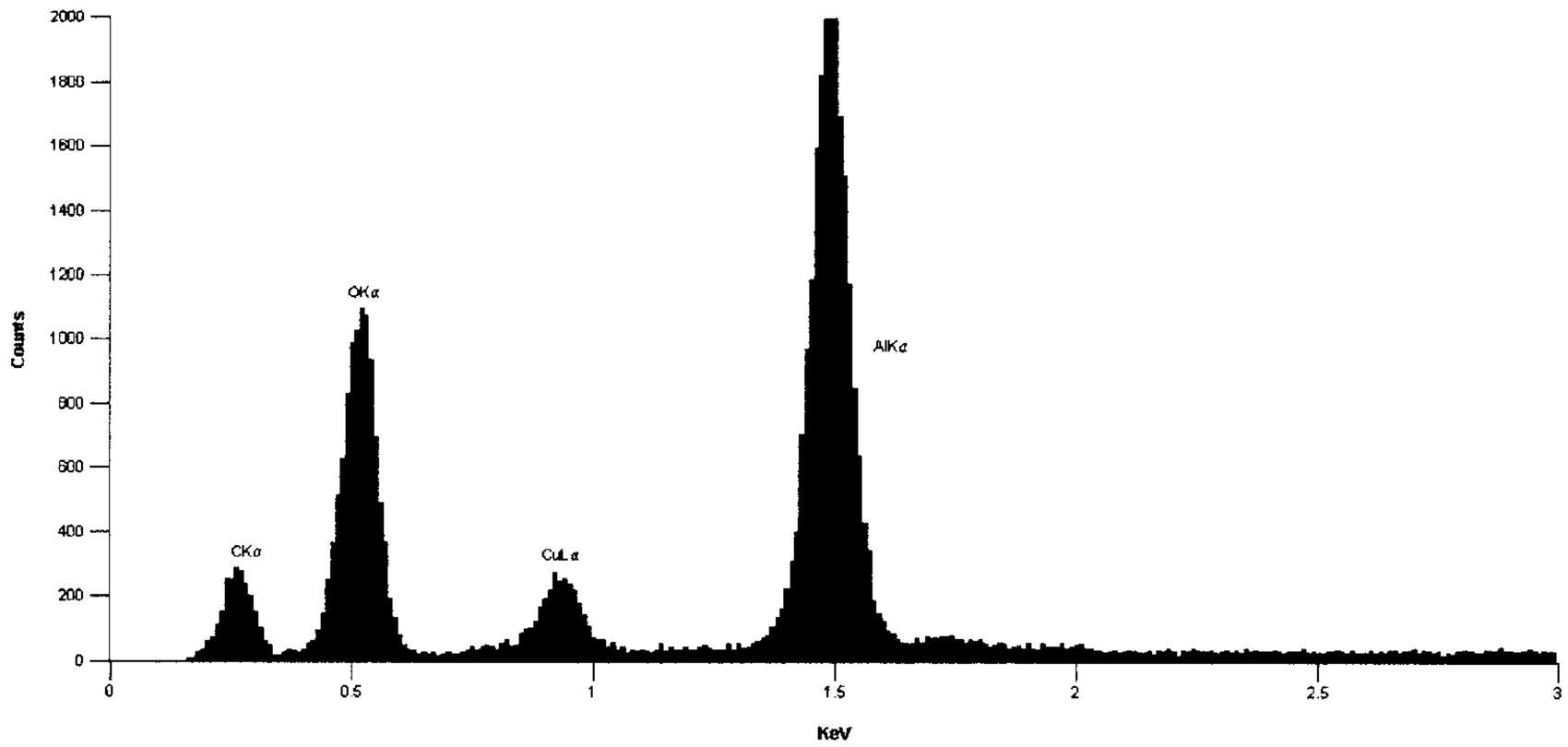

Figure 30. EDX spectra of tabular Al_2O_3 particles coated with Cu using hydrazine as reducing agent.

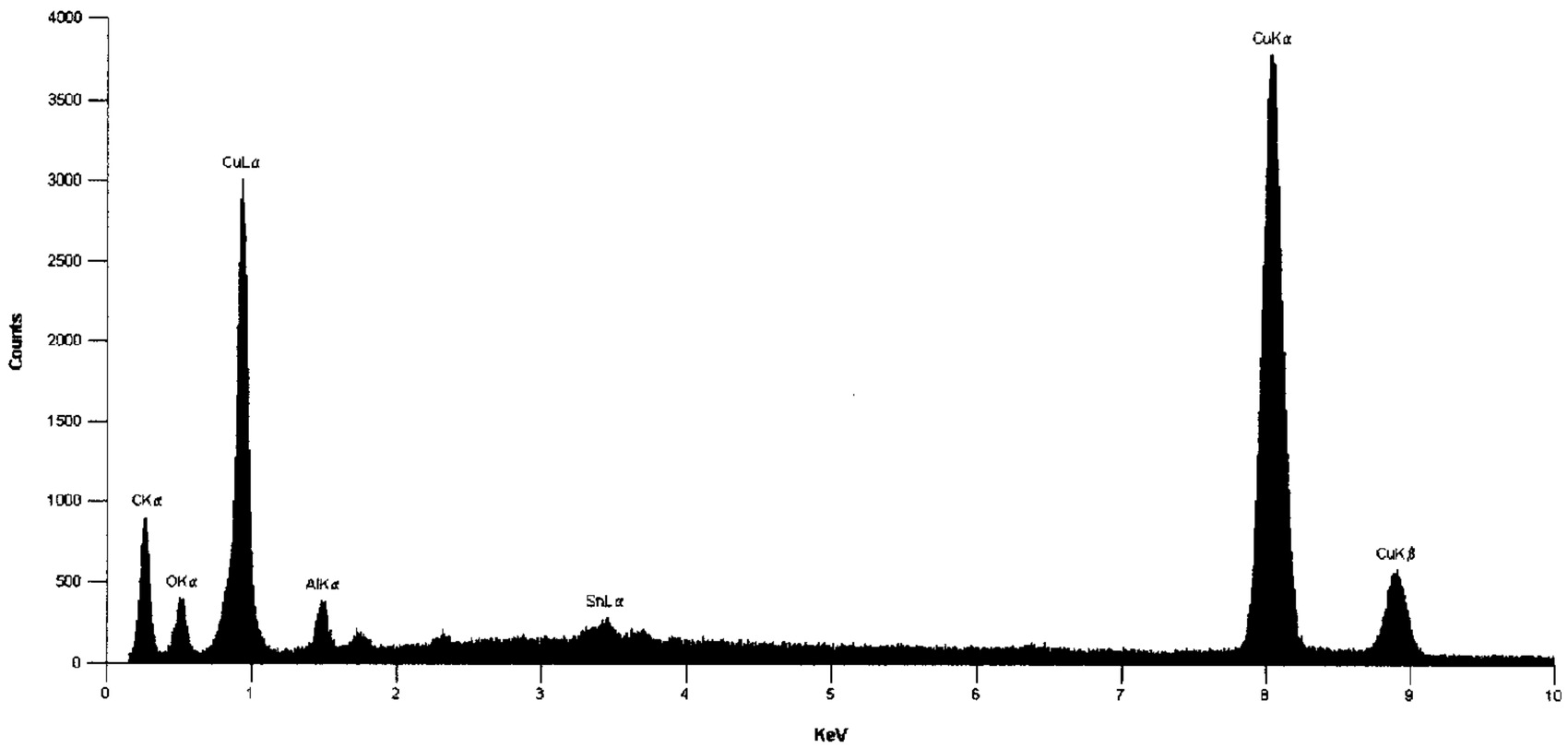

Figure 31. EDX spectra (spot analysis) of a small discrete particle from analysis of spherical Al_2O_3 particles coated with Cu using formaldehyde as reducing agent. This spectra displays a high Cu concentration >90 wt%. The small Sn peak is a remnant of the activation stage for Cu plating.

- EDX analysis of Al_2O_3 particulate containing composites displayed that there was no magnesium present in the matrix regions, "away" from the Al_2O_3 particulates, after a 5-hour sinter (Figure 32).

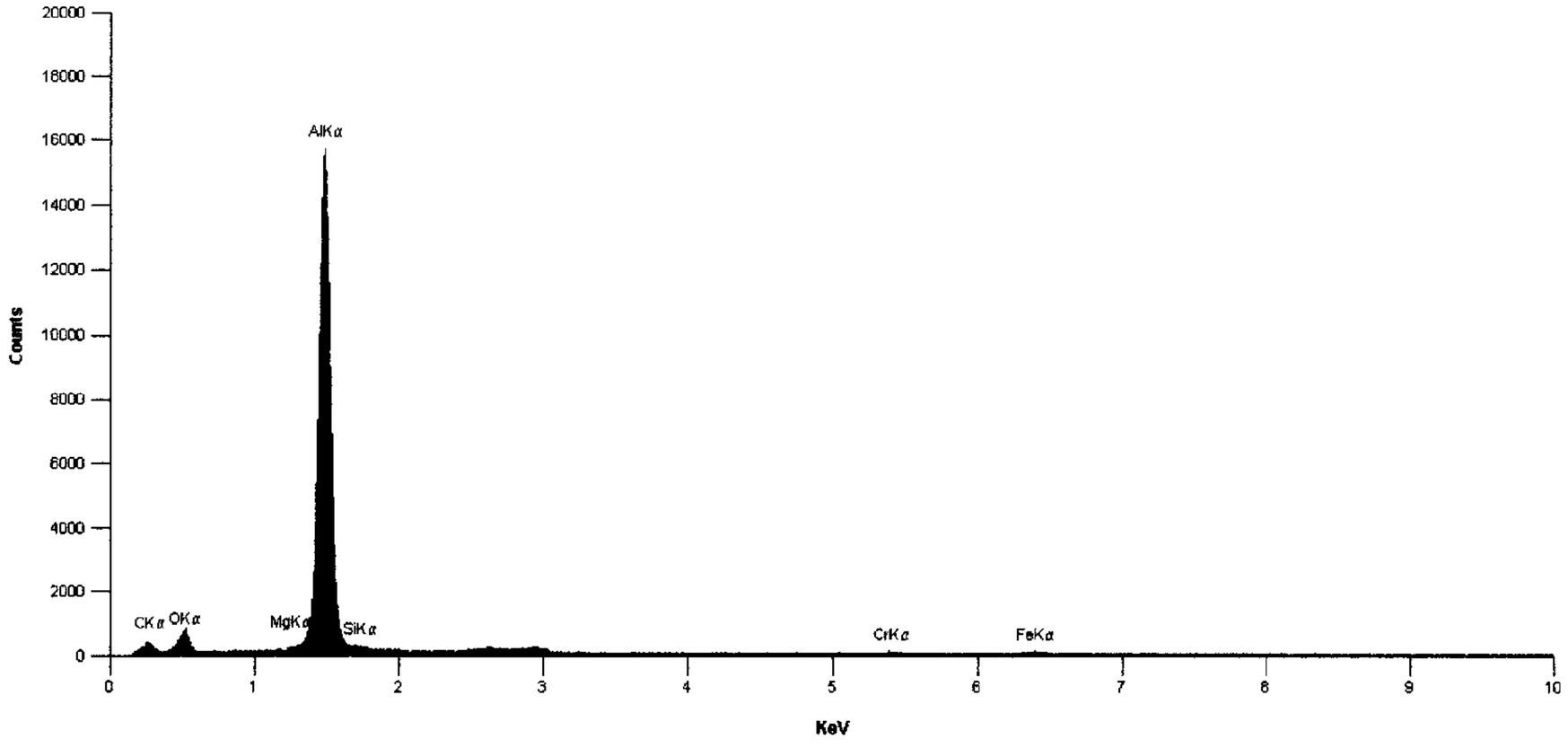

Figure 32. EDX spectra from a matrix area "away" from Al_2O_3 particulates. Note no Mg and limited Si concentrations are observed. This spectra was obtained following a 5-hour sinter treatment.

With the 5-hour sinter time, large concentrations of Mg were found at the interface region between the Al_2O_3 particulates and the 6061 matrix. This is demonstrated in Figure 33.

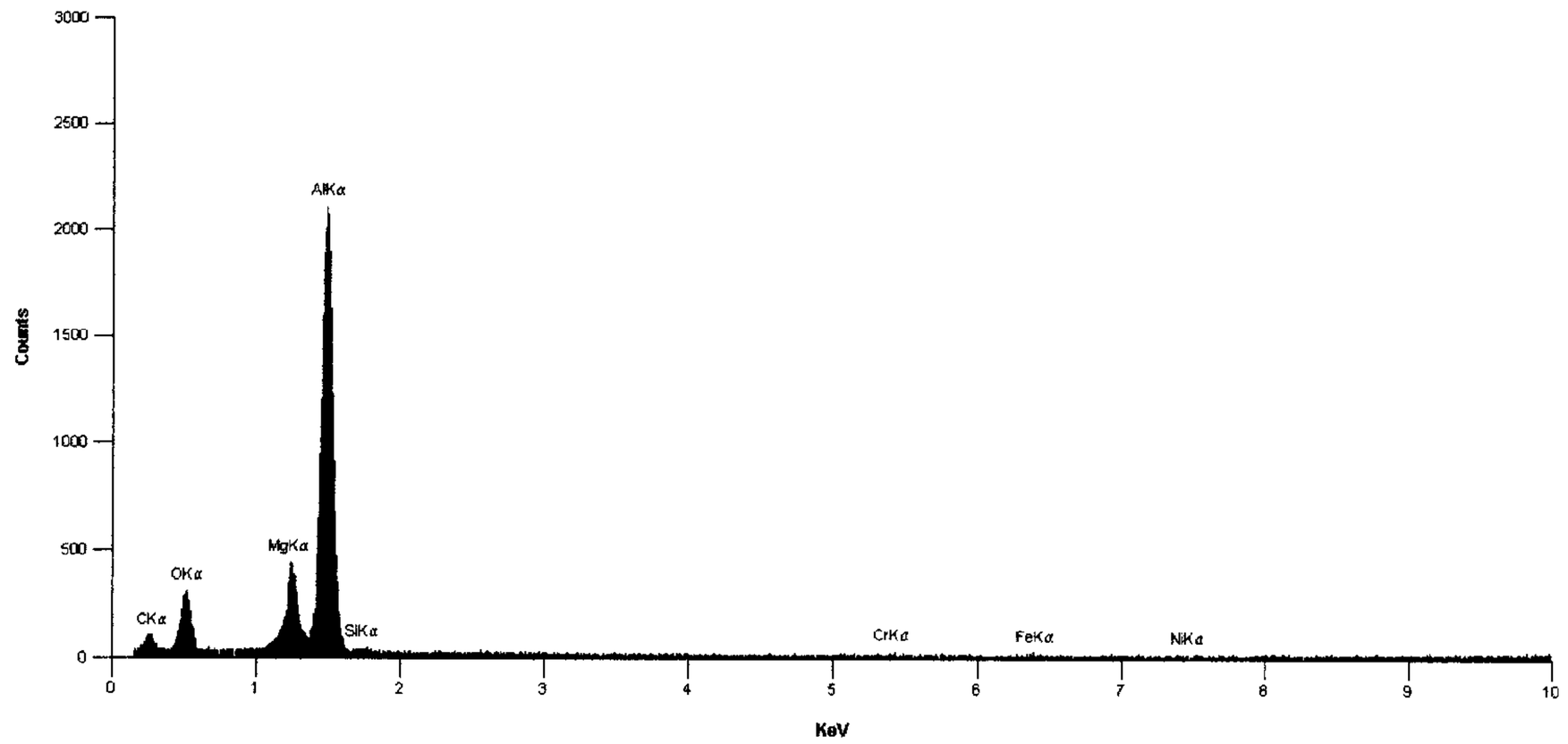

Figure 33. EDX spectra showing increased Mg concentrations near to interface of Al_2O_3 particle and 6061 matrix.

- With a 30-minute sinter time, the above observations were much less pronounced, as seen in spectra, Figure 34.

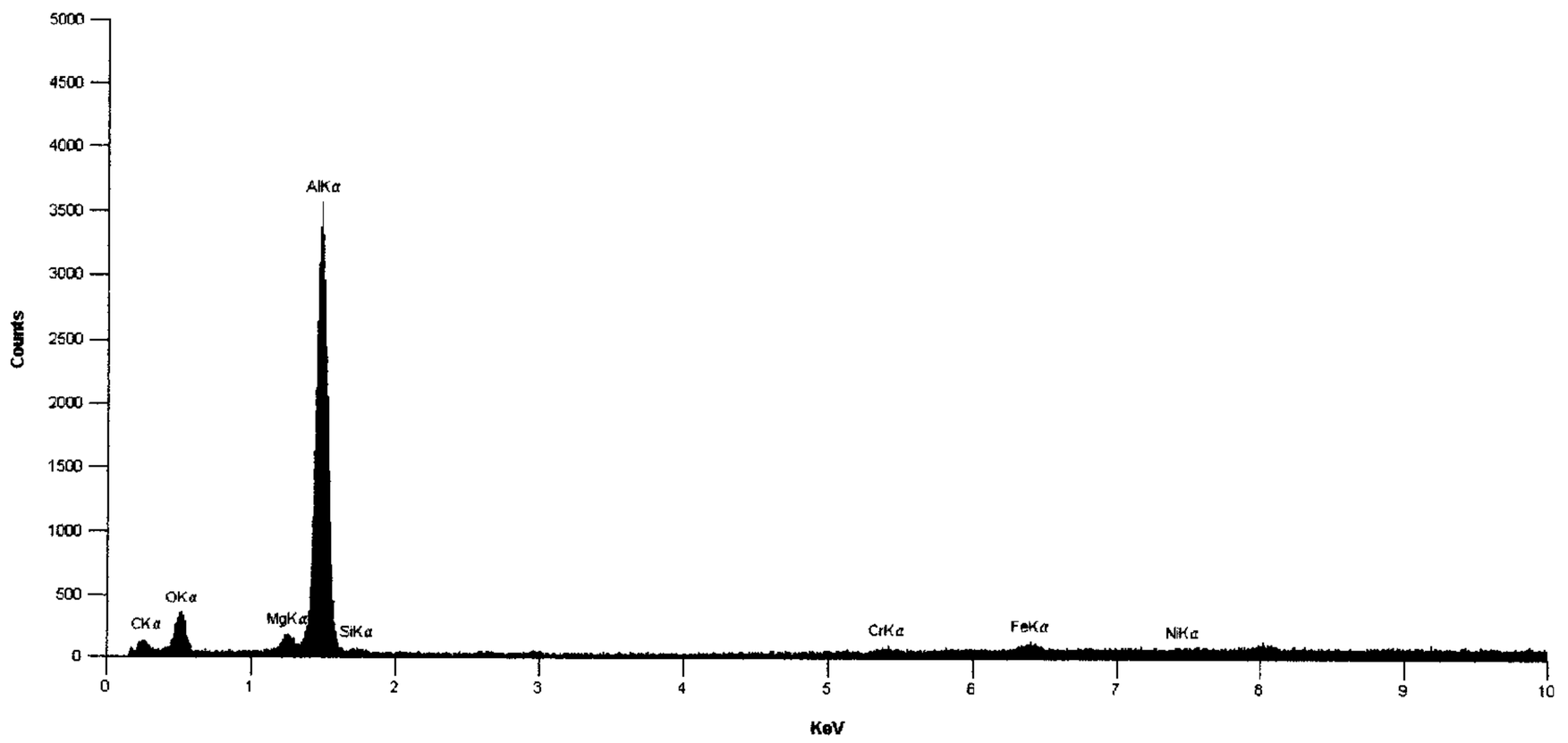

Figure 34. EDX spectra showing reduced Mg concentrations near to Al_2O_3 - 6061 matrix interface.

An SEM micrographic image (appendix 1. Plate 22) displays the areas in the composite materials, which displayed high and low concentrations of Mg.

Also identified from EDX analysis was the localised high concentrations of Si at or near to the surface of 5 hour sintered composites. Figure 35 below shows the EDX spectra obtained from a localised area of Si at the edge of an Al_2O_3 containing composite. Similar Si concentration was found at the surface of the monolithic 6061 alloy, which was also sintered for 5 hours. (see appendix 1. Plate 23. for an example micrograph of an area within monolithic 6061 alloy where a high Si concentration was found.

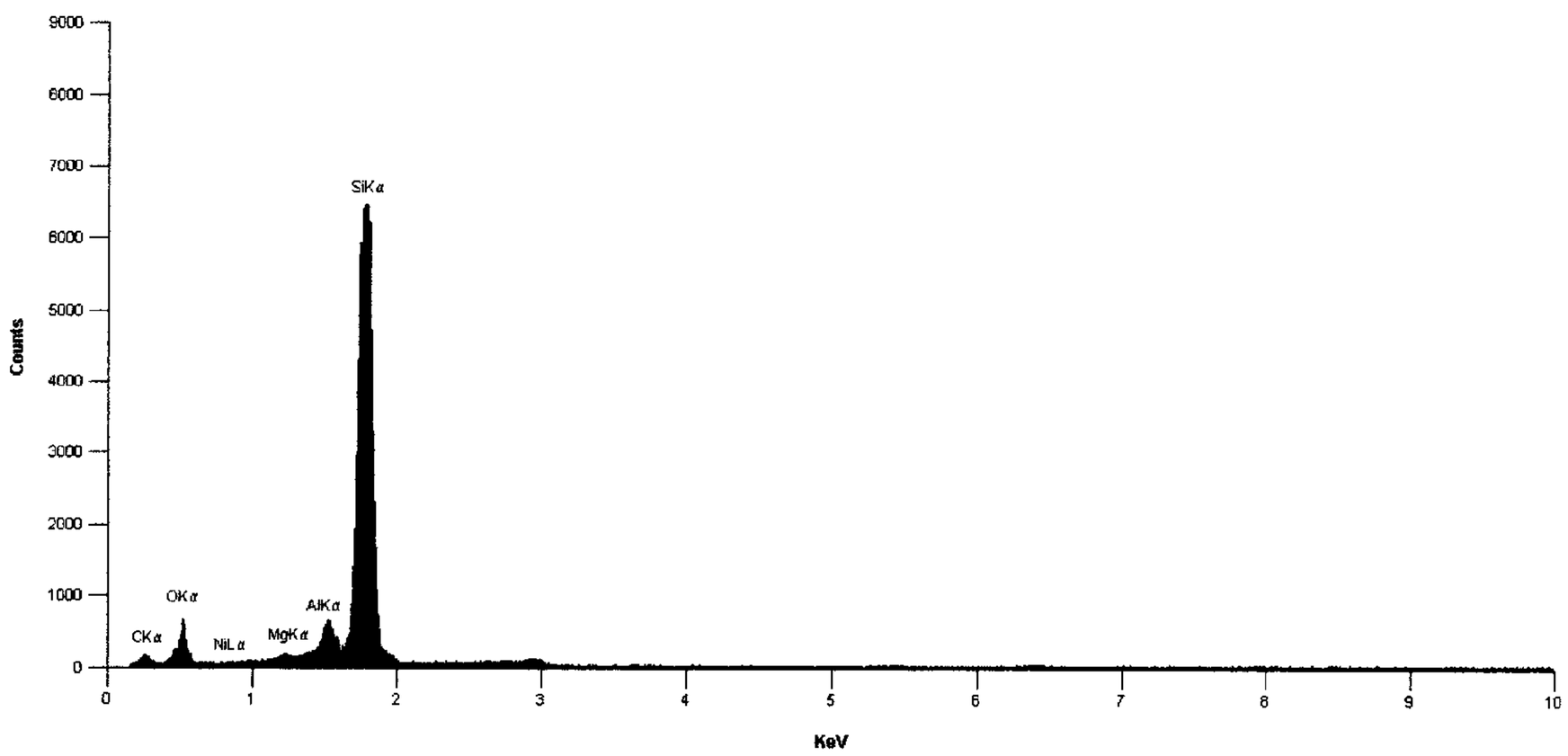

Figure 35. EDX spectra (spot analysis) showing a high concentration of Si on surface of Al_2O_3 containing composite.

- From EDX analysis it is found that adding 5-wt% Si to the Al_2O_3 containing composites the Mg concentration can be maintained at a higher level within the matrix for sinter times of one hour. See Figures 36, 37, 38 and 39 below.

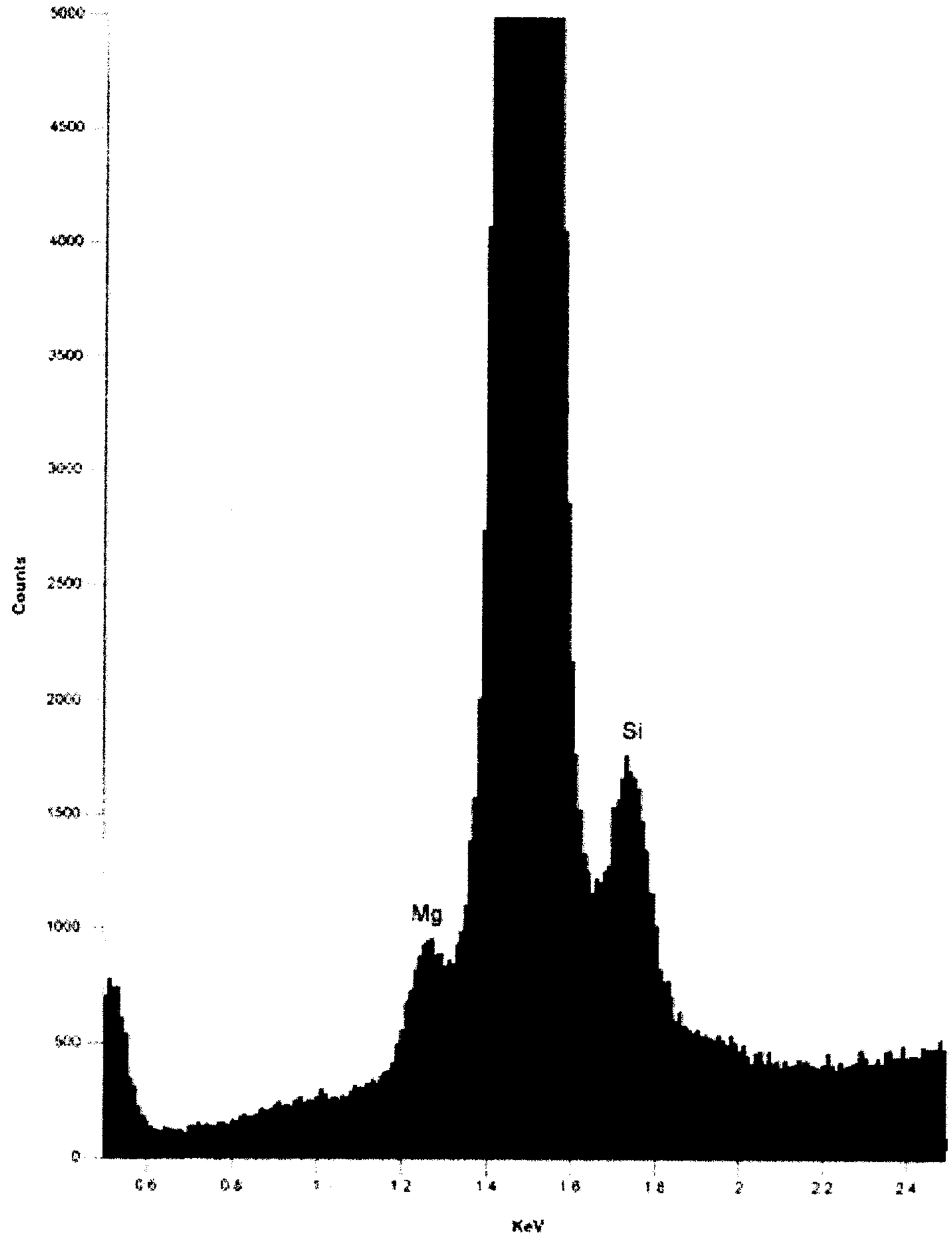

Figure 36. Spectrograph of matrix area in Al 6061/5% Si/10%Al_2O_3 after 1 hr sinter at 600°C. Note Mg retention in matrix.

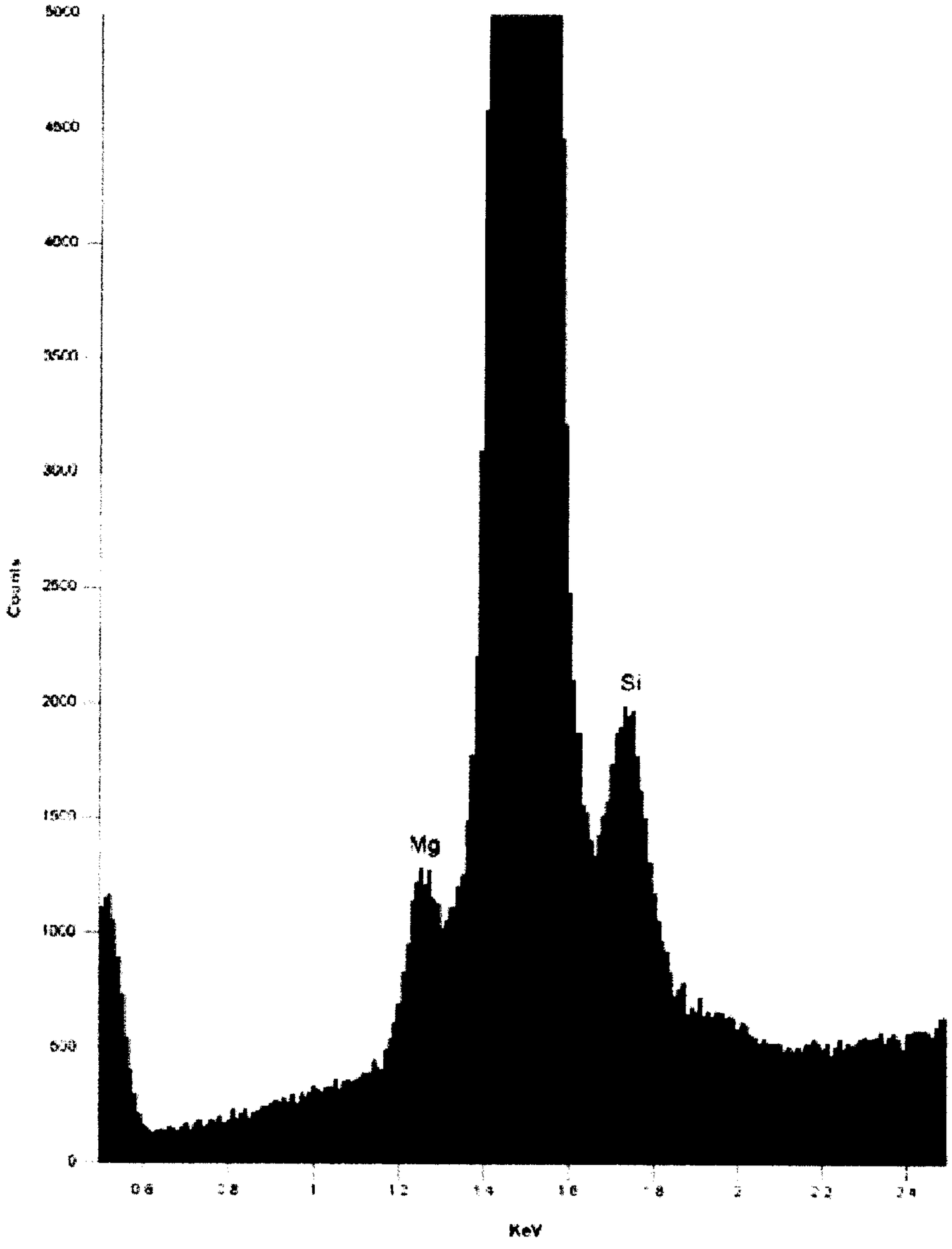

Figure 37. Spectrograph of area around Al_2O_3 particle in Al 6061/5% Si/10%Al_2O_3 after 1 hr sinter at 600°C. Note increase in Mg concentration compared to Figure 36.

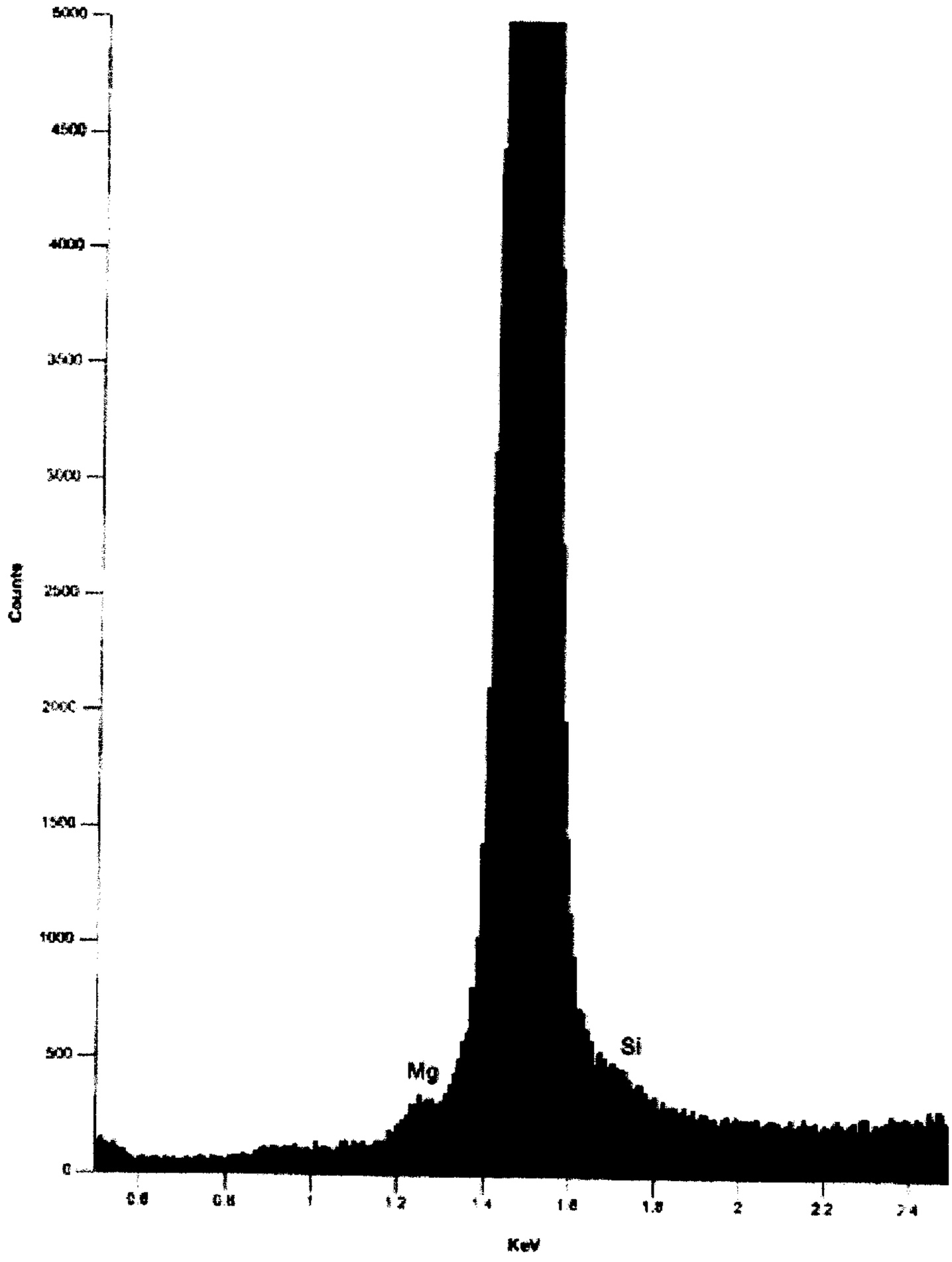

Figure 38. Spectrograph of matrix area in Al 6061/10%Al_2O_3 after 1 hr sinter at 600°C. Note depletion of Mg in matrix compared to Figures 36 and 37, which had added Si.

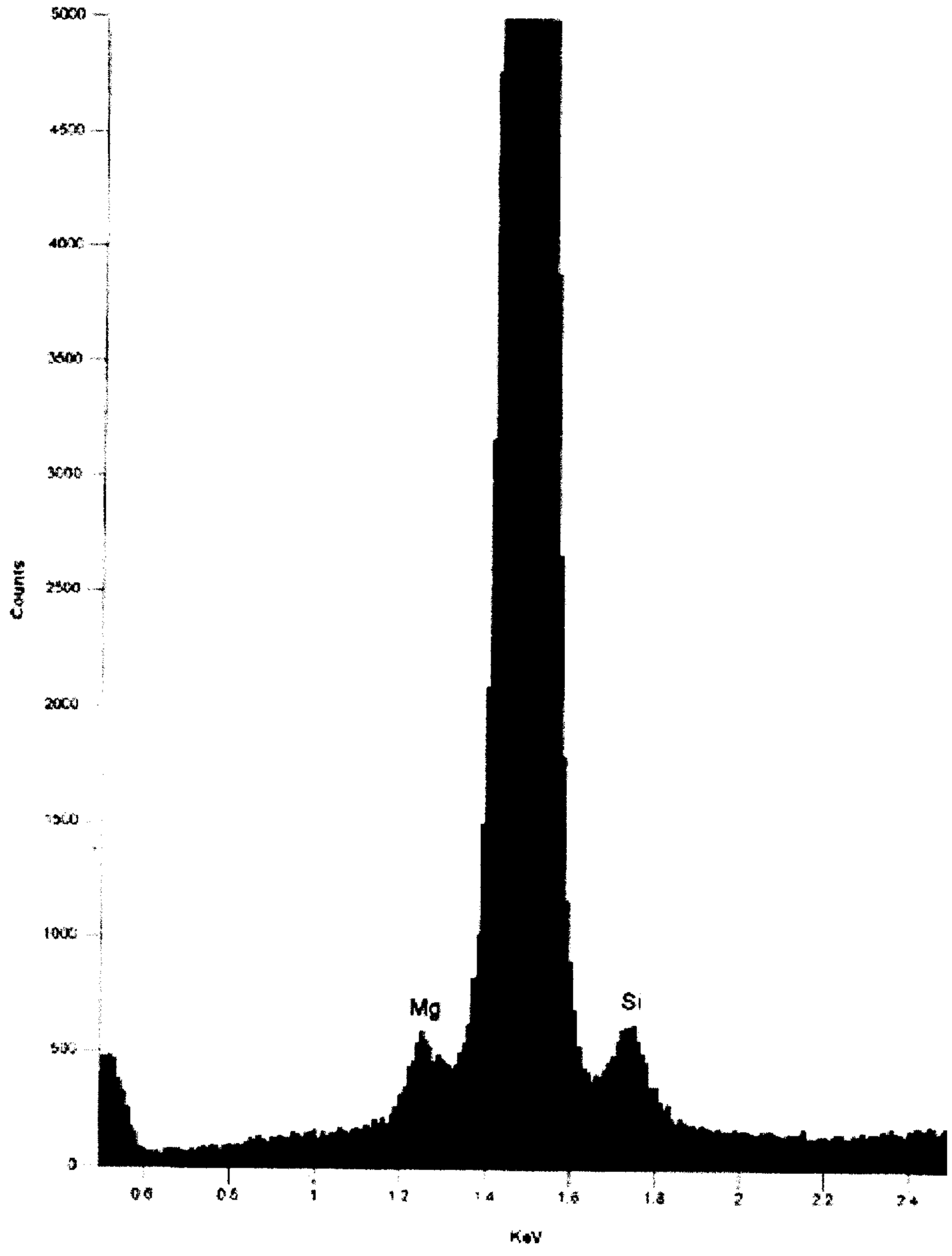

Figure 39. Spectrograph of area around Al_2O_3 particle in Al 6061/10%Al_2O_3 after 1 hr sinter at 600°C. Note Mg concentration is increasing around the Al_2O_3 particulate compared to the matrix spectra in Figure 38.

Chapter 5.

Discussion of Results.

5.1. Introduction.

In this chapter the results presented in chapter 4 will be discussed.

5.2. Density Measurements.

Final densities of the monolithic alloys were found to be very satisfactory with 98 - 99 % theoretical density being measured. Similarly good densities were achieved with SiC reinforced composites. However, with increasing Al_2O_3 content there was an observed decrease in measured density. This is attributed to agglomeration of the particulates, which causes localised sintering difficulties. The addition of Si and Mg to Al_2O_3 containing composites resulted in no improvement in the density of the metal matrix composites.

There was no effect of sinter time on the density pattern observed above. This would support the suggestion of Al_2O_3 particulates agglomeration being the root cause of observed density reduction.

5.3. Hardness Measurements.

Age hardening of the monolithic 6061 alloy resulted in peak hardness values at 8 hours heat treatment time.

As shown in Table 15 (5 hour sinter), there was an increase observed on the addition of SiC compared to the monolithic alloy. However, any inclusion of Al_2O_3 particulates resulted in a marked reduction in measured hardness values. From

SEM/EDXA analysis strong evidence of magnesium migration from the "body of the matrix" towards the Al_2O_3 particulates was recorded. It is postulated that this magnesium depletion in the matrix prevents the formation of Mg_2Si, thereby nullifying the age hardening mechanism. This would support the decreased hardness observed. However, in Table 16, it is seen that this reduction in hardness is much less pronounced for a 30-minute sinter time. Again, this is supported by SEM/EDXA observations showing reduced magnesium depletion in the "body of the matrix".

Increasing the magnesium concentration by elemental addition (to attempt to compensate for magnesium migration) still resulted in low hardness values. However, when elemental silicon was added (Table 18), shorter sinter times resulted in higher hardness levels being retained for thirty minutes and one-hour sinter times. hardness levels then fall for longer sinter times. This would corroborate EDXA results, which showed silicon migration from the matrix to the surface, over longer sinter periods.

There appears to be a dynamic mass migration of silicon to the surface, and magnesium to the Al_2O_3 interfacial regions, and that this phenomenon is influenced by the presence of extra elemental silicon, as well as sinter time. One possible explanation for the magnesium migration is the lowering of the systems energy due to the formation of spinel ($MgAl_2O_4$), and has been observed by other researchers [Janowski 1990; Suery 1993]. It is postulated that a similar lowering of energy within the system is the driving force for the silicon migration to the materials surface. Further detailed research would be required to determine the effect of factors such as diffusion rates of magnesium and silicon, under various conditions, on the chemical kinetics of this system.

5.4. Wear Results.

As shown in Figure 19, there is an improvement in the wear resistance of the composites when the SiC content is increased. This is to be expected because of the superior wear properties of the SiC reinforcement. The effect of size of SiC reinforcement is demonstrated in Figures 25 and 26. They again show that increasing the percentage of reinforcement results in enhanced wear resistance, but they also show that the larger sized SiC (23μm) out performs the smaller size (7μm) particulates. From a surface area point of view, the smaller sized particles should have superior wear resistance but they may be less well embedded into the matrix. A possible explanation for this observed behaviour is that if reinforcement pull out is part of the wear mechanism, then the smaller contact area between reinforcement and matrix for individual smaller particulates would account for easier removal of the particulates, thereby contributing more to the wear mechanism.

For the 5-hour sinter Al_2O_3 reinforced metal matrix composites, the general trend is one of improved wear resistance compared to the monolithic alloy. However, the fact that the matrix hardness (which may infer wear resistance) decreases with the presence of Al_2O_3 particulates, may counteract the expected wear resistance benefit from the ceramics additions.

For thirty-minute sinter times with composites containing Al_2O_3 the wear resistance is improved (Figures 23 and 24), the addition of excess silicon improves the performance of the one hour sintered composites. This improvement in wear resistance is attributed to the retention of magnesium in the matrix and an improvement in the structural integrity of the overall composite.

The results obtained for aluminium 2000 series alloy and composite were used only as a comparison and no definite wear pattern was established.

The observations of material displacement due to ductile wear, which results in material being removed from the wear surface but is still attached to the wear sample, was seen to a great extent in the monolithic alloys which were wear tested (appendix 1. Plate 3). This attachment of material leads to incorrect wear measurements when the method of wear assessment is measuring mass loss from a sample. It is noted that ductile wear was not observed to a great extent in any of the composite wear samples. Therefore, the wear performance of the monolithic alloys can be considered to be poorer than the measurements taken in this study would suggest. It can be concluded that the wear comparisons between composite and alloy should be more marked.

The wear patterns observed for both monolithic alloy and composite materials displayed similar patterns. Both showed grooving or gouging on the wear surface. The Al_2O_3 containing composites displayed ceramic fragmentation, which would add to the overall wear mechanism. The fragmented particles would be displaced from the wear surface and result in a three-body wear mechanism possibly causing increased wear.

5.5. Surface Effect Observations from adding Elemental Si and Mg.

When 5 wt% Mg was added to the composites (attempt to reduce Mg depletion from the matrix) the surface was observed to blister. This is attributed to concentration gradients of Al and Mg throughout the composite resulting in excessive liquid formation due to the conditions being satisfied for the creation of localised eutectics in the Al - Mg system. This is supported by the phase diagram (Figure 40) for Al - Mg [Scientific Group 2002], which shows a large portion, would be liquid at various concentrations at the sinter temperature of 600°C. The addition of silicon to the composite resulted in a less rough surface than the composite or the monolithic alloy.

This is attributed to concentration gradients occurring throughout the composite resulting in less liquid (melting) forming. The phase diagram (Figure 41) shows a large concentration range, which would not be liquid at the sinter temperature of 600°C [Scientific Group 2002].

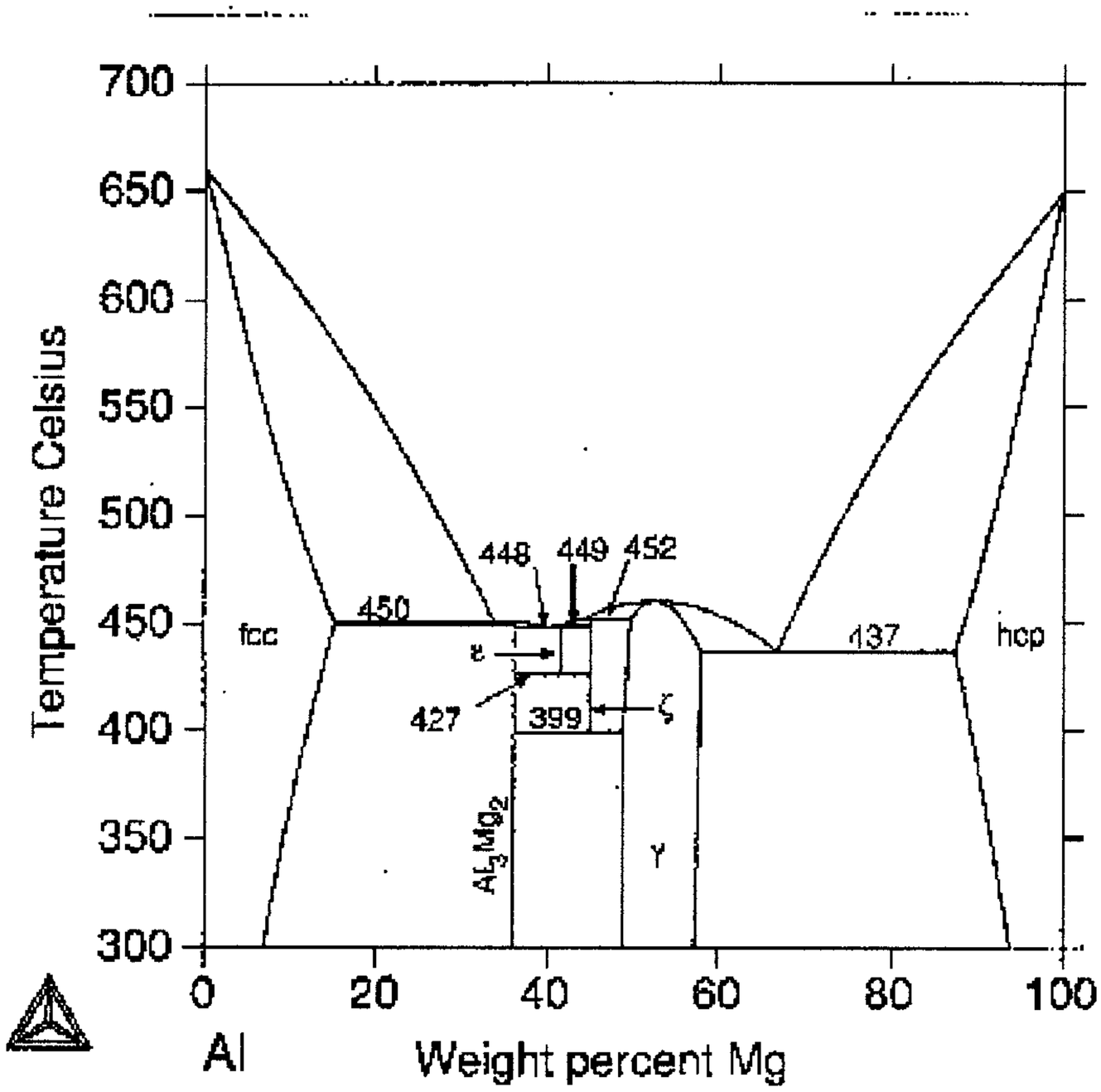

Al-Mg Crystal Structure Data

Phase	Pearson Symbol	Struktur Bericht	Prototype	Model
fcc	cF4	A1	Cu	RK
Al_3Mg_2	cF1168		Cd_2Na	CE
ε				CE
ζ				CE
γ	cI58	A12	(αMn)	CE
hcp	hP2	A3	Mg	RK

N. Saunders,Chalpad Vol 14 (1990) pp 61-70

Figure 40. Phase diagram for the binary Al - Mg system [Scientific Group 2002].

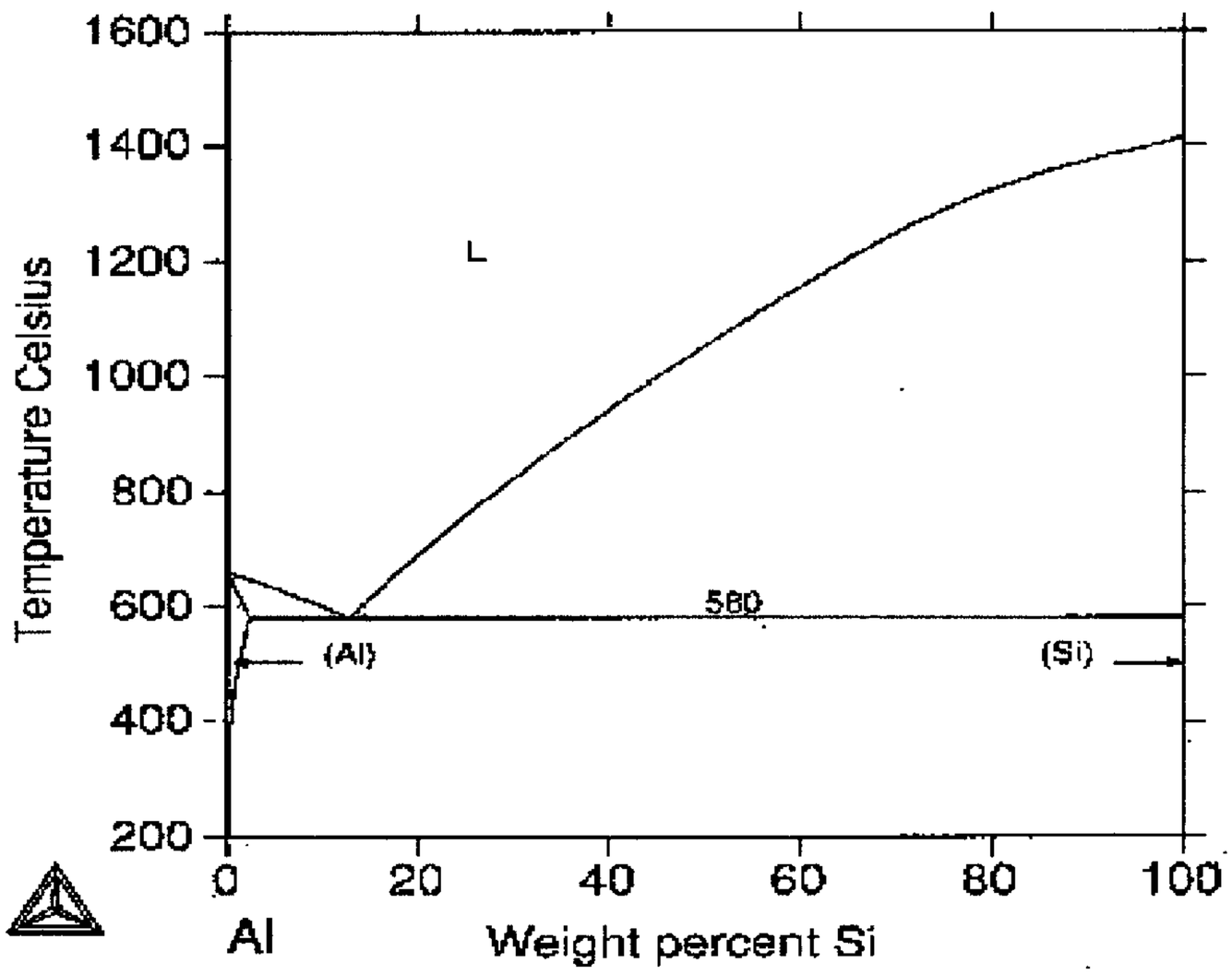

Al-Si Crystal Structure Data

Phase	Pearson Symbol	Struktur Bericht	Prototype	Model
(Al)	cF4	A1	Cu	RK
(Si)	cF8	A4	C(diamond)	RK

D. Ludecke, Z. Metallkde Vol 77, (1986) p 278-283

Figure 41. Phase diagram for Al - Si binary system [Scientific Group 2002].

5.6. Electroless Coating of Al_2O_3 Particles.

The copper coating of Al_2O_3 tabular particles using the formaldehyde process showed extensive agglomeration of the particles. Also observed in the spherical particulates coated using the formaldehyde process were discrete small particles of copper. It is suggested here that the agglomeration of the tabular type particulates is due to their shape and to small particles of copper "binding" them together. The tabular or irregular shaped particulates will have a greater surface area and more surface energy (sharp corners, crevices), therefore a greater attraction for particles. It is postulated that the greater surface area of irregular particulates compared to spherical particulates also allows more of each particle to come into contact with each other thereby lowering the surface energy of the system. The presence of small particles of copper observed in the spherical shaped copper baths are attributed to poor copper coating on to the ceramic particles. This may be due to the stages required for copper deposition, namely sensitisation and activation stages. If these stages are not carried out effectively then the copper deposition will be hindered. The large copper peaks observed for the particulates coated with copper using the formaldehyde method are attributed to a large percentage of elemental copper being "free", that is not coating the ceramic but existing as separate "flakes" of copper.

The hydrazine method proved to be much more successful. The spherical particulates appeared to be coated with a film of copper with no agglomeration and the irregular shaped Al_2O_3 displayed much less agglomeration than the previous formaldehyde method had shown. This superior copper deposition is attributed to the relative simplicity of the method, with only a copper bath necessary and no activation or sensitisation steps, which have the potential to prevent deposition. Again there was more agglomeration for the tabular/irregular shaped particulates than for the spherical

shaped ceramic, this agglomeration is attributed to surface energy interaction between particulates.

Chapter 6.

Conclusions

6.1. Conclusions.

- With extended sinter times, one hour and over, the effect on Al_2O_3 - aluminium 6061 composites is detrimental. Mg migration towards the interfacial region between the Al_2O_3 reinforcement and the 6061 matrix is observed. The Mg concentration at the interface increases with sinter time.
- There may be a preferential reaction for the formation of $MgAl_2O_4$ resulting in a reduction of Mg_2Si precipitates, also the increased dislocation density (less order, higher energy) surrounding the Al_2O_3 particles may have an effect on the Mg distribution.
- The depletion of Mg in the matrix leads to a reduction in matrix hardness, because the intermetallic Mg_2Si cannot form in the age hardening process.
- The addition of Si to the composite mixture aids the retention of Mg in the matrix for up to one-hour sinter times.
- The addition of Mg into the composite mix has no beneficial effect, in fact it is detrimental to the material and severe blistering on the surface is observed.
- Silicon migration to the surface of the composites was observed over long sinter times, greater than one hour.
- Age hardening of the composites aluminium 6061 matrix was not successful for longer sinter times (greater than 30 minutes) when Al_2O_3 is used as the reinforcement.
- From experimental work the most effective method of producing composites, up to 5 mm thick, using cold pressing and vacuum sintering has been found to be:

Pressing at 400 MPa; Vacuum sinter at 600°C for 30 minutes; Solution heat treat for 30 minutes at 530°C then water quench; Precipitation (ageing) heat treat for 7 hours at 175°C then air cool.

- EDAX analysis supports the theory that there is magnesium depletion in the matrix leading to reduced measured hardness values in Al_2O_3 containing composites. EDAX shows low concentrations of magnesium in matrix with higher concentrations being found at interfacial regions, which becomes more apparent for longer sinter times.
- Ductile wear is observed mainly in monolithic aluminium 6061 alloys (this phenomenon was not observed to any extent in composite wear samples) - this moving of attached material was not taken into account when determining wear performance (wear determined by measuring mass loss - not mass movement).
- For Al_2O_3 containing composites the 30-minute sinter time produced better wear and hardness results - possibly due to the retention of magnesium in the matrix and the reduced amount of spinel ($MgAl_2O_4$) formation at interfaces.
- With increasing Al_2O_3 content, there was a measured reduction in composite densities - possibly due to agglomeration of the Al_2O_3 particulates, resulting in localised sintering problems.
- Addition of silicon and/or magnesium resulted in no improvement of density - this having no effect on particulate agglomeration.
- Varying the sinter time for Al_2O_3 containing composites had no effect on the final densities measured.
- The wear resistance of SiC containing composites showed an improvement when SiC content was increased.

- The wear performance of SiC containing composites showed an improvement when the composite contained large particles (23μm) compared to composites containing smaller particles (7μm).
- It was noted that there was a greater degree of pull out of the larger (23 μm) SiC particles than for the smaller (7 μm) particles. An example of the pullout observed is given as a micrograph from a composite containing 7 μm SiC particles in Appendix 1 25. This improved performance for the composites containing the larger particles may be due to more surface area of each larger individual particulate in contact with the matrix, compared to the smaller (low surface area for each individual particulate in contact with matrix) particulates.
- Al_2O_3 containing composites did not perform as well as SiC composites. This may be due to agglomeration, the low hardness of the matrix making a small contribution to wear resistance and the Al_2O_3 particulates fragmenting while bearing most of any forces applied during wear testing.
- The observed wear mechanism for Al_2O_3 containing composites is fragmentation of particulates leading to gouging and three body wear mechanism.
- The addition of magnesium to composites resulted in excessive surface blistering during sintering - this is attributed to local Mg/Al concentrations liquefying.
- The copper coating of Al_2O_3 particulates displayed that the method using hydrazine gave better results than tests using formaldehyde as the reducing agent. The hydrazine method showed a uniformity of coating and no discrete copper particles (as were observed in the formaldehyde tests).
- For both hydrazine and formaldehyde copper-coating experiments the spherically shaped Al_2O_3 was found to produce a better copper covering with reduced agglomeration compared to the irregular tabular shaped particulates.

- Sinter times should be kept to a minimum for Al_2O_3 - aluminium 6061 composites as no benefit in terms of hardness or density was observed for longer sinter times.
- The method of producing discontinuously reinforced aluminium based composites has proven successful using a simple blending, cold pressing and vacuum sintering technique.
- Age hardening treatments were successful for monolithic aluminium 6061 alloy and SiC containing composites.
- It was found that when the matrix consisted of 2000 series aluminium alloy (containing 4wt% Cu) these composites outperformed the 6000 series (containing Mg and Si) matrix for wear resistance.

6.2. Recommendations for Future Research.

The following are recommendations for future research, which will continue from the study presented in this thesis.

- To copper coat Al_2O_3 particulates using the hydrazine coating method presented in this thesis, and include them in an aluminium 6061 matrix to form a composite.
- To investigate the sintering temperatures and times to establish whether the copper coated reinforcements are of benefit to retaining magnesium within the matrix of aluminium 6061 - based composites.
- Further research heat treatments of the copper coated reinforcement compared to non-coated composite materials and examine if revision of times and temperatures are required to achieve improved composite performance.
- To examine the wear performance of composites containing copper coated reinforcements to identify if the copper improves the wear resistance of the composites.
- To investigate other mechanical properties of composites containing copper coated reinforcements, for example is there any change in bend strength, fatigue performance or hardness.
- Investigate any possible corrosion problems that may occur by including copper coated reinforcements into aluminium alloys. Due to the more reactive nature of aluminium compared to copper could the aluminium behave as a sacrificial metal when combined as a coating on the reinforcement within the composite?

- Pursue the findings found during this research, which found that 2000 series aluminium alloy when used as the matrix material, outperformed the 6000 series alloy in wear resistance studies.
- Examine and compare the interfacial regions between Al_2O_3 reinforcements and 2000 series and 6000 series aluminium alloys. identify any deleterious or beneficial compounds found in the interfacial regions.
- An examination of the diffusion of alloying species (Mg, Si, Cu) in monolithic alloys compared to alloys used as the matrix in composites containing Al_2O_3 reinforcing particulates.

References

Abraham, S., Pai, B. C., Satyanarayana, K. G. and Vaidyan, V. K. *Copper coating on fibres and their composites with aluminium matrix.* Journal of Materials Science. **27.** 1992. pp. 3479-3486.

Alahelisten, A., Bergman, F., Olsson, M. and Hogmark, S. *On the Wear of Aluminium and Magnesium Metal Matrix Composites.* Wear, 1993. **165** (2). pp. 221-226.

Alliston-Grenier, A. *Guidelines for laboratory Wear Testing.* The 1996 Donald Julius Groen Prize Lecture, Institute of Mechanical Engineering. December 1996.

Anan'in, V. N., Romanenkov, V. E. and Smirnova, T. A. *The Sintering Mechanism of Aluminium Powder.* Dokl. Akad. Nauk BSSR, **31** (9). 1987. pp. 818-820.

Antoniou, R.A. *Wear Behaviour of Aluminium-based MMCs Containing SiC Particulates.* In: Proceedings First Australian Surface Engineering Conference. Adelaide: (March 1992). pp.51-54.

Appendino, P. and Badini, C. *6061 Aluminium Alloy-SiC Particulate Composite: A Comparison Between Ageing Behaviour in T4 and T6 Treatments.* Materials Science and Engineering, 1991. **A135.** pp. 275-279.

Archard, J. F. *Contact and Rubbing of Flat Surfaces.* Journal of Applied Physics, 1953. **24.** pp. 981-988.

Arsenault, R.J. and Romero, J.C. *A Comparison of Interfacial Arrangements of SiC/Al Composites.* Scripta Metallurgica et Materialia. 1995, **32**(11), pp. 1783-1787.

Askeland, D.R. *The Science and Engineering of Materials.* 3rd ed. London: Chapman and Hall, 1998.

ASTM Standard G40. *Standard terminology relating to wear and erosion.* American Society for Testing and Materials, 1999.

Baptista, A.P.M. and Pinto, M.A. *Tribological Properties of Sintered and Forged Aluminium Composites.* In: International Conference on Composite Materials 9. Madrid: 1993. pp. 510-517.

Bhatgadde, L. G. and Mahaptra, S. *A Novel Electroless Technique for Copper Metallization of Alumina Substrates.* Solid State Technology. Dec. 1983. pp. 181-184.

Blackburn, L. D., Herzog, J. A., Meyerer, W. J., Snide, J. A., Stuhrke, W. F. and Brisbane, A. W. *MAMS Internal Research on Metal Matrix Composites.* MAM-TM 66-3. 1966.

British Standards Institution (15 June 1993) BS EN 23369:1993 (ISO 3369:1975) *Impermeable sintered metal materials and hardmetals. Determination of density.* London, BSI.

Callister, W.D. *Materials Science and Engineering: An Introduction*. 3rded. New York: John Wiley and Sons Inc. 1994.

Calhoun, R. B. and Dunand, D. C. *Dislocations in Metal Matrix Composites.* In: Kelly, A and Zweben, C. Comprehensive Composite Materials, Vol. 3. Oxford: Elsevier Science, 2000. pp. 27-60.

Chung, S. and Hwang, H. A Micro structural Study of the Wear Behaviour of SiC_p/Al Composites. *Tribology International.* 1994, **27**(5). pp. 307-314.

Clyne, T. W. *An Introductory Overview of MMC Systems, Types and Developments.* In: Kelly, A and Zweben, C. Comprehensive Composite Materials, Vol. 3. Oxford: Elsevier Science, 2000. pp. 1-26.

Davis, J.R. (editorial manager) *Metals Handbook: Vol 2. Properties and Selection: Nonferrous Alloys and Special Purpose Materials.* 10th ed. U.S.A.: ASM International, 1990, pp. 210-215.

Deckert, C. A. *Electroless Copper Plating.* In: ASM Handbook, Volume 5, Surface Engineering. ASM International, materials Park, Ohio. 1994. pp. 311-322.

Dunn, B. *New Materials in Space.* Materials World, 2000, **8**(1). pp. 13-15.

Dynan, S. Canumalla, S. Bhagat, R.B. Green, D.J. and Pangborn, R.N. *Processing and Mechanical Properties of Metal Matrix Composites*. In: International Conference on Composite Materials 9. Madrid: 1993. pp. 889-896.

Eremenko, V. N., Natanzon, Ya. V. and Petrishchev, V. Ya. *Kinetics of Reaction of Pyrolytic Graphite with Liquid Aluminium.* Adgez. Rasplavov, Naukova Dumka, Kiev: 1974. pp. 160-164. Abstract obtained from online Cambridge Scientific Abstract Service, http://www.csa1.co.uk (Aluminium Industry Abstracts).

Foo, K.S., Banks, W. M., Craven, A. J. and Hendry, A. *Interface Characterization of an SiC Particulate/6061 Aluminium Alloy Composite.* Composites. 1994, **25**(7), pp. 677-683.

Gao, Y., Jia, J., Loehman, R. E., Ewsuk, K. G. and Fahrenholtz, W. G. *Microstructure and composition of Al-Al_2O_3 composites made by reactive metal penetration.* Journal of Materials Science, 1996. **31**. pp. 4025-4032.

Garg, A. K. and De Jonghe, L. C. *Metal-coated colloidal particles.* Journal of Materials Science. **28.** 1993. pp. 3427-3432.

Generous, J.D. and Montgomery, W.C. *Aluminium P/M - Properties and Applications.* In: Klar, E. Powder Metallurgy. Applications, Advantages and Limitations. Ohio: American Society for Metals. 1983, pp. 211-234.

Goodfellows. *Catalogue.* CD-ROM, 2000.

Greenwood, N.N. and Earnshaw, A. *Chemistry of the Elements.* Oxford: Pergamon Press, 1993.

Gurcan, A.B. and Baker, T.N. *Wear Behaviour of AA6061 Aluminium Alloy and its Composites.* Wear. 1995, **188.** pp. 185-191.

Gutin, S. S., Panov, A. A. and Khlopin, M. I. *Effect of Oxide Films on the Sintering of Aluminium Powders.* Poroshkovaya Metall. (4) Apr. 1972. pp.32-35.

Hallstedt, B., Liu, Z-K. and Agren, J. *Reactions in Al_2O_3-Mg metal matrix composites during prolonged heat treatment at 400, 550 and 600 ℃.* Materials Science and Engineering. **A169.** 1993. pp. 149-157.

Harris, B. *Engineering Composite Materials.* 2nd edition. London: IOM Communications Ltd. 1999.

Hausner, H. H. and Mal, M. K. *Handbook of Powder Metallurgy*, 2nd edition. New York: Chemical Publishing Co. Inc. 1982.

Hexemer, R. and Pierce, R. *Advances in MMCs and CMCs.* Ceramic Industry, 2000. **150**(6). pp. 31-38.

Hill, R. G., Nelson, R. P. and Hellerich, C. L. *Composites Work at Battelle-Northwest.* Battelle Memorial Institute, Pacific Northwest Laboratory, 16th Refractory Composites Working Group, Seattle, Washington, October 1969.

Hong, S. I., Gray III, G. T. and Wang, Z. *Microstructure and Stress-strain Responses of Al-Mg-Si Alloy Matrix Composites Reinforced with 10 vol.% Al_2O_3 Particulates.* Materials Science and Engineering A. **A221.** 1996. pp. 38-47.

Hong, S. I. and Seo, Y. S. *Effect of Microstructure on Wear Behavior of Al-Mg-Si Alloy Matrix-10 vol.% Al_2O_3 Composite.* Materials Science and Engineering, . **A265**. 1999. pp. 29-41.

Horng, C. F., Lin, S. J. and Liu, K.S. *Formation of $MgAl_2O_4$ in Al_2O_3-(Al-4wt%Mg) Composites.* Materials Science and Engineering, **A150.** 1992. pp. 289-294.

Hull, D. and Clyne, T.W. *An Introduction to Composite Materials.* Cambridge: Cambridge University Press, 1996.

Hunt, W. H. P*articulate Reinforced MMCs.* In: Kelly, A and Zweben, C. Comprehensive Composite Materials, Vol. 3. Oxford: Elsevier Science, 2000. pp. 701-716.

Hutchings, I. M., Wilson S. and Alpas, A. T. *Wear of Aluminium-based Composites.* In: Kelly, A and Zweben, C. Comprehensive Composite Materials, Vol. 3. Oxford: Elsevier Science, 2000. pp. 701-716.

Hutchings, I. M. *Tribology Friction and Wear of Engineering Materials.* London: Edward Arnold, 1992.

Janowski, G. M. and Pletka, B. J. *The Influence of Interfacial Structure on the Mechanical Properties of Liquid-phase-sintered Aluminium-Ceramic Composites.* Materials Science and Engineering, **A129.** 1990. pp. 65-76.

Johnson, K. *Discontinuously reinforced Aluminium has come of Age.* [WWW] Aluminium Metal Matrix Composites Consortium. http://www.almmc.com/ (09 March 2001).

Jost, H. P. and Schofield, J. *Energy Saving Through Tribology: A techno-economic Study.* Proceedings of the Institution of Mechanical Engineers. June 1981. **195**. pp. 151-173.

Kevorkijan, M. *Development of Aluminium Based Composites for Automotive Applications.* Metalurgija. 1998, **37**(2). pp. 67-74.

Kindl, B., Teng, Y. H. and Liu, Y. L. *Protective coatings for commercial particulates.* Composites. **25** (7). 1994. pp. 671-676.

King, J. E. *Advanced Ceramic and Metallic Composites: Reinforcements and Matrices.* Lecture: Programme for Industry. University of Cambridge. 1991.

Klein, M. J. and Metcalfe, A. G. *Effect of Interfaces in Metal Matrix Composites on Mechanical Properties.* AFML-TR-71-189, October 1971.

Koerner, R.M. *Triaxial Stress State Compaction of Powders.* In: Kuhn, H.A. and Lawley, A. (eds.) Powder Metallurgy Processing, New Techniques and Analyses. London: Academic Press Inc. (London) Ltd. 1978, pp. 33-49.

Kondoh, K., Kimura, A. and Watanabe, R. *Effect of magnesium on deoxidizing reaction of particle surface oxide film at elevated temperature. Sintering phenomenon of aluminium alloy powder particle and analysis on particle surface structure.* Quarterly Journal of the Japan Welding Society (Japan), vol. **19**(1). Feb. 2001. pp. 167-173.

Krieder, K.G. *Introduction to Metal Matrix Composites.* In: Broutman, L.J. and Krock, R.H. (eds.) Composite Materials vol. 4. Metal Matrix Composites. London: Academic Press Inc. (London) Ltd. 1974, pp. 1-34.

Lansdown, A.R. and Price, A.L. *Materials to Resist Wear. A Guide to their Selection and Use.* Oxford: Pergamon Press Ltd. 1986. pp. 21-22.

Lansdown, A.R. and Price, A.L. *Materials to Resist Wear: A Guide to their Selection and Use.* Oxford: Pergamon Press Ltd. 1986. pp. 111-117.

Lawley, A. *Analysis of Mechanical Property-Structure Relations in Powder Forgings.* In: Kuhn, H. A. and Lawley, A. Powder Metallurgy Processing; New Techniques and Analyses. London: Academic Press 1978. pp. 139-171.

Lee, K. B., Kim, Y. S. and Kwon, H. *Fabrication of Al-3 Wt Pct Mg Matrix Composites reinforced with Al_2O_3 Particulates by the Pressureless Infiltration Technique.* Metallurgical and Materials Transactions A. 1998, **29A**(12), pp. 3087-3095.

Leonida, G. *Electroless Copper Plating.* Handbook of Printed Circuit Design, Manufacture, Components and Assembly. Electrochemical Publications Ltd. Ayr, Scotland. 1989. pp. 262-267.

Levitt, A. P. *Whisker Technology.* New York: Wiley, 1970.

Li, X. Y. and Tandon, K. N. *Subsurface Microstructures generated by Dry Sliding Wear on As-cast and Heat Treated Al Metal Matrix Composites.* Wear, 1997. **203-204.** pp. 703-708.

Liu, X., Shih, W. Y. and Shih, W-H. *Effects of Copper Coating on the Crystalline Structure of Fine Barium Titanate Particles.* Journal of the American Ceramic Society. **80** (11). 1997. pp. 2781-2788.

Liu, Y.B. Lim, S.C. Lu, L. and Lai, M.O. *Fabrication of Metal-Matrix-Particulate Composites Using Powder Metallurgy Techniques.* In: International Conference on Composite Materials 9. Madrid: 1993. pp. 770-778.

Lloyd, D. J. and Jin, I. *Melt Processed Aluminium Matrix particle Reinforced Composites.* In: Kelly, A and Zweben, C. eds. Comprehensive Composite Materials, Vol. 3. Oxford: Elsevier Science, 2000. pp. 555-578.

Lorimer, G. W. *Sequences of intergranular nucleation and precipitation at grain and subgrain boundaries.* In: Proceedings of an International Conference on Solid to Solid Phase Transformations. Eds. Aaronson, H. I., Laughlin, D. E., Skerka, R. f. and Wayman, C. M.. TMS-AIME, Warrendale, PA. Aug. 1981. pp. 613-635.

Lu, D., Gu, M., Shi, Z., Wu, Z. and Jin, Y. *Effect of Interfacial Reaction on the Wear and Friction Properties of Aluminium Matrix Composites Reinforced by Graphite and Silicon Carbide Particles.* Xiyou Jinshu Cailiao yu Gongcheng (Rare Metal materials and Engineering) (China), 2000. **29**(1). pp. 35-38. Abstract obtained from online Cambridge Scientific Abstract Service, http://www.csa1.co.uk (Aluminium Industry Abstracts).

Lumley, R. N., Sercombe, T. B. and Schaffer, G. M. *Surface oxide and the role of magnesium during the sintering of aluminium.* Metallurgical and Materials Transactions A (USA), **30A**, (2). Feb. 1999. pp. 457-463.

Maruyama, B. and Rabenberg, L. *Oxidation Model of Interface Reactions in Aluminium / Graphite Composites.* Conference Proceedings, Interfaces in Metal-Matrix Composites, New Orleans, Louisiana, USA. 2-6 March, 1986. The Metallurgical society / AIME, pp. 233-238. Abstract obtained from online Cambridge Scientific Abstract Service, http://www.csa1.co.uk (Aluminium Industry Abstracts).

Matweb. *The Online Materials Information Resource.* [WWW] Materials Property Database. http://matls.com (30 April 2001).

Mel'nikov, V. G., Zamyatina, N. I., Yudina, T. F. and Aleshonkova, E. A. *Electroless Deposition of Metals on Alumina Powder.* Soviet Power Metallurgy Metals Ceramics. **5.** 1980. pp. 307-309.

Metcalfe, A. G. *Introduction and Review.* In: Metcalfe, A. G. Composite Materials Volume 1, Interfaces in Metal Matrix Composites. London: Academic Press. 1974. pp.1-30.

Metcalfe, A. G. *Physical Chemical Aspects of the Interface.* In: Metcalfe, A. G. Composite Materials Volume 1, Interfaces in Metal Matrix Composites. London: Academic Press. 1974. pp. 65-123.

Moore, T. L. *DMIC Memorandum 243.* Battelle Memorial Institute, Columbus, Ohio. 1969.

Mortensen, A. *Melt Infiltration of Metal Matrix Composites.* In: Kelly, A and Zweben, C. eds. Comprehensive Composite Materials, Vol. 3. Oxford: Elsevier Science, 2000. pp. 521-554.

Muhly, J. D. In: Maddin, R. ed. *The Beginning of the use of Metals and Alloys.* Cambridge, Massachusetts. MIT Press, 1988. pp. 2-20.

Narayan, M., Surappa, M. K. and Pramila Bai, B. N. *Dry Sliding wear of Al alloy 2024-Al_2O_3 particle Metal Matrix Composite.* Wear, 1995. **181-183**. pp. 563-570.

Ochiai, S. In: Ochiai, S. ed. *Mechanical Properties of Metallic Composites.* Marcel Dekker, New York, 1994. pp. 473-510.

Okuma, S. *Sintering Mechanism of Aluminium and the Anodization of Aluminium Sintered Bodies.* Electrocomponent Science and Technology. **6** (1). 1979. Pp. 23-29.

Parvizi-Majidi, A. In: Chou, T. W. ed. *Structure and Properties of Composites.* Weinheim: VCH, 1993.

Pepper, R. T., Rossi, R. C., Upp, J. W. and Riley, W. C. *The Room Temperature Mechanical Behavior of Aluminium-graphite Composites.* A.S.M. Materials Engineering Congress, Cleveland, Ohio, October 20 1970.

Polmear, I.J. *Light Alloys: Metallurgy of the Light Metals.* London: Edward Arnold Ltd. 1981. pp. 25.

Prangnell, P. B. *Precipitation Behaviors in MMCs.* In: Kelly, A and Zweben, C. eds. Comprehensive Composite Materials, Vol. 3. Oxford: Elsevier Science, 2000. pp. 61-90.

Rabinowicz, E. *Friction and Wear of Materials.* New York: John Wiley and Sons Inc. 1965.

Rajan, T. P. D., Pillai, R. M. and Pai, B. C. *Reinforcement Coatings and Interfaces in Aluminium Metal Matrix Composites.* Journal of Materials Science. 1998, **33**, pp. 3491-3503.

Schiroky, G. H., Miller, D. V., Aghajanian, M. K. and Fareed, A. S. *Fabrication of CMCs and MMCs using Novel Processes.* Key Engineering Materials. 1997, **127-131**, pp. 141-152.

Scientific Group Thermodata Europe. [*WWW*]*http://www.met.kth.se/pd/element/Al-Mg.html.* March 2002.

Sears, F. W., Zemansky, M. W. and Young, H. D. *University Physics.* 7th ed. Reading, Massachusetts, USA: Addison-Wesley Publishing Company. 1987.

Sharp, D. W. A. *Dictionary of Chemistry.* 2nd. ed. London: Penguin, 1990.

Smith, D.W. *Elements of Powder Metallurgy.* In: Klar, E. (ed.) Powder Metallurgy. Applications, Advantages and Limitations. Ohio: American Society for Metals. 1983, pp. 7-38.

Spowart, J. E. and Deve, H. E. *Compressive Failure of Metal Matrix Composites.* In:
Kelly, A and Zweben, C. eds. Comprehensive Composite Materials, Vol. 3. Oxford: Elsevier Science, 2000. pp. 221-245.

Stone, I.C. and Tsakiropoulos, P. *The Spatial Distribution of Reinforcement in PM Al/SiC_p MMCs and its Effect on their Processing and Properties.* In: International Conference on Composite Materials 9. Madrid: 1993. pp. 271-278.

Strangwood, M., Hippsley, C. A. and Lewandowski, J. J. *Segregation to SiC/Al interfaces in Al based metal matrix composites.* Scripta Metallurgica et Materialia, 24 (8). (Aug 1990), pp 1483-1487.

Strangwood, M., Hippsley, C. A. and Lewandowski, J. J. *Interfacial segregation in Al based metal matrix composites.* In: Low Density, High Temperature Powder Metallurgical Alloys. Eds. Fazier, W. E., Koczac, M. J. and Lee, P. W. TMS, Warrendale, PA. 1991. pp. 97-108.

Suery, M. and L'Esperance, G. *Interfacial Reactions and Mechanical Behaviour of Aluminium Matrix Composites Reinforced with Ceramic Particles.* Key Engineering Materials. 1993. **79-80**. pp. 33-46.

Teng, Y. H. and Boyd, J. D. *Measurement of interface strength in Al/SiC particulate composites.* Composites. **25** (10). 1994. pp. 906-912.

Tinklepaugh, J. R. and Crandall, W. B. eds. *Cermets.* New York: Reinhold Publishing, 1960.

Tsukada, M and Ohfuji, S-I. *Interface Reaction of Al/W and Chemical Properties of Al-W Bimetallic Bonding.* Journal of Vacuum Science and Technology A (USA). 1995. **13** (5). pp. 2525-2531.

Unsworth, J. P. and Bandyopadhyay, S. *Effect of thermal ageing on Hardness, Tensile Strength and Impact Properties of an Alumina Microsphere-reinforced Aluminium Metal-matrix Composite.* Journal of Materials Science. **29.** 1994. pp. 4645-4650.

Upadhyaya, G. S. *Powder Metallurgy Technology.* Cambridge: Cambridge International Science Publishing, 1997.

Varma, S.K. *et al.* *Control of Grain Size and Distribution of Particles in a (6061 alloy)$_m$ / (Al_2O_3)$_p$ Composite by Solutionizing Treatment.* Metallurgical and Materials transactions A: Physical Metallurgy and Materials Science. 1996, **27A**(7), pp. 2023-2034.

Wang, J., Furukawa, M., Horita, Z., Nemoto, M., Ma, Y. and Langdon, T. G. *The Age-hardening Characteristics of an Al-6061 / Al_2O_3 Metal Matrix Composite.* Metallurgical and Materials transactions A: Physical Metallurgy and Materials Science. 1995, **26A**(3), pp. 581-587.

Zhang, Z., Zhang, L. and Mai, Y. *The Running-in Wear of a Steel/SiC_p-Al Composite System.* Wear. 1996, **194.** pp. 38-43.

Zhao, X., Jiang, J. X., Xiong, D. G. and Yang, G. *Interfacial Reactions and Reaction Kinetics Between Silicon Carbide and Aluminium.* In: International Conference on Composite Materials 9. Madrid: 1993. pp. 697-705.

Zhong, W. M., L'Esperance, G. and Suery, M. *Interfacial Reactions in Al-Mg (5083)/Al_2O_3p Composites During Fabrication and Remelting.* Metallurgical and Materials Transactions A. **26A.** 1995. pp. 2625-2635.

Appendix 1.

Photographic Plates.

Micrographs showing the shape of alumina particles. The micrographs on this page are taken from Alcan Chemicals (Europe) Data Sheet 461.

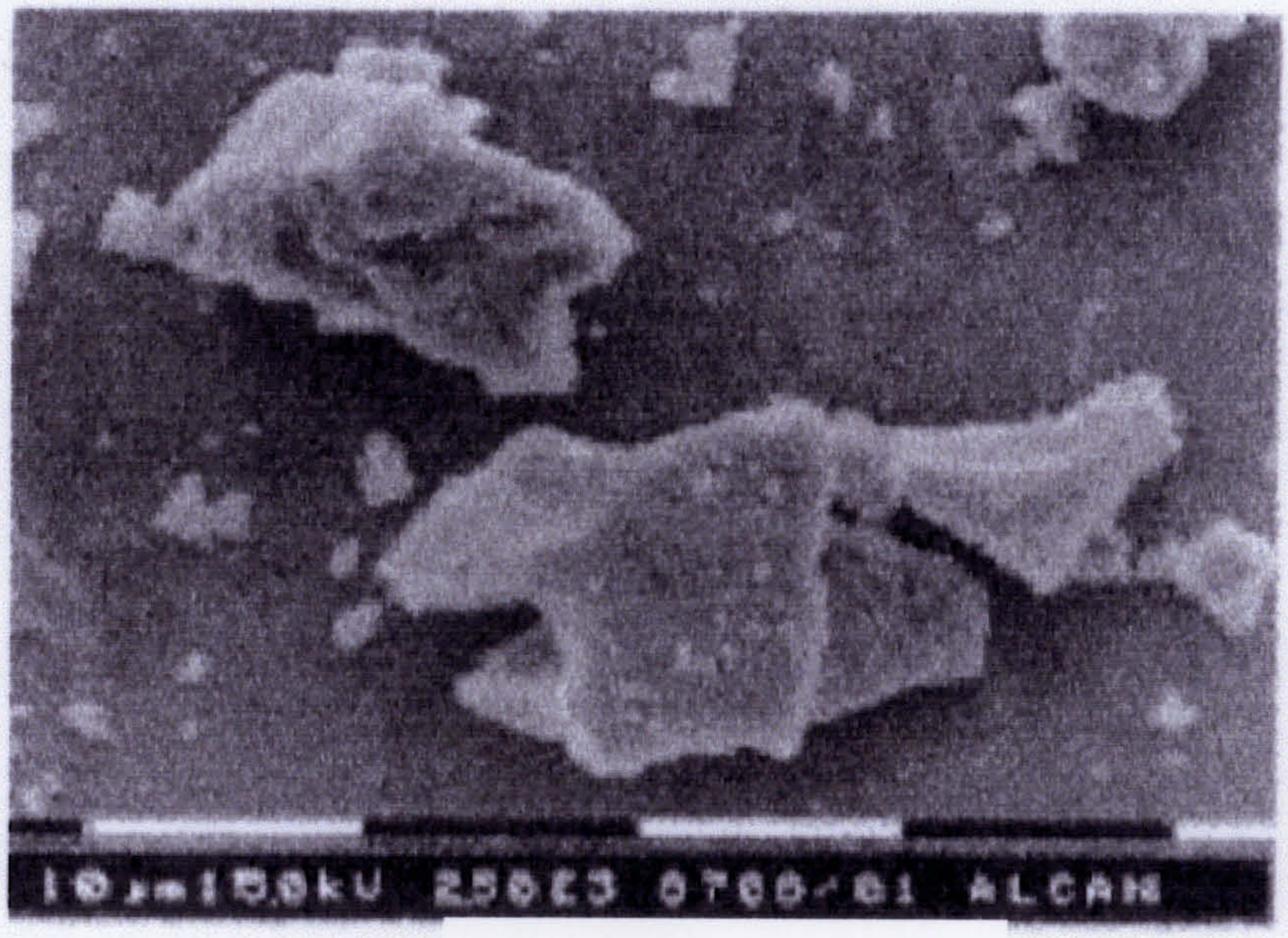

Plate 1. Tabular alumina.

Plate 2. Spherically shaped alumina.

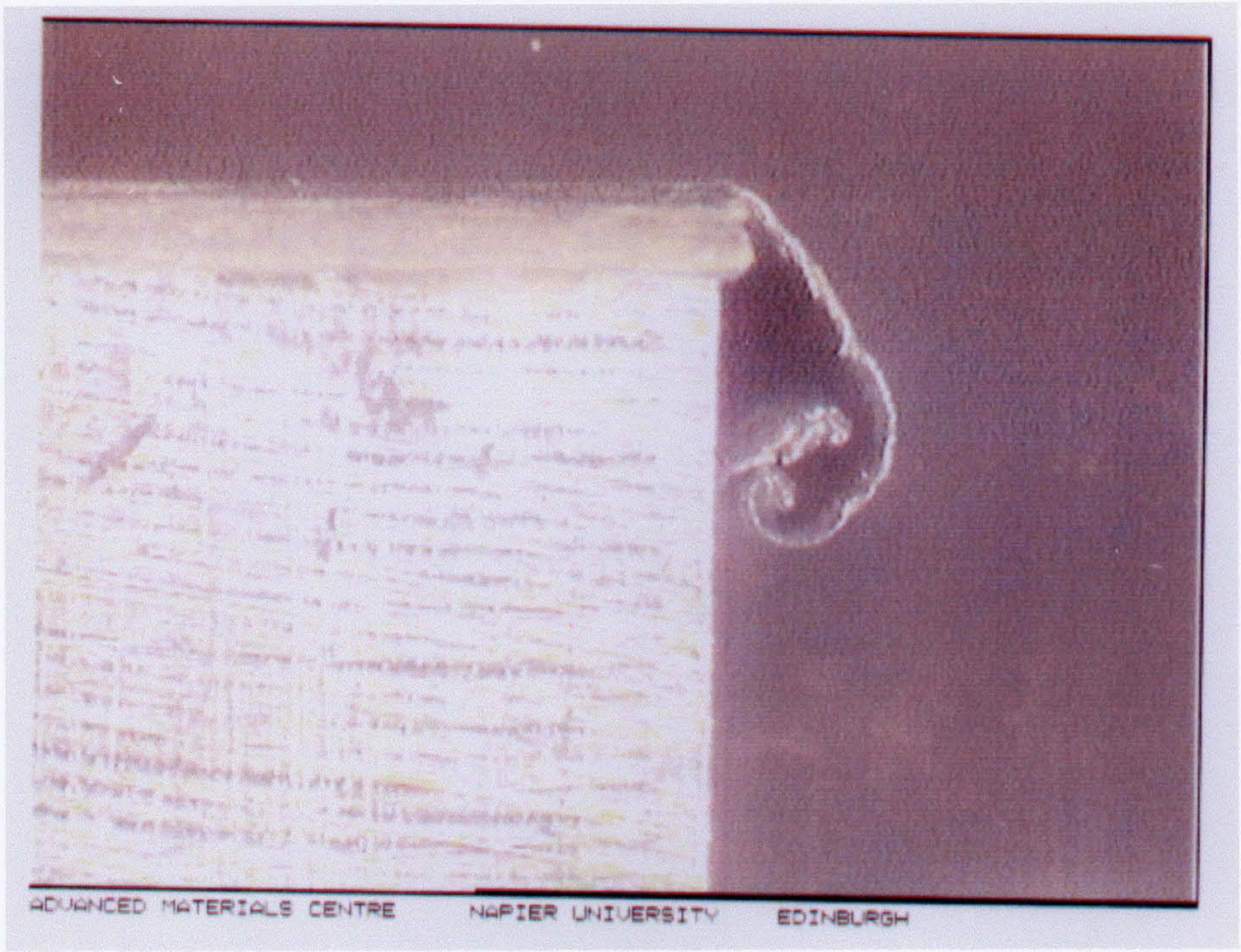

Plate 3. Microscopic picture (magnification x 40) showing ductile deformation at trailing edge of monolithic 6061 wear sample.

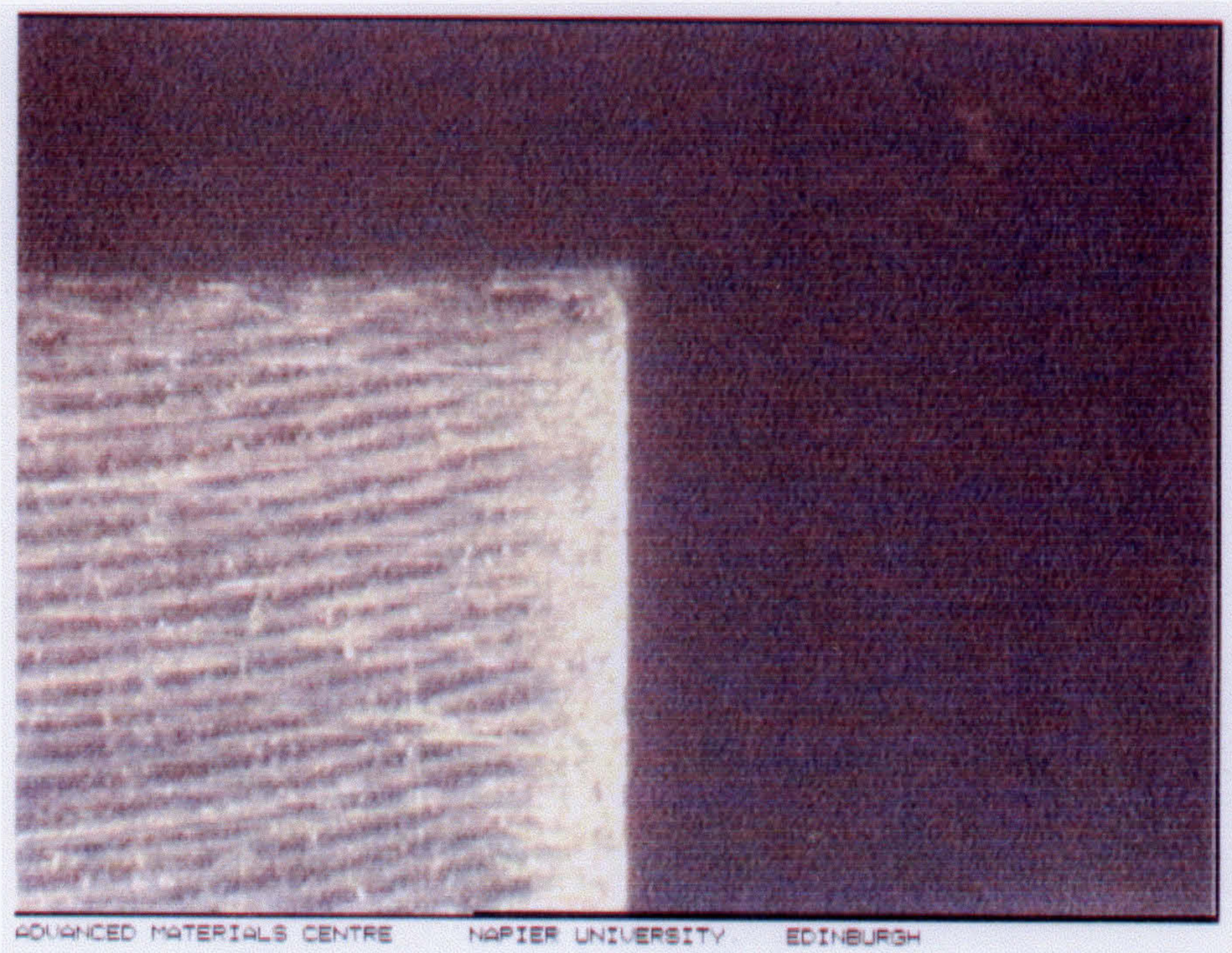

Plate 4. Microscopic photograph (magnification x 40)of trailing edge of Alumina-containing composite wear sample.

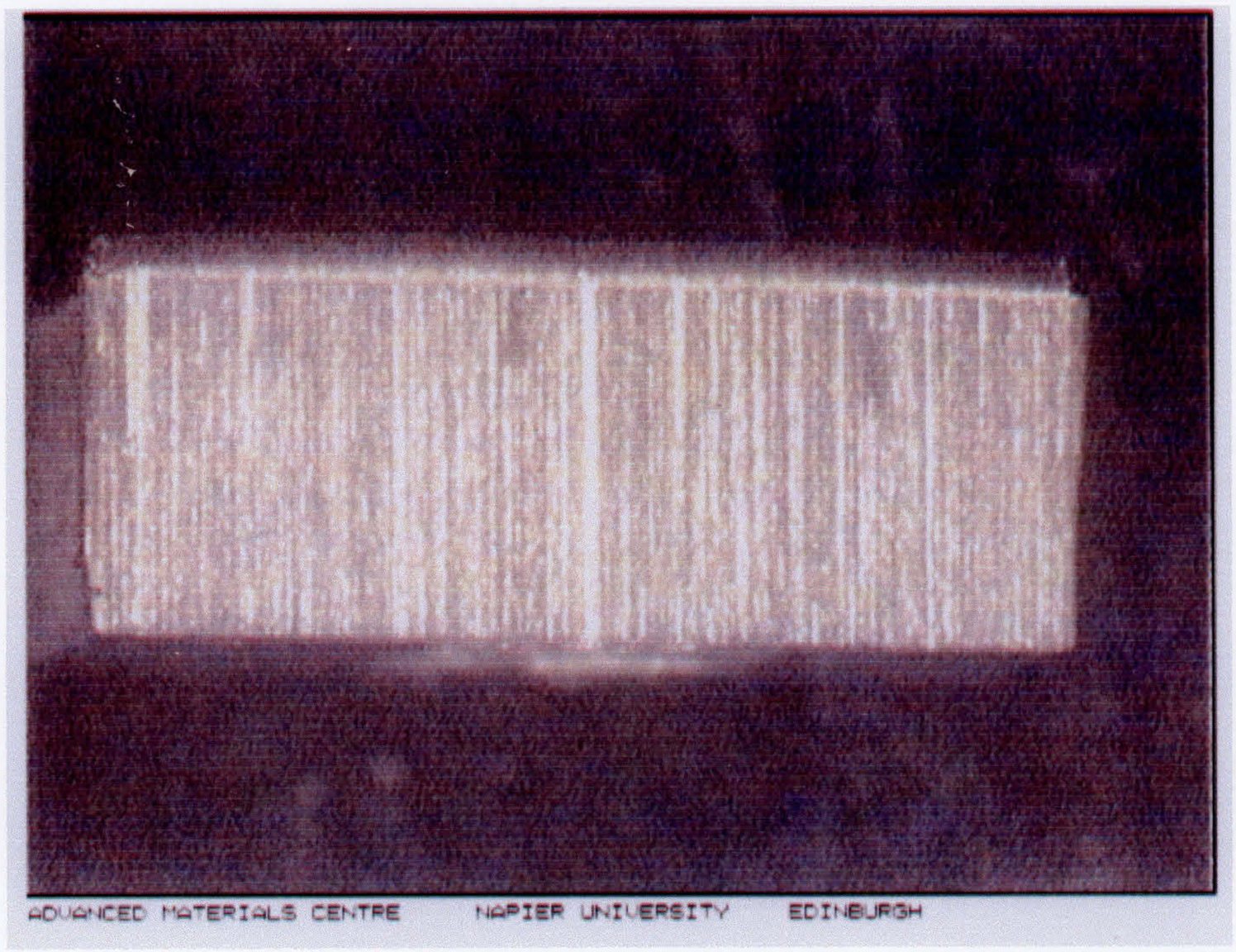

Plate 5. Microscopic photograph (magnification x 10) displaying wear surface pattern for monolithic 6061 alloy.

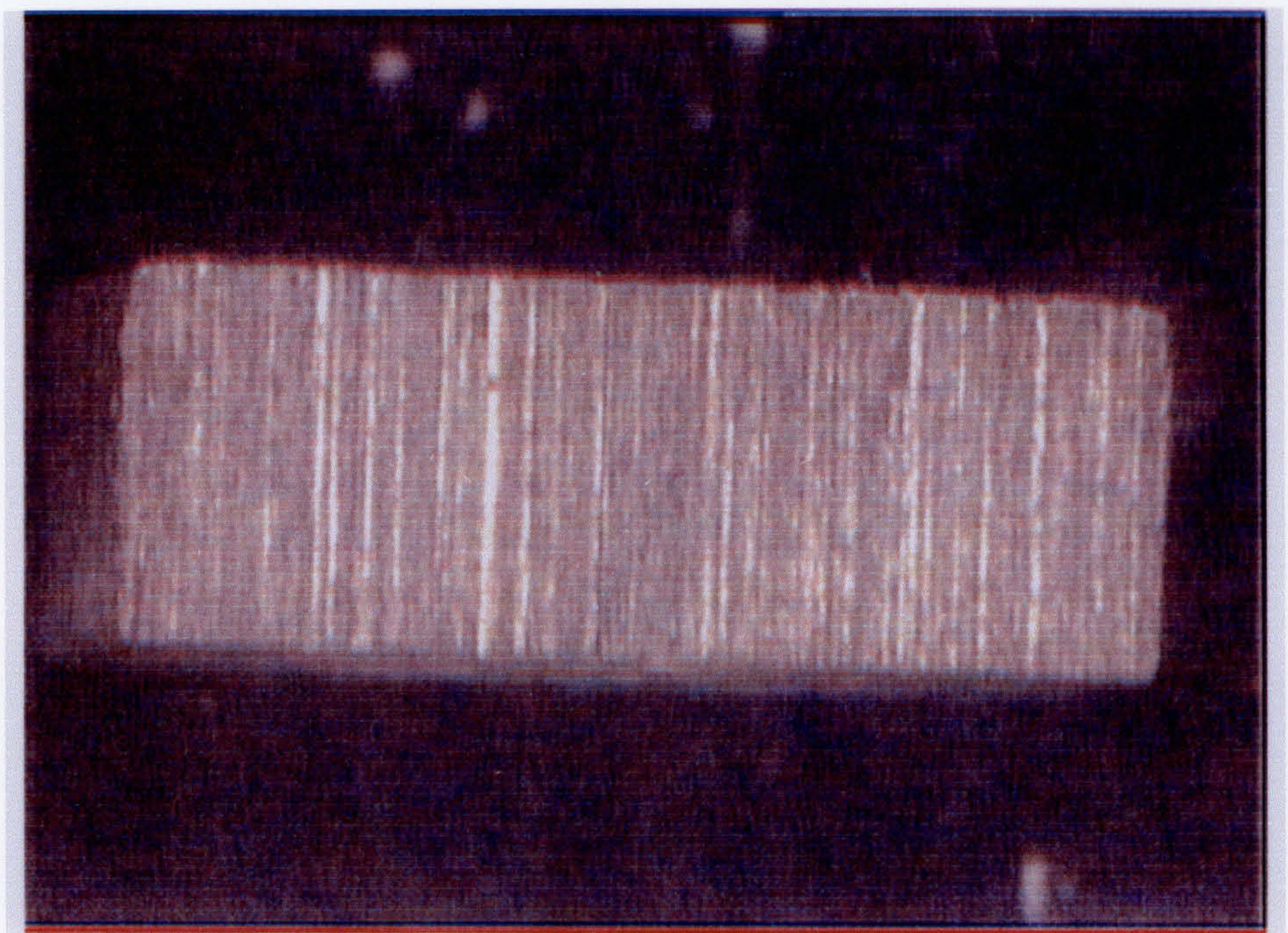

Plate 6. Microscopic photograph (magnification x 10) displaying wear surface pattern for alumina containing 6061 composite.

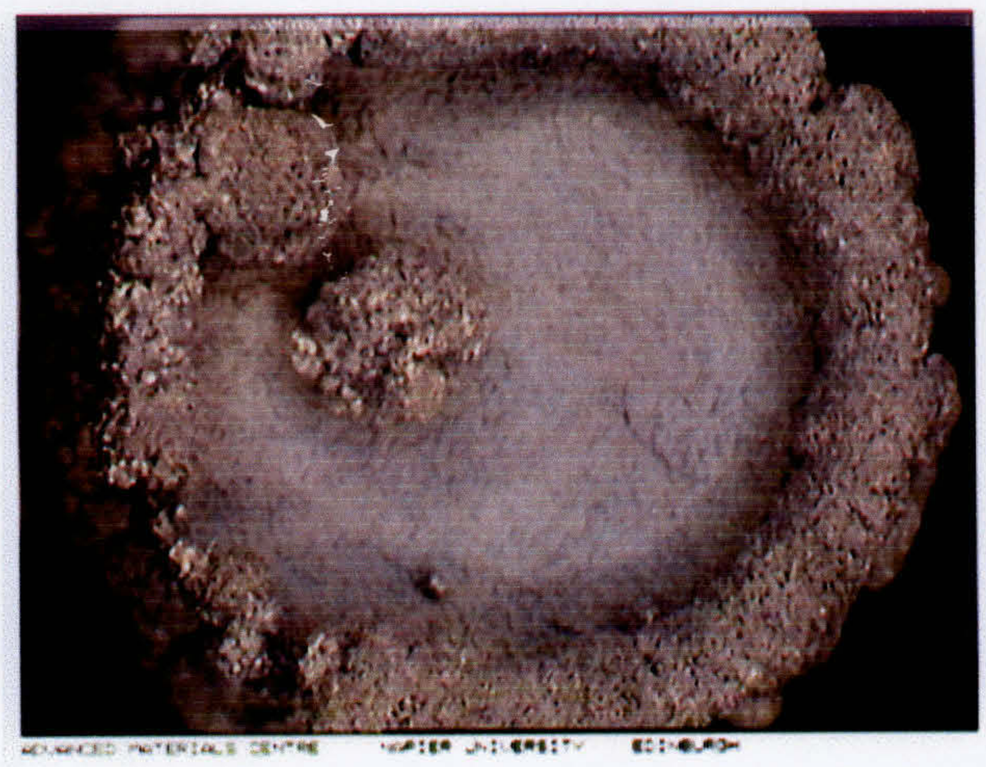

Plate 7. The surface of an AA6061/5 wt % Mg/10 vol % Al_2O_3 composite. Extreme bubbling and blistering is observed.

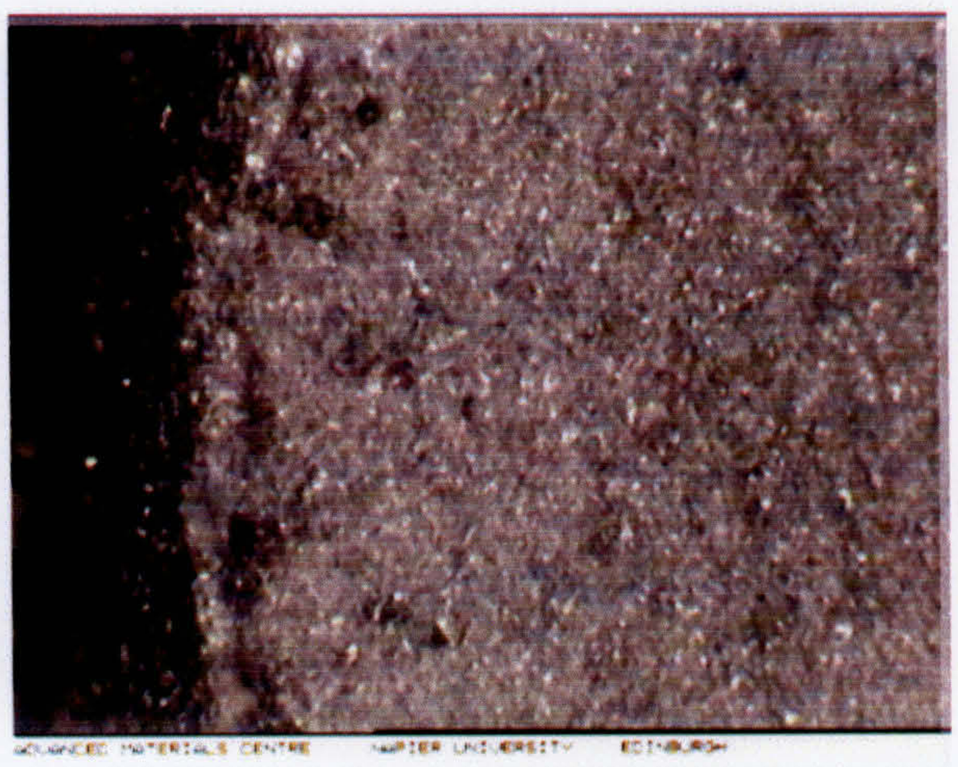

Plate 8. The surface of monolithic AA6061. Moderate roughness with no excessive blistering.

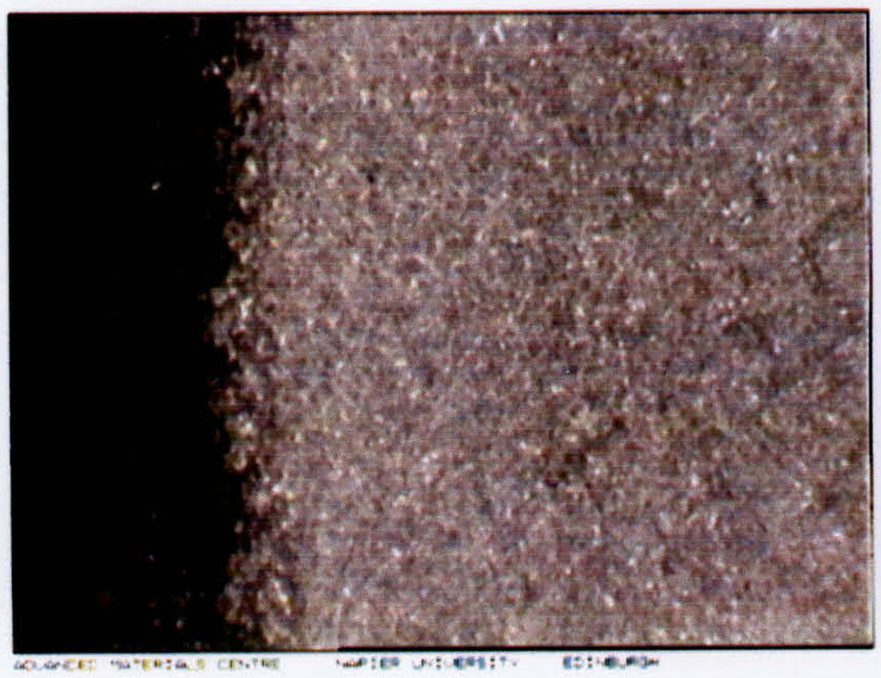

Plate 9. The surface of an AA6061/10 vol % Al_2O_3 composite. Surface is similar to the monolithic alloy.

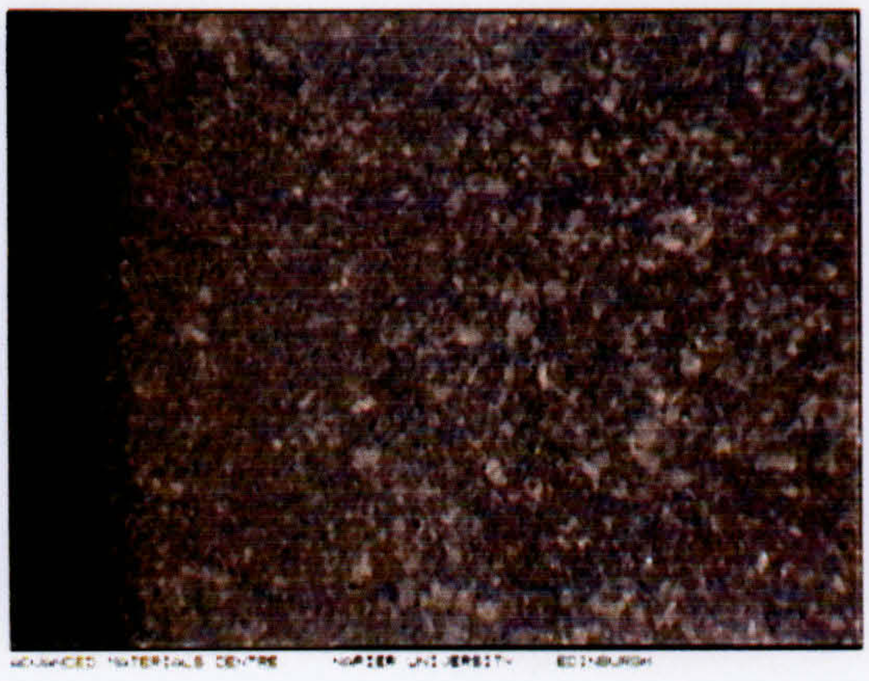

Plate 10. The surface of an AA6061/5 wt % Si/10 vol % Al_2O_3 composite. The surface displays low roughness with no blistering.

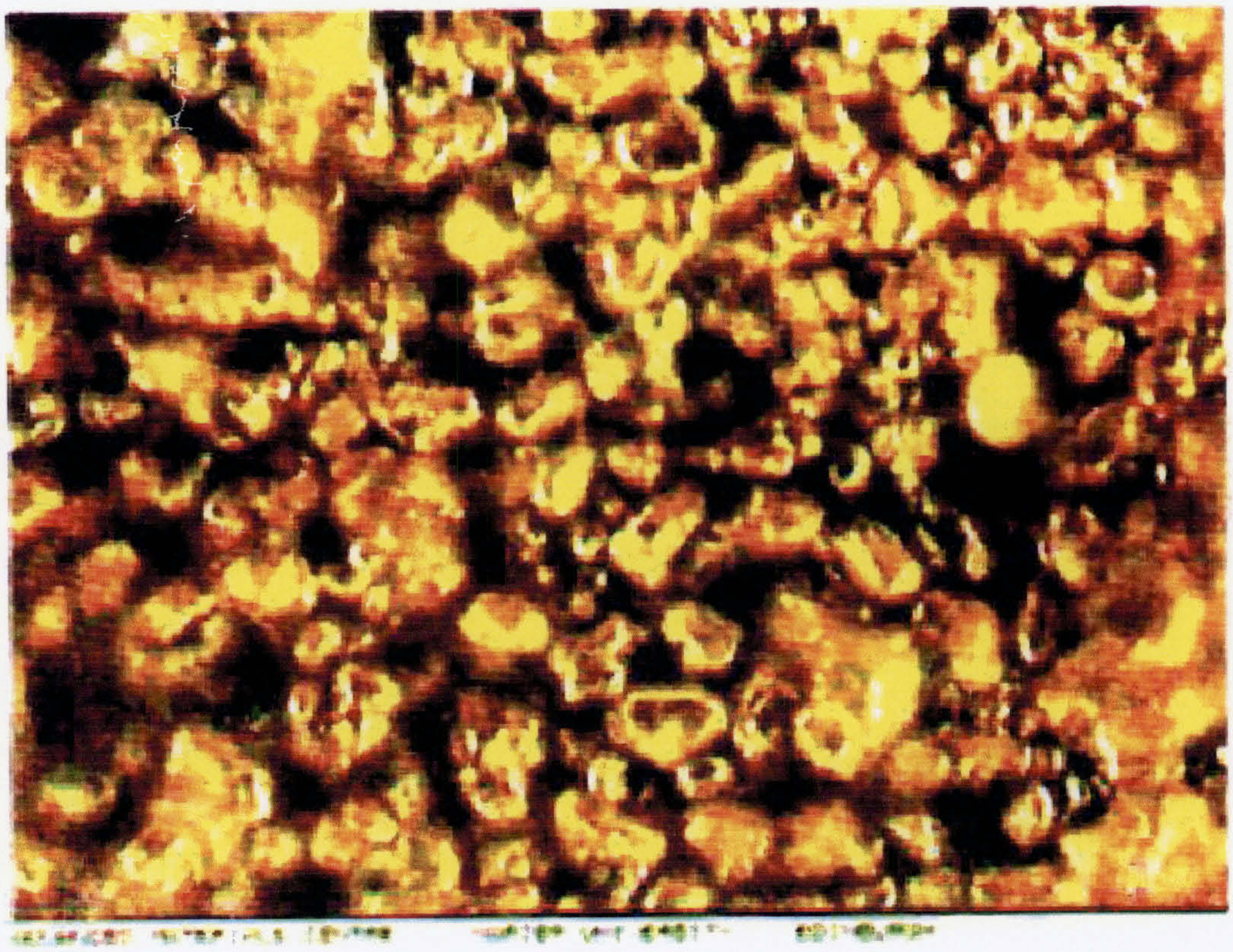

Plate 11. Photograph of copper coated spherical Al_2O_3 (magnification x 40)

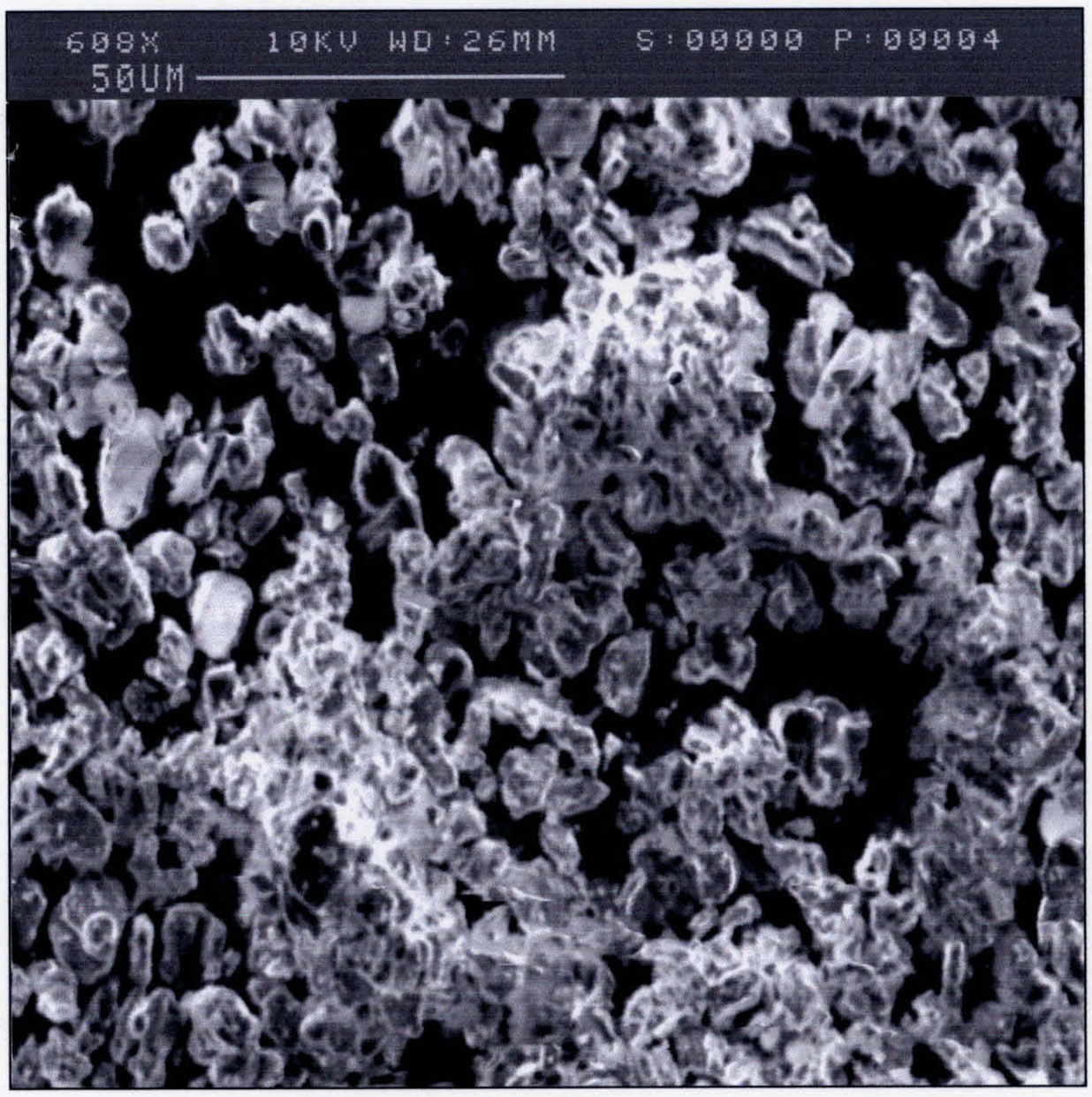

Plate 12. SEM micrograph of Al_2O_3 tabular shaped particles coated with Cu using formaldehyde as reducing agent. Note there is extensive agglomeration.

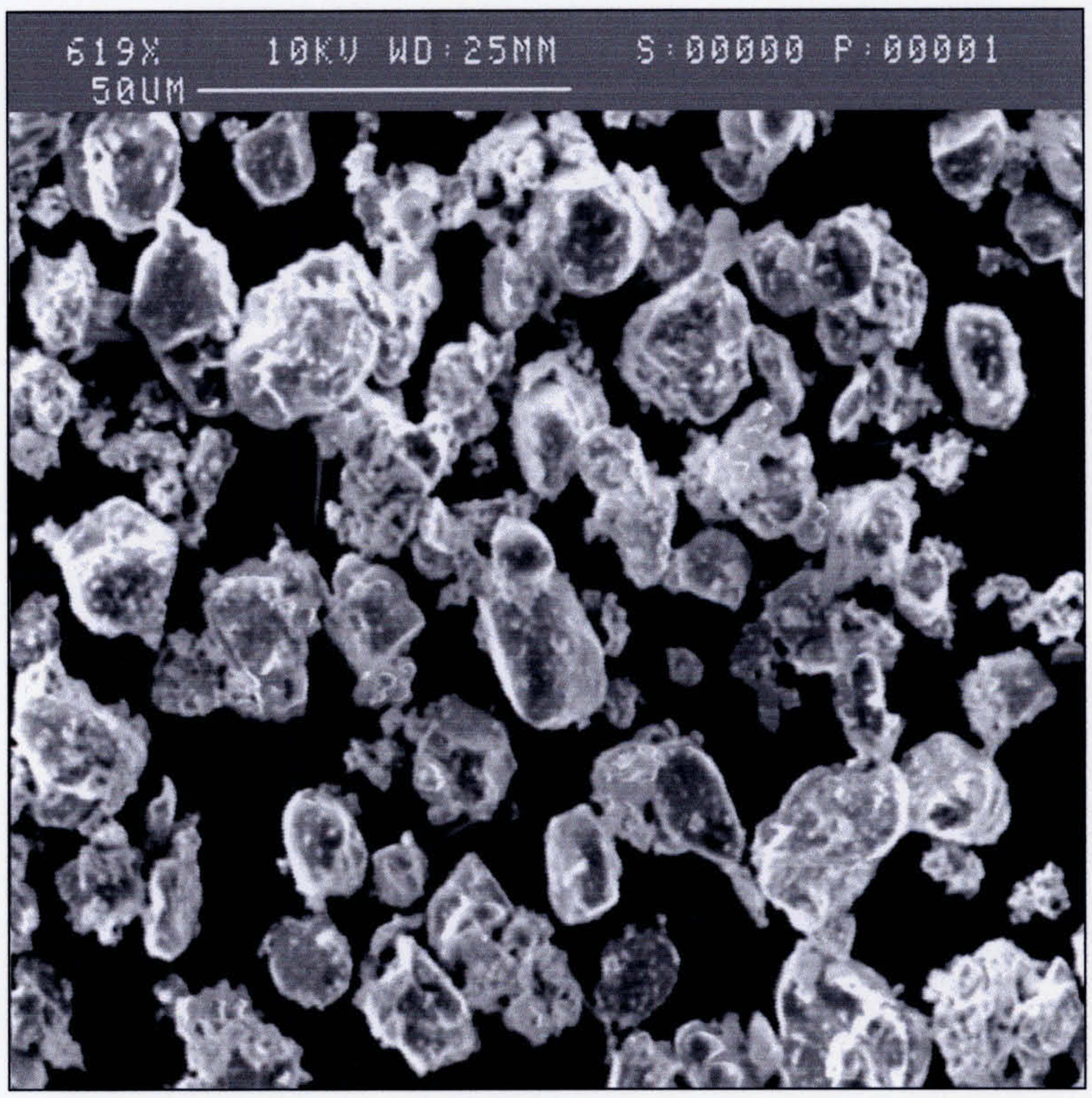

Plate 13. SEM micrograph of Al_2O_3 spherical shaped particles coated with Cu using formaldehyde as reducing agent. Note there is little agglomeration. There are however discrete particles of Cu present.

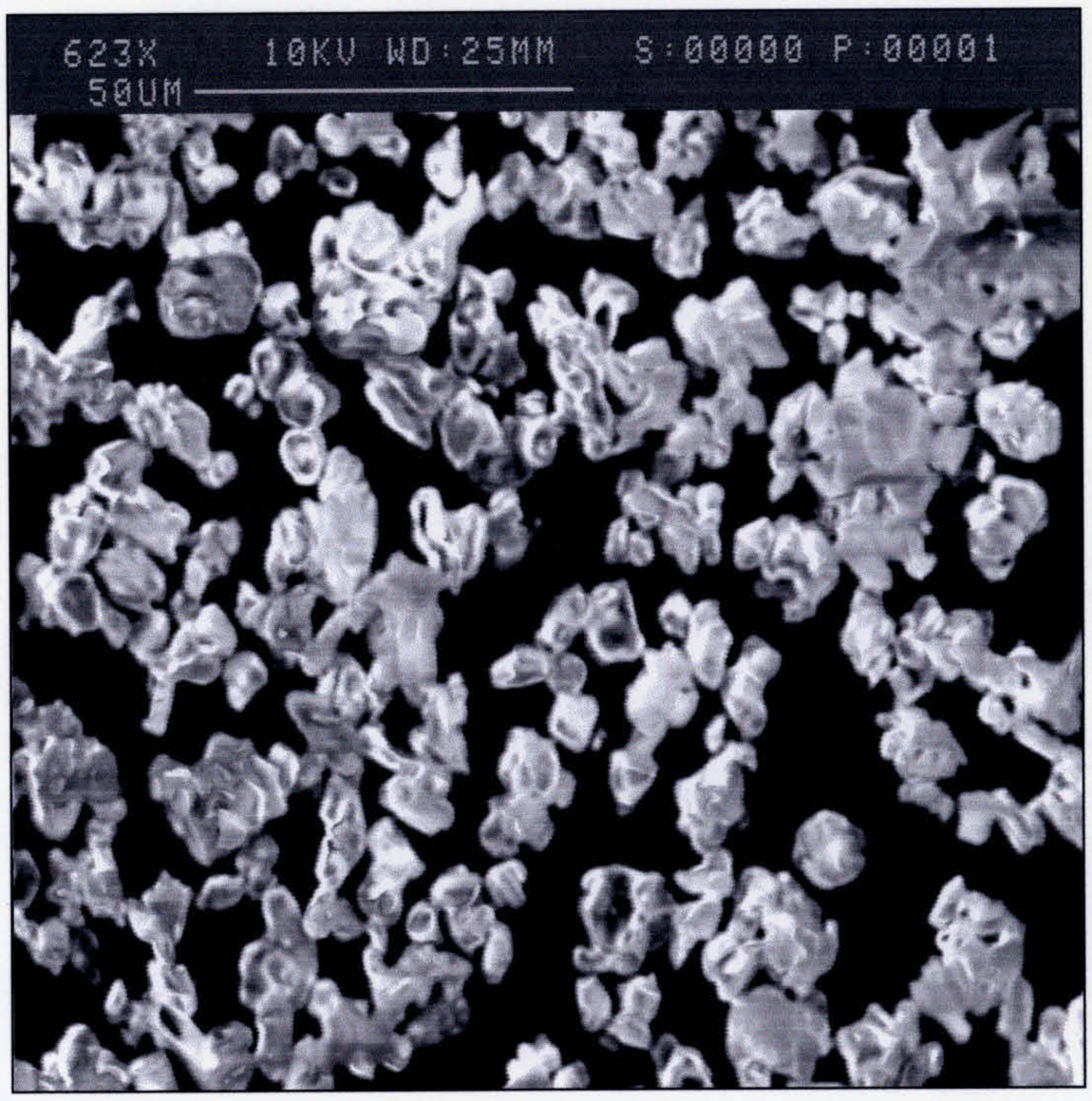

Plate 14. SEM micrograph of Al_2O_3 tabular shaped particles coated with Cu using hydrazine as reducing agent. There is some agglomeration observed with no discrete Cu present.

Plate 15. SEM micrograph of Al_2O_3 spherical shaped particles coated with Cu using hydrazine as reducing agent. Note there is little agglomeration with no discrete Cu present.

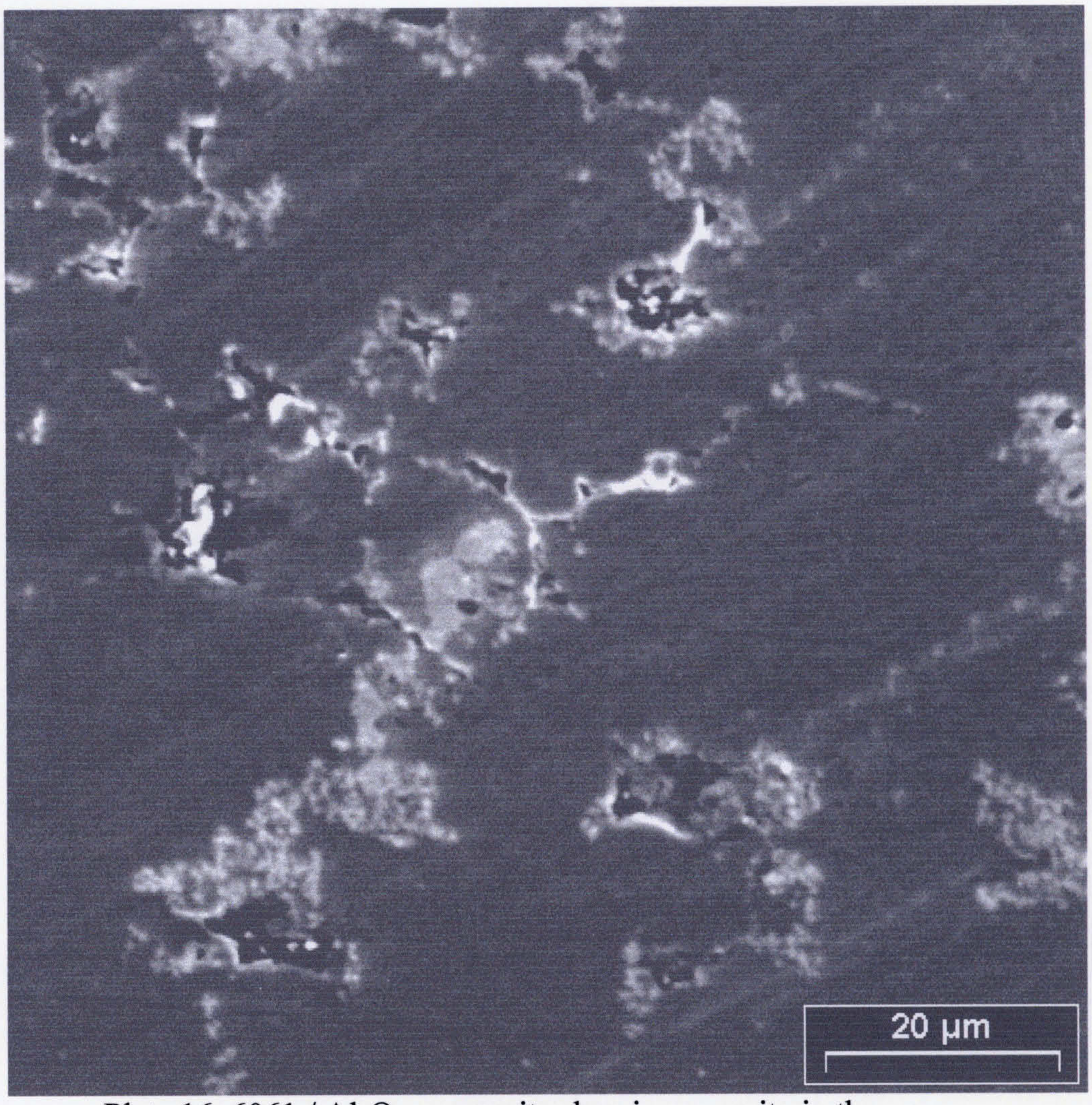

Plate 16. 6061 / Al_2O_3 composite showing porosity in the Al_2O_3 reinforcement regions.

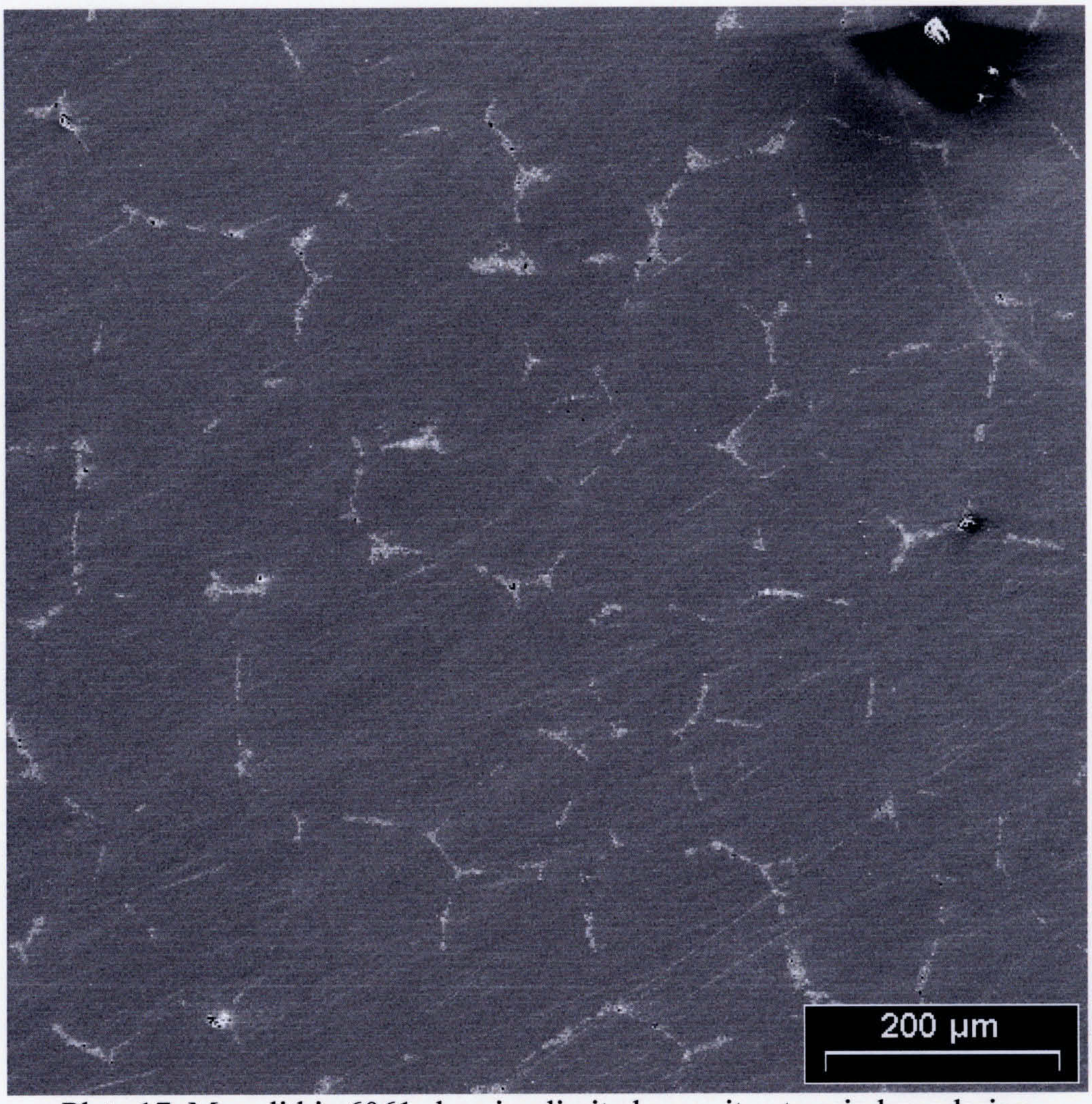

Plate 17. Monolithic 6061 showing limited porosity at grain boundaries.

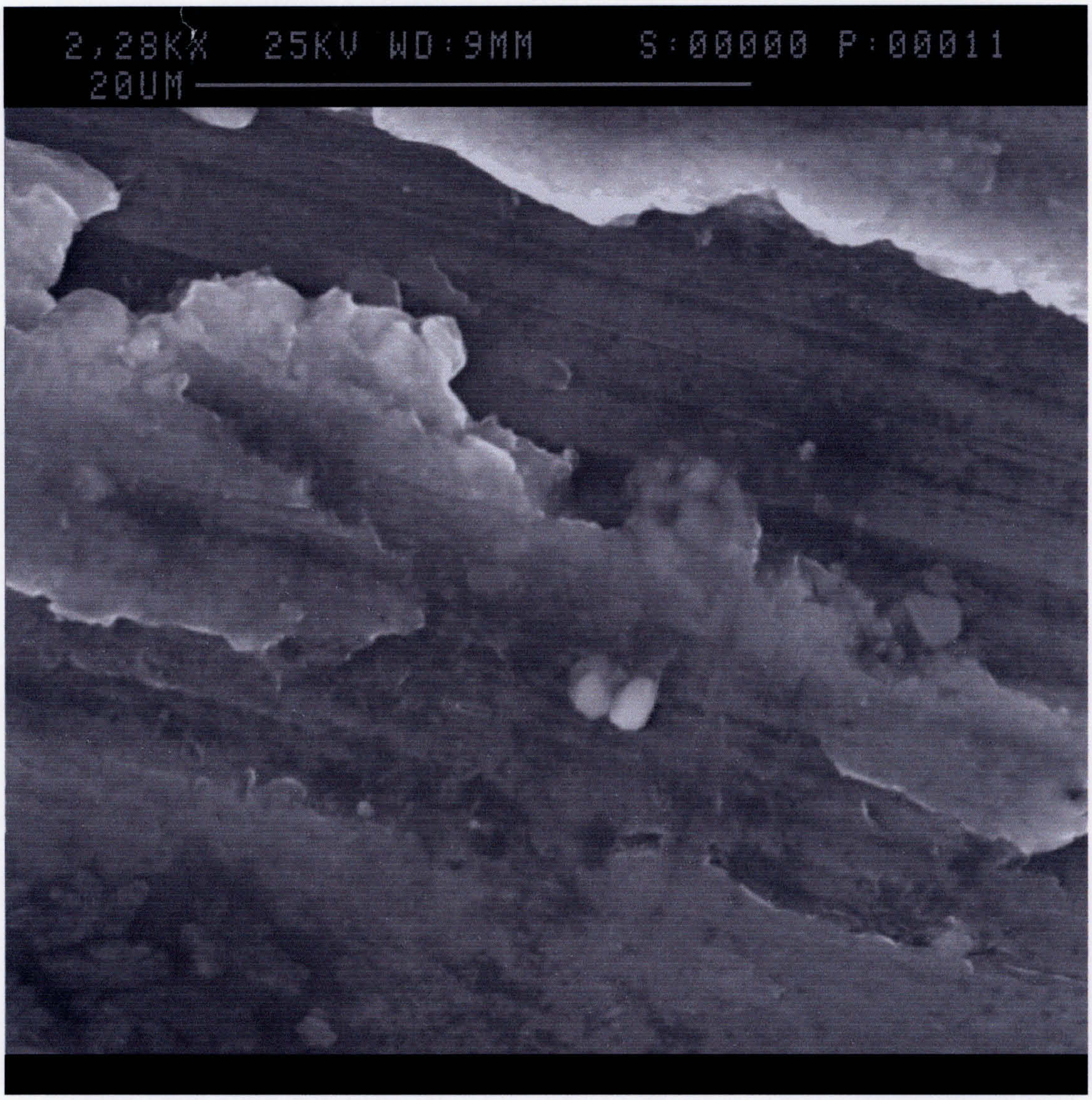

Plate 18. Wear pattern of a 6061/Al_2O_3 composite showing gouging.

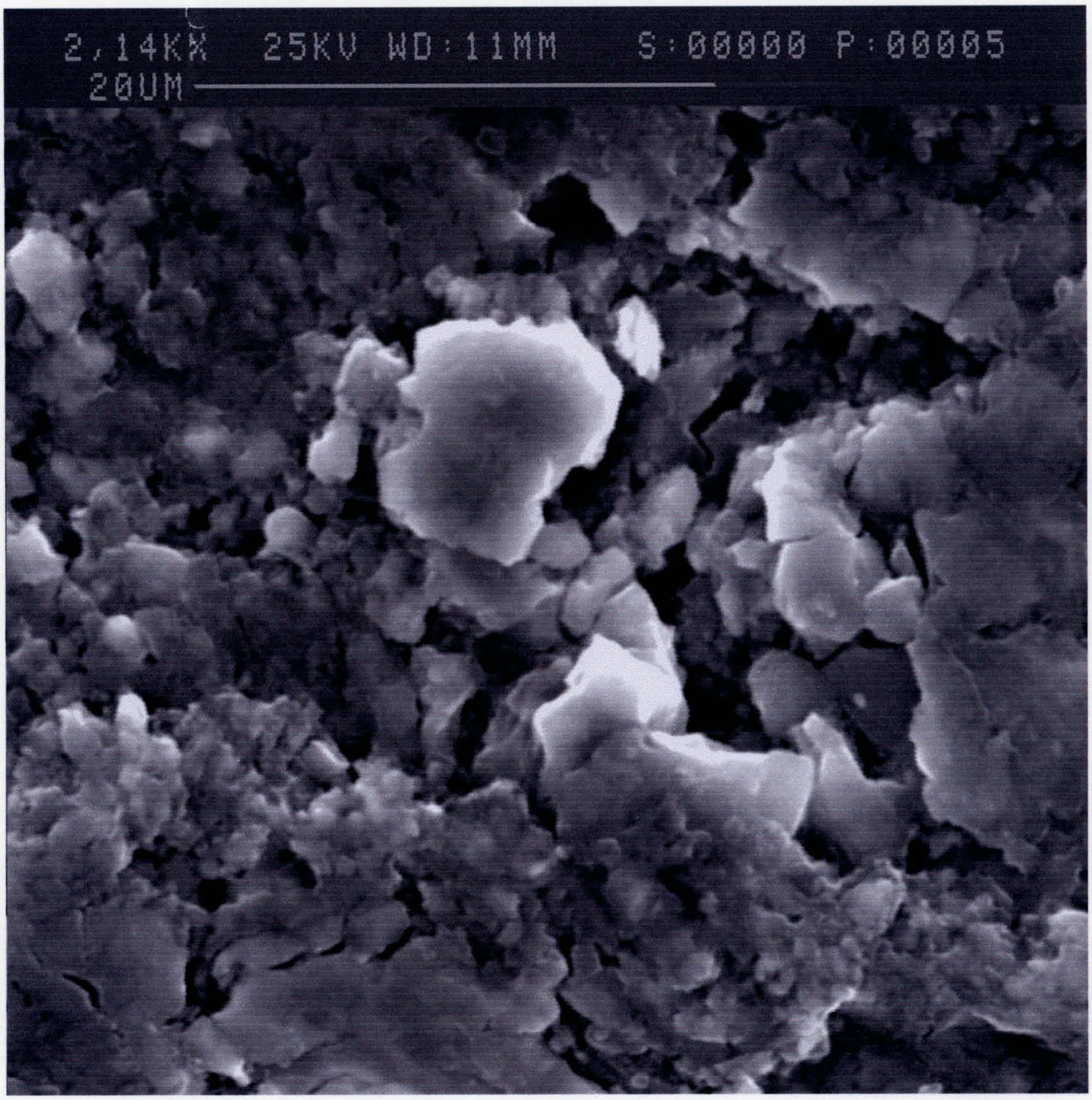

Plate 19. Wear of a 6061/Al_2O_3 composite within a region of pitting, showing fragmentation of the alumina particles.

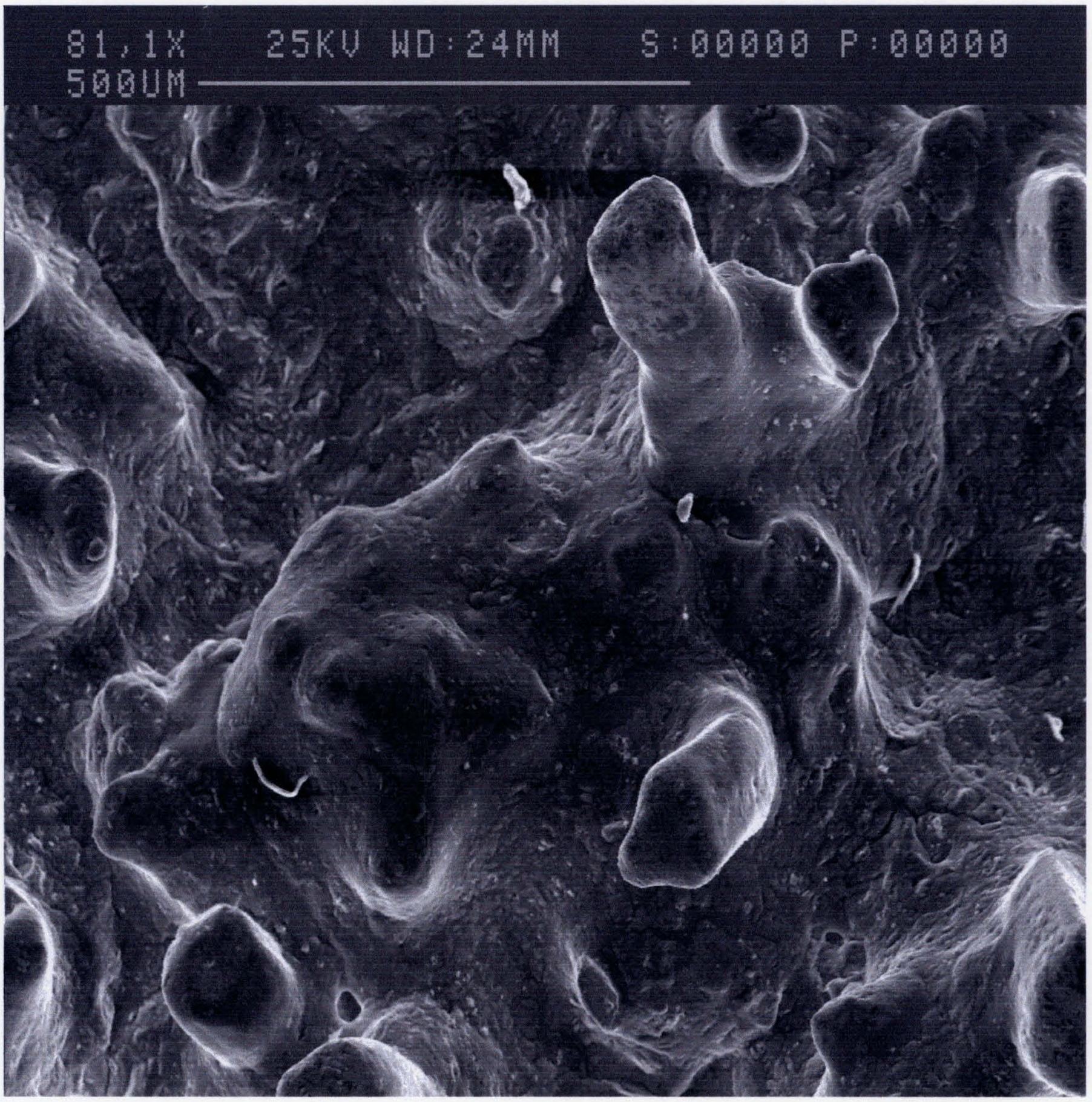

Plate 20. Aluminium alloy 6061 surface after 5-hour sinter.

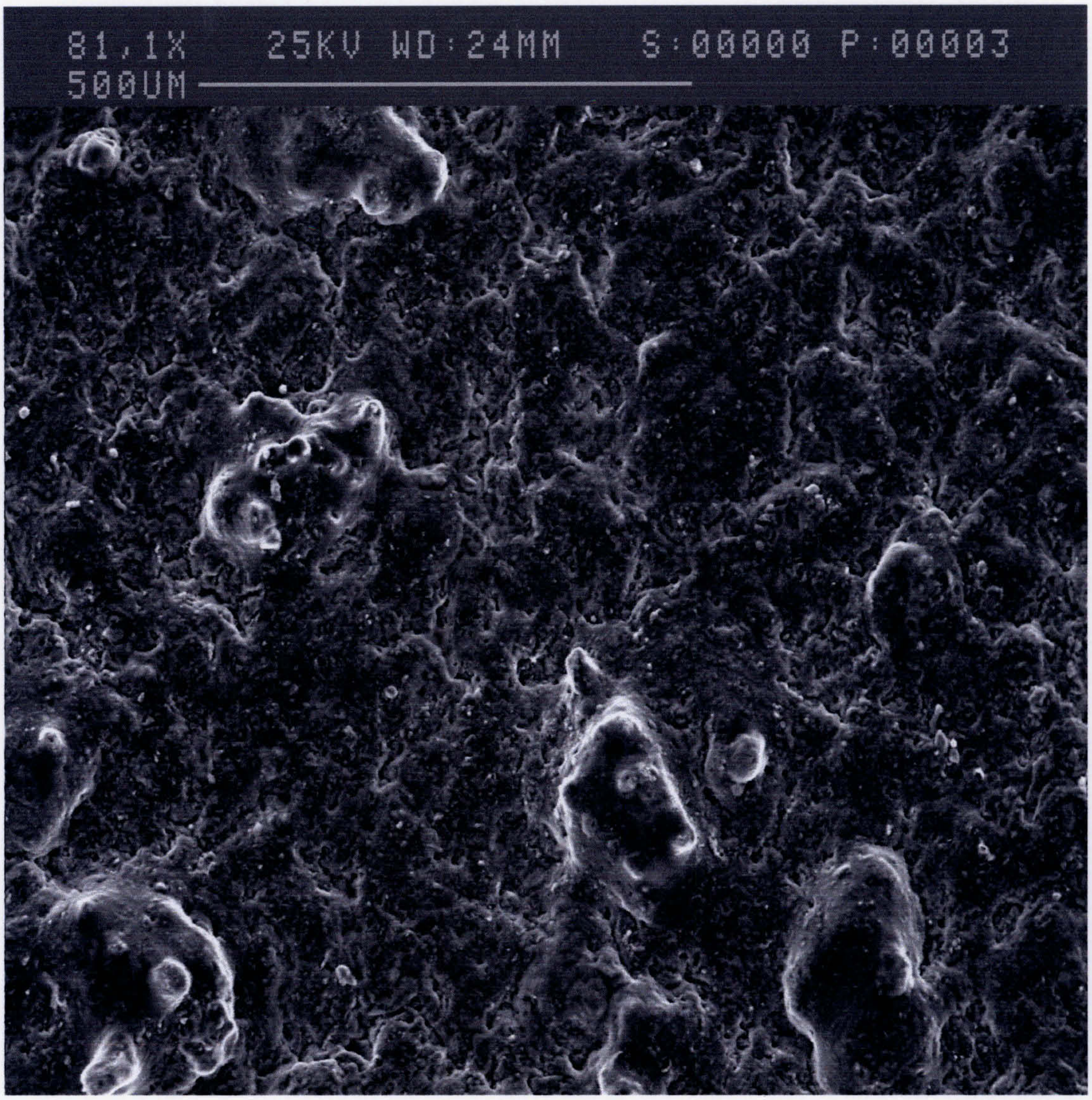

Plate 21. Aluminium alloy 6061 surface after 0.5-hour sinter.

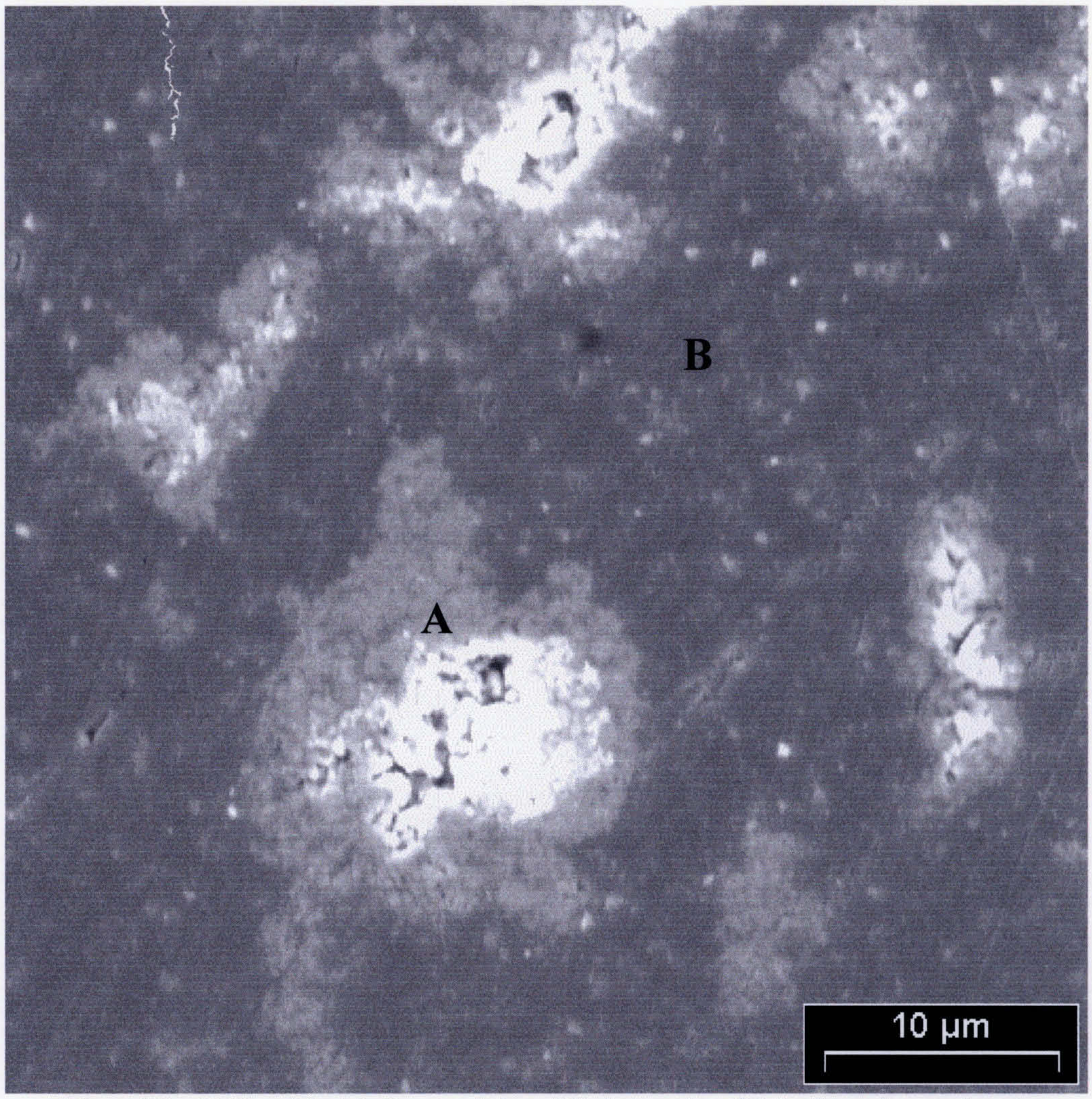

Plate 22. 6061 with Al_2O_3 particles. High levels of Mg found at point A (close to interface between reinforcement and matrix) and no Mg concentrations were found at point B ("away" from reinforcement) in composites sintered for 5 hours.

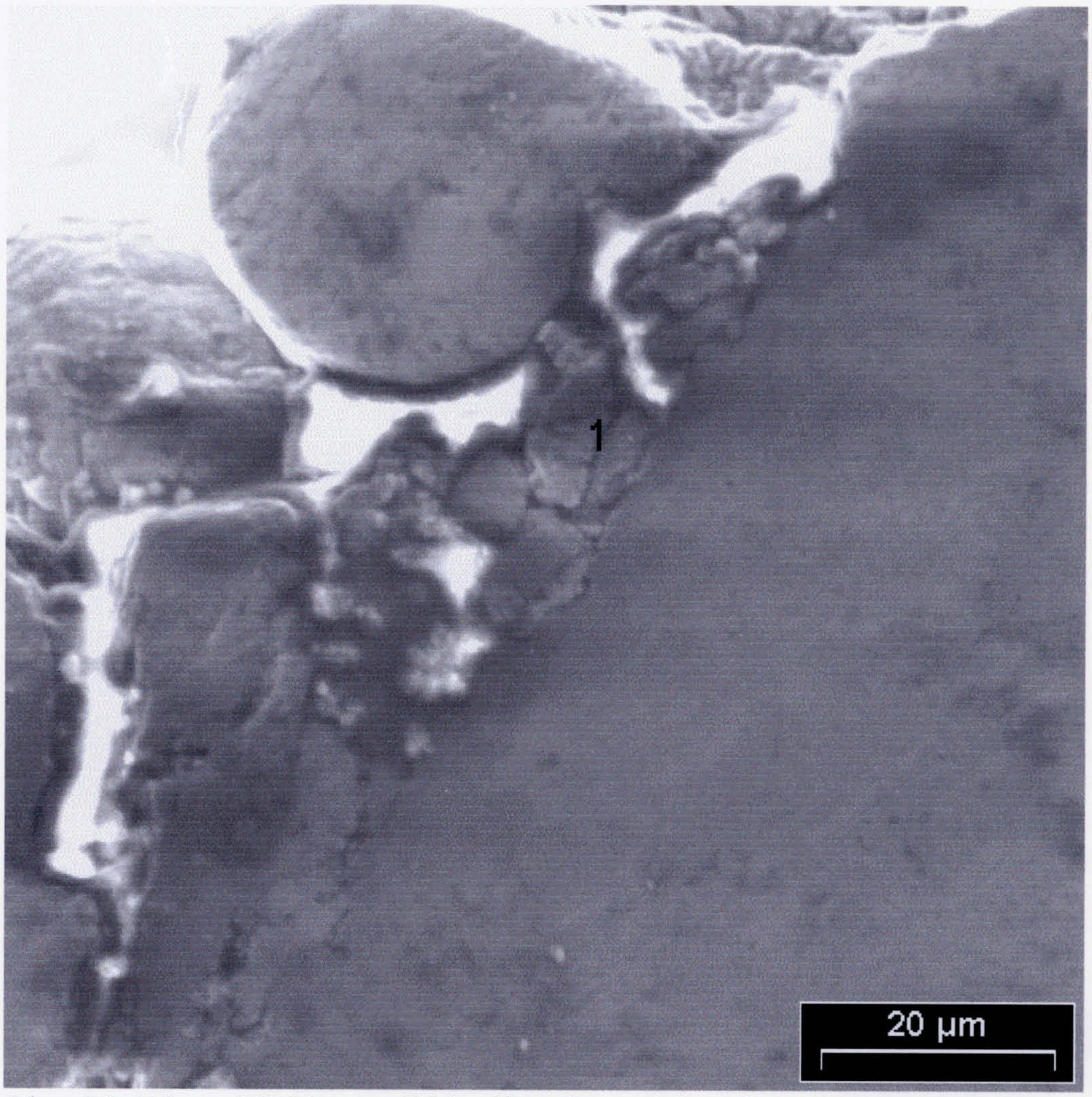

Plate 23. Edge of 6061 monolithic alloy sintered for 5 hrs at 600°C, at point 1 a high level of Si was found.

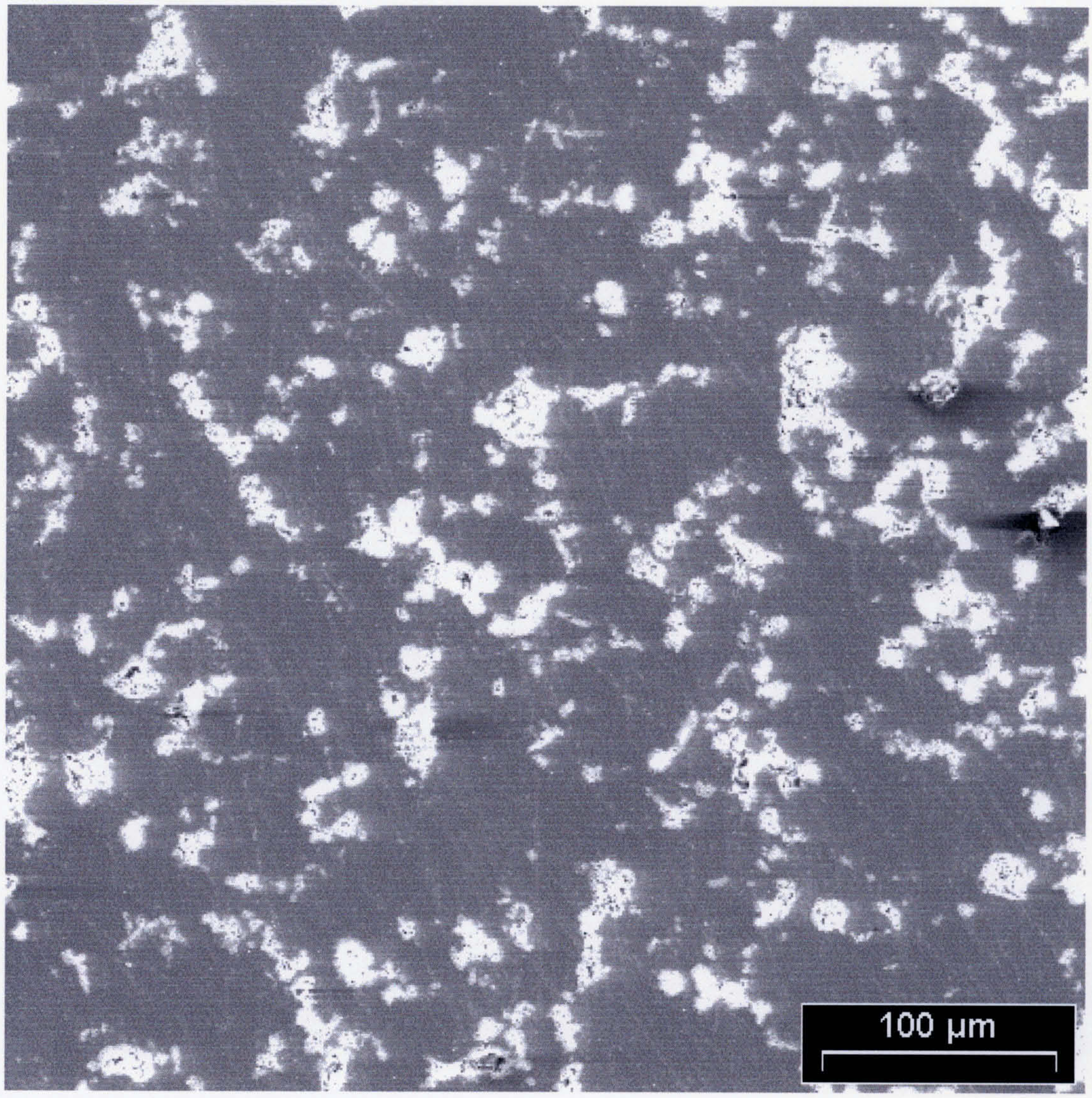

Plate 24. Micrograph displaying Al_2O_3 distribution in Al 6061 matrix.

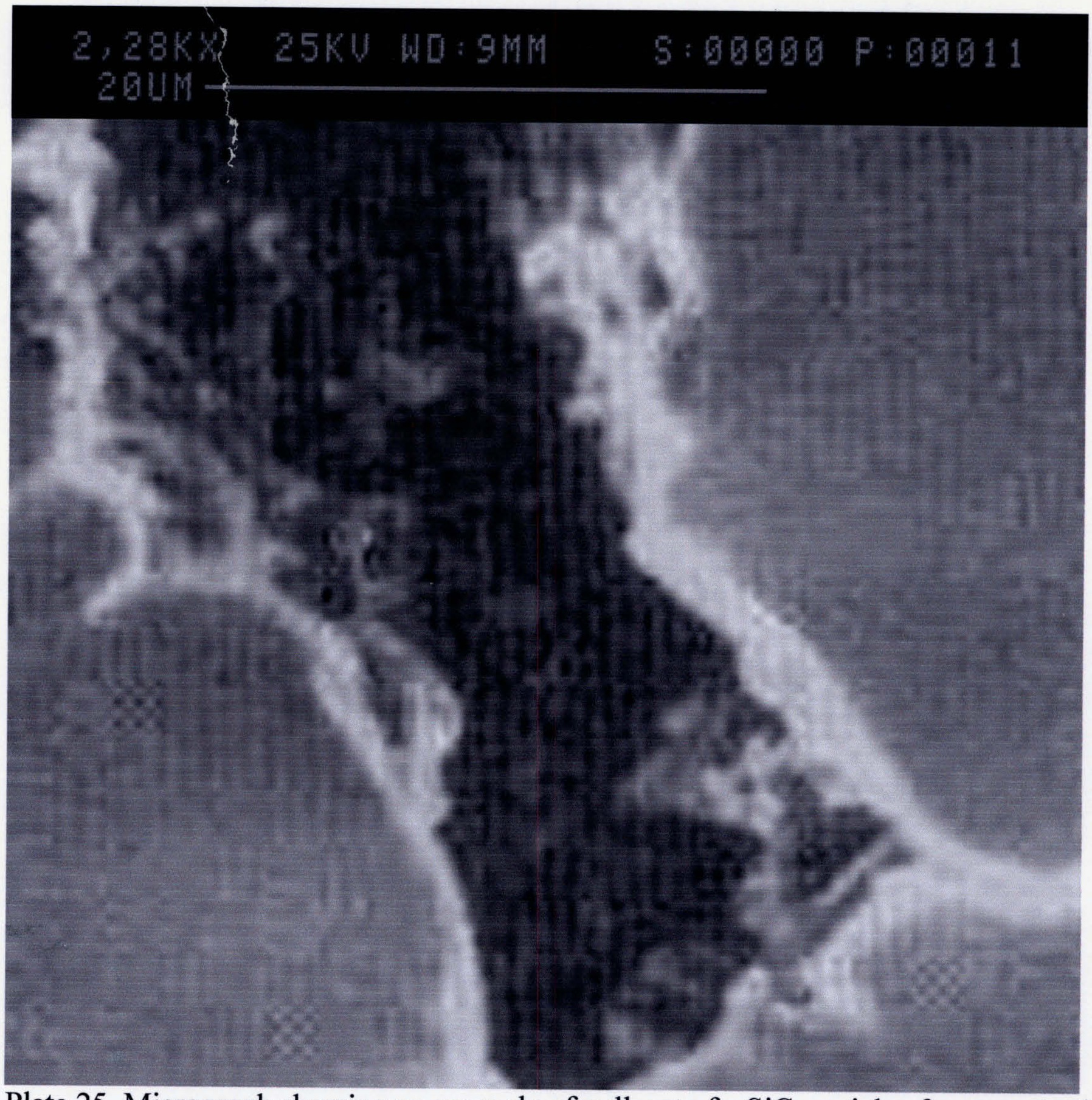

Plate 25. Micrograph showing an example of pull-out of a SiC particle after wear testing in an aluminium 6061 alloy matrix reinforced with 7μm SiC particulates.

Appendix 2.

COSHH Assessment.

The materials safety data sheets found in this appendix were downloaded from:

"The Physical and Theoretical Chemistry Laboratory
Oxford University Chemical and Other Safety Information" located at
http://www.liv.ac.uk/Chemistry/Links/links.html

Safety data for hydrazine hydrate

General

Synonyms: hydrazine monohydrate, diamide hydrate, aqueous hydrazine, hydrazine hydroxide, hydrazinium hydroxide
Use:
Molecular formula: $N_2H_4.H_2O$
CAS No: 7803-57-8
EC No:

Physical data

Appearance: colourless fuming liquid
Melting point: -52 C
Boiling point: 120 - 121 C
Vapour density:
Vapour pressure: 5.2 mm Hg at 20 C
Density (g cm^{-3}): 1.027
Flash point: 74 C (closed cup)
Explosion limits: 3.4 - 100%
Autoignition temperature: 280 C
Water solubility: miscible

Stability

Incompatible with a wide variety of materials, including oxidizing agents, heavy metal oxides, dehydrating agents, alkali metals, rust, silver salts. Combustible. **Contact with many materials may cause fire or explosive decomposition. May react explosively with a variety of materials, including dehydrating agents, heavy metal oxides, perchlorates. Contact with cadmium, gold, brass, molybdenum and stainless steel containing > 0.5% molybdenum may cause rapid decomposition. Vapour may explode in fire.** Note wide explosive limits - flammable from 4 to 100% hydrazine in air. **Read safety data sheet fully before use.**

Toxicology

Toxic, and may be fatal, if inhaled, swallowed or absorbed through the skin. Expected to be a human carcinogen. Eye contact may cause serious damage. May cause CNS, eye, liver, kidney and lung damage. Possible sensitizer. Corrosive. Material is very irritating to respiratory tract, even a low concentrations. Typical OEL 0.02 ppm (8h TWA)

Toxicity data

ORL-RAT LD50 129 mg kg^{-1}
ORL-MUS LD50 83 mg kg^{-1}
SKN-RBT LDLO 20 mg kg^{-1}
IHL-RAT LC50 0.75 mg/l/4h
ORL-GPG LD50 40 mg kg^{-1}

Transport information

IATA packing group 2. IATA sub-risk 61. Adr No 8/44B. UN No 2030. IATA class 8. Transport category 2. Not permitted on passenger flights.

Personal protection

Safety glasses, gloves, good ventilation. Treat as a possible carcinogen. Remove all sources of ignition from the working area. **Prepare a risk assessment before starting work.**

Safety data for formaldehyde, 37% solution

General

Synonyms: formalin, formic aldehyde, methylene oxide, oxomethane, paraform
Molecular formula: CH_2O
CAS No: 50-00-0
EC No: 200-001-8

Physical data

Appearance: colourless liquid, typically 37% formaldehyde in water
Melting point:
Boiling point:
Specific gravity: 1.083
Vapour pressure: 55 mm Hg at 37 C
Flash point: 56 C
Explosion limits: 7% - 73%
Autoignition temperature: 572 F

Stability

Stable. Substances to be avoided include strong bases, strong acids, strong oxidising agents, aniline, phenol, isocyanates, anhydrides. Combustible.

Toxicology

Causes burns. **Very toxic by inhalation, ingestion and through skin absorption. Readily absorbed through skin. Possible cancer hazard. Mutagen. May cause damage to kidneys. May cause allergic reactions. May cause sensitisation. May cause heritable genetic damage.** Lachrymator. Very destructive of mucous membranes and upper respiratory tract, eyes and skin.

Toxicity data

ORL-RAT LD50 100 mg kg^{-1}
SKN-RBT LD50 270 mg kg^{-1}

Personal protection

Safety glasses. Gloves. Good ventilation.

Safety data for aluminium

General

Synonyms: aluminum
Molecular formula: Al
CAS No: 7429-90-5
EC No: 231-072-3

Physical data

Appearance: silver foil, shot or powder
Melting point: 660 C
Boiling point:
Vapour density:
Vapour pressure:
Specific gravity: 2.7
Flash point:
Explosion limits:
Autoignition temperature:

Stability

Stable. Powder is flammable. Moisture and air sensitive. Incompatible with strong acids, caustics.

Toxicology

Powder may be harmful by ingestion or inhalation.

Transport information

Non-hazardous for air, sea and road freight.

Personal protection

Safety glasses if using granules or powder.

Safety data for aluminium oxide

General

Synonyms: aluminum oxide, alumina, aluminium sesquioxide, alundum, abramant, Alumite, Poraminar, Microgrit WCA, Ludox CL and numerous other trade names
Molecular formula: Al_2O_3
CAS No: 1344-28-1
EC No: 215-691-6

Physical data

Appearance: White granules or powder
Melting point: 2030 C
Boiling point: 2977 C
Vapour density:
Vapour pressure: 1 mm Hg at 2158 C
Specific gravity: 4.0
Flash point:
Explosion limits:
Autoignition temperature:
Solubility in water: negligible

Stability

Stable. Incompatible with strong acids, strong bases, CF3, ethylene oxide, halocarbons, OF2, sodium nitrate, vinyl acetate. [Used as adsorbent, refractory material, catalyst, GC analysis component.]

Toxicology

Harmful by inhalation. May be harmful by ingestion. May irritate eyes or skin. 8h TWA typically 10mg/m3.

Toxicity data
INHL-MOUSE TCLO 352 mg m^{-3}

Personal protection

Good ventilation. Safety glasses.

Safety data for silicon carbide

General

Synonyms:
Use:
Molecular formula: SiC
CAS No: 409-21-2
EC No: 206-992-8

Physical data

Appearance: light grey powder
Melting point: 2700 C
Boiling point:
Vapour density:
Vapour pressure:
Density (g cm^{-3}): 3.22
Flash point:
Explosion limits:
Autoignition temperature:
Water solubility: insoluble

Stability

Toxicology

Skin, eye and respiratory irritant. Nuisance dust. Experimental tumorigen.

Transport information

Non-hazardous for air, sea and road freight.

Personal protection

Adequate ventilation. Safety glasses.

Safety data for copper

General

Synonyms: bronze powder, arnwood copper, copper shot, anac 110, copper bronze, Raney copper
Molecular formula: Cu
CAS No: 7440-50-8
EINECS No: 231-159-6

Physical data

Appearance: reddish lustrous malleable metal
Melting point: 1083 C
Boiling point: 2595 C
Specific gravity: 8.92
Vapour pressure:
Flash point:
Explosion limits:
Autoignition temperature:

Stability

Stable. Incompatible with strong acids, active halogen compounds, chlorine, fluorine, iodine, bromine, ammonia. May react explosively with strong oxidizing agents.

Toxicology

Dust may cause respiratory irritation.

Toxicity data
IPR-MUS LD50 3.5 mg kg^{-1}

Transport information

UN Nos: 3089 (very fine powder), 3077 (fine powder); otherwise considered non-hazardous for air, sea and road freight.

Personal protection

Suitable ventilation if handling powder.

Safety data for copper (II) sulfate

General

Synonyms: cupric sulfate, cupric sulphate, blue vitriol, copper (II) sulfate 5-hydrate, copper sulphate
Molecular formula: Cu S O_4 $5H_2O$ (if hydrated)
CAS No: 7758-99-8
EC No: 231-847-6

Physical data

Appearance: blue odourless crystalline solid (white or grey powder if anhydrous)
Melting point: 110 C (600 C, with decomposition, if anhydrous)
Boiling point:
Vapour density:
Vapour pressure:
Specific gravity: 2.28 (hydrated) 3.6 (anhydrous)
Flash point: none
Explosion limits: none
Autoignition temperature:
very soluble in water

Stability

Stable. Incompatible with strong reducing agents, hydroxylamine.

Toxicology

Harmful by inhalation or ingestion. Dust may ulcerate membranes. Prolonged exposure may cause dermatitis. Possible irritant. No UK exposure limit (as at 13.8.01) **Very toxic to aquatic organisms.**

Toxicity data
ORL-RAT LD50 300 mg kg^{-1}

Personal protection

Safety glasses. Effective ventilation.

Safety data for ammonium chloride

General

Synonyms: sal ammoniac, ammonium muriate, amchlor, ammoneric, darammon, sal ammonia, slammonite, salmiac
Molecular formula: NH_4Cl
CAS No: 12125-02-9
EC No: 235-186-4
EC index no: 017-014-00-8

Physical data

Appearance: white crystalline powder
Melting point: 340 C (sublimes)
Boiling point:
Vapour density: 1.9
Vapour pressure: 1 mm Hg at 160 C
Specific gravity: 1.527
Flash point:
Explosion limits:
Autoignition temperature:

Stability

Stable. Incompatible with strong acids, strong bases.

Toxicology

Harmful if swallowed. May be harmful by inhalation. Skin, eye and respiratory irritant.
Typical TLV 10 mg m^{-3} Typical STEL 20 mg m^{-3}

Toxicity data
(The meaning of any abbreviations which appear in this section is given here.)
ORL-INF LDLO 2000 mg kg^{-1}
ORL-RAT LD50 1650 mg kg^{-1}
IMS-RAT LD50 30 mg kg^{-1}
UNR-RAT LD50 550 mg kg^{-1}

Transport information

Non-hazardous for air, sea and road freight.

Personal protection

Handle with care.

Safety data for magnesium

General

Synonyms: magnesium ribbon
Molecular formula: Mg
CAS No: 7439-95-4
EC No: 231-104-6

Physical data

Appearance: silver or grey rod, turnings or ribbon
Melting point: 650 C
Boiling point: 1107 C
Vapour density:
Vapour pressure: 1 mm at 621 C
Specific gravity: 1.73
Flash point: 634 C (closed cup)
Explosion limits:
Autoignition temperature: 510 C

Stability

Stable. Reacts violently with halogens, chlorinated solvents. Air and moisture sensitive. Incompatible with acids, acid chlorides, strong oxidizing agents. **Highly flammable.**

Toxicology

Harmful if swallowed or inhaled. Severe irritant. Vessicant.

Transport information

UN Major hazard class 4.1 Packing group III

Personal protection

Safety glasses.

Safety data for silicon

General

Synonyms:
Molecular formula: Si
CAS No: 7440-21-3
EINECS No:

Physical data

Appearance: grey lustrous solid or grey powder
Melting point: 1410 C
Boiling point: 2355 C
Vapour density:
Vapour pressure:
Density (g cm^{-3}): 2.33
Flash point:
Explosion limits:
Autoignition temperature:

Stability

Stable. Fine powder is highly flammable. Incompatible with oxidizing agents, bases, carbonates, alkali metals, lead and aluminium oxides, halogens, carbides, formic acid.

Toxicology

Generally regarded as safe. Typical TLV (TWA) 10 mg/m3.

Toxicity data
ORL-RAT LD50 3160 mg kg^{-1}

Transport information

Non-hazardous for air, sea and road freight.

Personal protection

Minimize contact.

1 - PRODUCT IDENTIFICATION

PRODUCT NAME: STANNOUS CHLORIDE, DIHYDRATE
FORMULA: SNCL2 2H2O
FORMULA WT: 225.63
CAS NO.: 10025-69-1
NIOSH/RTECS NO.: XP8700000
COMMON SYNONYMS: TIN(II)CHLORIDE, DIHYDRATE; TIN DICHLORIDE, DIHYDRATE
PRODUCT CODES: 3980,3986
EFFECTIVE: 09/08/86
REVISION #02

PRECAUTIONARY LABELLING

BAKER SAF-T-DATA(TM) SYSTEM

HEALTH	-	2	MODERATE
FLAMMABILITY	-	0	NONE
REACTIVITY	-	1	SLIGHT
CONTACT	-	2	MODERATE

HAZARD RATINGS ARE 0 TO 4 (0 = NO HAZARD; 4 = EXTREME HAZARD).

LABORATORY PROTECTIVE EQUIPMENT

SAFETY GLASSES; LAB COAT; VENT HOOD; PROPER GLOVES

PRECAUTIONARY LABEL STATEMENTS

WARNING
CAUSES IRRITATION AND MAY CAUSE BURNS.
HARMFUL IF SWALLOWED, INHALED, OR ABSORBED THROUGH SKIN
AVOID CONTACT WITH EYES, SKIN, CLOTHING.
AVOID BREATHING DUST. KEEP IN TIGHTLY CLOSED CONTAINER. USE WITH ADEQUATE
VENTILATION. WASH THOROUGHLY AFTER HANDLING. IN CASE OF FIRE, SOAK WITH WATER.
IN CASE OF SPILL, SWEEP UP AND REMOVE. FLUSH SPILL AREA WITH WATER.

SAF-T-DATA(TM) STORAGE COLOR CODE: ORANGE (GENERAL STORAGE)

2 - HAZARDOUS COMPONENTS

COMPONENT	%
CAS NO.	
STANNOUS CHLORIDE, DIHYDRATE	90-100
10025-69-1	

FOR INFORMATION ONLY; ANHYDROUS FORM 7772-99-8

3 - PHYSICAL DATA

BOILING POINT: N/A

VAPOR PRESSURE(MM HG): N/A

MELTING POINT: 37 C (99 F)

VAPOR DENSITY(AIR=1): N/A

SPECIFIC GRAVITY: 2.71

EVAPORATION RATE: N/A

(H2O=1)

(BUTYL ACETATE=1)

SOLUBILITY(H2O): APPRECIABLE (MORE THAN 10 %) % VOLATILES BY VOLUME: 0

APPEARANCE & ODOR: WHITE ODORLESS CRYSTALS.

4 - FIRE AND EXPLOSION HAZARD DATA

FLASH POINT (CLOSED CUP N/A

FLAMMABLE LIMITS: UPPER - N/A % LOWER - N/A %

FIRE EXTINGUISHING MEDIA
USE EXTINGUISHING MEDIA APPROPRIATE FOR SURROUNDING FIRE.

SPECIAL FIRE-FIGHTING PROCEDURES
FIREFIGHTERS SHOULD WEAR PROPER PROTECTIVE EQUIPMENT AND SELF-CONTAINED
BREATHING APPARATUS WITH FULL FACEPIECE OPERATED IN POSITIVE PRESSURE MODE.
MOVE CONTAINERS FROM FIRE AREA IF IT CAN BE DONE WITHOUT RISK. USE WATER
TO KEEP FIRE-EXPOSED CONTAINERS COOL.

UNUSUAL FIRE & EXPLOSION HAZARDS
CLOSED CONTAINERS EXPOSED TO HEAT MAY EXPLODE.
NOTE: DECOMPOSES AT MELTING POINT.

TOXIC GASES PRODUCED

HYDROGEN CHLORIDE

---

5 - HEALTH HAZARD DATA

SOME EXPERIMENTS WITH TEST ANIMALS INDICATED THAT THIS SUBSTANCE MAY BE
ANTICIPATED TO BE A CARCINOGEN.

THRESHOLD LIMIT VALUE (TLV/TWA): 2 MG/M3 (PPM)

PERMISSIBLE EXPOSURE LIMIT (PEL): 2 MG/M3 (PPM)

TOXICITY: LD50 (ORAL-RAT)(MG/KG) - 700
LD50 (IPR-MOUSE)(MG/KG) - 66

CARCINOGENICITY: NTP: NO IARC: NO Z LIST: NO OSHA REG: NO

EFFECTS OF OVEREXPOSURE
INHALATION OF DUST MAY CAUSE IRRITATION TO UPPER RESPIRATORY TRACT.
DUST MAY IRRITATE OR BURN MUCOUS MEMBRANES.
CONTACT WITH SKIN OR EYES MAY CAUSE SEVERE IRRITATION OR BURNS.
PROLONGED
CONTACT MAY CAUSE SKIN SENSITIZATION. SUBSTANCE IS READILY ABSORBED
THROUGH THE SKIN.
INGESTION MAY CAUSE IRRITATION AND BURNING TO MOUTH AND STOMACH.

INGESTION MAY CAUSE NAUSEA, VOMITING, HEADACHES, DIZZINESS,
GASTROINTESTINAL IRRITATION.

TARGET ORGANS
EYES, SKIN, RESPIRATORY SYSTEM

MEDICAL CONDITIONS GENERALLY AGGRAVATED BY EXPOSURE
NONE IDENTIFIED

ROUTES OF ENTRY
INHALATION, EYE CONTACT, SKIN CONTACT

EMERGENCY AND FIRST AID PROCEDURES
CALL A PHYSICIAN.
IF SWALLOWED, DO NOT INDUCE VOMITING; IF CONSCIOUS, GIVE LARGE AMOUNTS OF
WATER.
IF INHALED, REMOVE TO FRESH AIR. IF NOT BREATHING, GIVE ARTIFICIAL
RESPIRATION. IF BREATHING IS DIFFICULT, GIVE OXYGEN.
IN CASE OF CONTACT, IMMEDIATELY FLUSH EYES OR SKIN WITH PLENTY OF WATER FOR
AT LEAST 15 MINUTES WHILE REMOVING CONTAMINATED CLOTHING AND SHOES.
WASH CLOTHING BEFORE RE-USE.

---

6 - REACTIVITY DATA

STABILITY: STABLE HAZARDOUS POLYMERIZATION: WILL NOT OCCUR

CONDITIONS TO AVOID: HEAT, FLAME, MOISTURE

INCOMPATIBLES: BROMINE TRIFLUORIDE AND TRICHLORIDE, NITRATES,
ALKALIES, ALCOHOLS, AMMONIA,
SODIUM METAL, POTASSIUM METAL, STRONG OXIDIZING AGENTS,
CARBIDES

DECOMPOSITION PRODUCTS: HYDROGEN CHLORIDE, TIN OXIDE FUME

---

7 - SPILL AND DISPOSAL PROCEDURES

STEPS TO BE TAKEN IN THE EVENT OF A SPILL OR DISCHARGE
WEAR SELF-CONTAINED BREATHING APPARATUS AND FULL PROTECTIVE CLOTHING.
WITH CLEAN SHOVEL, CAREFULLY PLACE MATERIAL INTO CLEAN, DRY CONTAINER AND
COVER; REMOVE FROM AREA. FLUSH SPILL AREA WITH WATER.

DISPOSAL PROCEDURE
DISPOSE IN ACCORDANCE WITH ALL APPLICABLE FEDERAL, STATE, AND LOCAL ENVIRONMENTAL REGULATIONS.

---

8 - PROTECTIVE EQUIPMENT

VENTILATION: USE GENERAL OR LOCAL EXHAUST VENTILATION TO MEET
TLV REQUIREMENTS.

RESPIRATORY PROTECTION: A RESPIRATOR WITH DUST/MIST FILTER IS RECOMMENDED.
IF AIRBORNE CONCENTRATION EXCEEDS TLV, A SELF-
CONTAINED BREATHING APPARATUS IS ADVISED.

EYE/SKIN PROTECTION: SAFETY GLASSES WITH SIDESHIELDS, UNIFORM, NEOPRENE

GLOVES ARE RECOMMENDED.

---

9 - STORAGE AND HANDLING PRECAUTIONS

SAF-T-DATA(TM) STORAGE COLOR CODE: ORANGE (GENERAL STORAGE)

SPECIAL PRECAUTIONS

KEEP CONTAINER TIGHTLY CLOSED. SUITABLE FOR ANY GENERAL CHEMICAL STORAGE AREA.

---

10 - TRANSPORTATION DATA AND ADDITIONAL INFORMATION

DOMESTIC (D.O.T.)

PROPER SHIPPING NAME	STANNOUS CHLORIDE, SOLID (AIR ONLY)
HAZARD CLASS	ORM-B
UN/NA	NA1759
LABELS	NONE

INTERNATIONAL (I.M.O.)

PROPER SHIPPING NAME	CORROSIVE SOLIDS, N.O.S. (STANNOUS CHLORIDE, DIHYDRATE)
HAZARD CLASS	8
UN/NA	UN1759
LABELS	CORROSIVE

Safety data for sodium hydroxide

General

Synonyms: caustic soda, soda lye, white caustic
Molecular formula: NaOH
CAS No: 1310-73-2
EC No: 215-185-5

Physical data

Appearance: odourless white solid (often sold as pellets)
Melting point: 318 C
Boiling point: 1390 C
Vapour density:
Vapour pressure: 1 mm Hg at 739 C
Specific gravity: 2.12 g/ml
Flash point: n/a
Explosion limits: n/a
Autoignition temperature:

Stability

Stable. Incompatible with a wide variety of materials including many metals, ammonium compounds, cyanides, acids, nitro compounds, phenols, combustible organics. Hygroscopic. Heat of solution is very high and may lead to a dangerously hot solution if small amounts of water are used.

Toxicology

Very corrosive. Causes severe burns. May cause serious permanent eye damage. Very harmful by ingestion. Harmful by skin contact or by inhalation of dust. Typical TLV 2 mg m^{-1}.

Toxicity data

IPR-MUS LD50 40 mg kg^{-1}

Irritation data

EYE-MKY 1%/24h sev
SKN-RBT 500 mg/24h sev

Transport information

UN Major hazard class 8.0. Packing group II. UN No 1823. EMS No 8.0-06.

Personal protection

Safety glasses, adequate ventilation, Neoprene or PVC gloves.

Safety data for palladium chloride

Synonyms: palladium dichloride
Molecular formula: Pd Cl2
CAS No: 7647101
EC No:

Physical data

Appearance:
Melting point:
Boiling point:
Vapour density:
Vapour pressure:
Specific gravity:
Flash point:
Explosion limits:
Autoignition temperature:

Stability

Stable. [Used as a catalyst, photographic and electroplating reagent.]

Toxicology

ORL-RAT LD50 200 mg/kg. IPB-RAT LD50 70 mg/kg. IV-RAT 5 mg/kg.

Personal protection

Safety glasses and adequate ventilation.

Safety data for potassium sodium tartrate 4-hydrate

General

Synonyms: Rochelle salt
Molecular formula: $KOCO(CHOH)_2COONa\ 4H_2O$
CAS No: 6381-59-5
EC No:

Physical data

Appearance: white crystals
Melting point: 70 C
Boiling point:
Vapour density:
Vapour pressure:
Specific gravity: 1.79
Flash point:
Explosion limits:
Autoignition temperature:

Stability

Stable. Incompatible with strong oxidizing agents.

Toxicology

May act as an irritant, or be harmful by inhalation, ingestion or skin contact.

Transport information

Non-hazardous for air, sea and road freight.

Personal protection

Generally regarded as presenting only a low hazard - handle with normal care and attention.

Safety data for copper (II) acetate

Synonyms: cupric acetate
Molecular formula: (CH3COO)2CU H2O
CAS No:006046931
EC No:

Physical data

Appearance: blue-green powder
Melting point: 115 C
Boiling point: 240C
Vapour density: 6.8
Vapour pressure:
Specific gravity: 1.882
Flash point:
Explosion limits:
Autoignition temperature:

Stability

Stable. Incompatible with oxidizing agents.

Toxicology

Contact with dust may cause irritation. Harmful by inhalation and if swallowed.

Personal protection

Safety glasses. Effective ventilation.

Safety data for hydrochloric acid (concentrated)

General

Synonyms: muriatic acid, chlorohydric acid
Molecular formula: HCl
CAS No: 7647-01-0
EC No: 231-595-7

Physical data

Appearance: clear colourless or slightly yellow liquid with pungent odour. Concentrated acid is fuming.
Melting point: -25 C
Boiling point: 109 C
Specific gravity: 1.19
Vapour pressure:
Flash point:
Explosion limits:
Autoignition temperature:

Stability

Stable. Avoid heat, flames. Incompatible with most common metals, amines, metal oxides, acetic anhydride, propiolactone, vinyl acetate, mercuric sulphate, calcium phosphide, formaldehyde, alkalies, carbonates, strong bases, sulphuric acid, chlorosulphonic acid.

Toxicology

Extremely corrosive. Inhalation of vapour can cause serious injury. Ingestion may be fatal. Liquid can cause severe damage to skin and eyes. TLV 5 ppm.

Toxicity data
ORL-RBT LD50 900 mg kg^{-1}
IPR-MUS LD50 40 mg kg^{-1}
IHL-RAT LC50 3124 ppm/1h.
IHL-HMN LCLO 1300 ppm 30min

Transport information

UN No 1789. Packing group II. Major hazard class 8.0. Transport category 2.

Environmental information

Lethal to fish from 25 mg/l up. Toxic for aquatic organisms due to pH shift.

Personal protection

Safety glasses or face mask, gloves. Effective ventilation.

Appendix 3.

Published Papers.

Contained within this appendix are the titles of, and the abstracts from, two published papers, which have resulted directly from the research carried out in this thesis.

Paper 1.
Published in the Proceedings for 32nd International Symposium on Automotive Technology and Automation: Materials for Energy Efficient Vehicles. Vienna, Austria, June 1999.

Processing Variables in Aluminium-based Composites for Wear Resistant Applications in the Automotive Industry

C A Mitchell and A M Davidson
Napier University, Edinburgh, Scotland

99NM041

This paper presents the early results of an investigation into the wear resistance of metal matrix composites. One of the factors, which limits the more widespread use of such composites, is their relatively high manufacturing costs - both in terms of raw materials and processing. This work uses a low cost, pressureless sintering powder processing route to manufacture aluminium-based composites and also compares the performance of particulate alumina as the reinforcing medium with that of the more expensive silicon carbide. Initial findings point to improved wear resistance of the alumina-reinforced composites over the monolithic alloy and only slightly poorer performance than the silicon carbide equivalents. Of great importance, however, is the processing conditions employed in the manufacture of the alumina-reinforced composites. It has been found that prolonged sintering and/or heat treatment results in a decrease in hardness and wear resistance. Shorter processing times - at a cost of decreased theoretical density values - give comparable hardness measurements between the two types of reinforced composites and work currently being undertaken will determine whether or not this equivalence will extend to wear resistance. If this is the case then the employment of alumina, generally significantly less expensive than silicon carbide, will be most attractive in terms of wear resistant components in automotive applications.

Paper 2.
Published in Materials Science and Technology, Volume 16, July-August 2000.

Effect of Al_2O_3 particulates as reinforcement in age hardenable aluminium alloy composites

C A Mitchell and A M Davidson
Napier University, Edinburgh, Scotland

This paper investigates the behaviour of aluminium-based composites, reinforced with aluminium oxide particulates, manufactured using a powder processing route and various sintering times. It is found that a softening effect, compared with the monolithic material, coincides with migration of magnesium from the matrix to the matrix / reinforcement interface and to the specimen surface. The addition of 5-wt%Si to the matrix alloy results in a retention of hardness in the specimens given shorter sinter times (0.5 and 1 h). This coincides with reduced migration of magnesium from the matrix. It is postulated that excess silicon results in sufficient magnesium being retained in the matrix during short sinter times to take part in the formation of Mg_2Si precipitates necessary for the hardening of the Al alloy 6061 matrix.

MST/4559